Comparative Power Capture of Unmoored Floating Offshore Wind Turbines and Energy Ships

by

Patrick Connolly
B.Sc., University of Prince Edward Island, 2018

A Thesis Submitted in Partial Fulfillment of the
Requirements for the Degree of

MASTER OF APPLIED SCIENCE

in the Department of Mechanical Engineering

We acknowledge with respect the Lekwungen peoples on whose traditional territory the university stands and the Songhees, Esquimalt and W̱SÁNEĆ peoples whose historical relationships with the land continue to this day.

Comparative Power Capture of Unmoored Floating Offshore Wind Turbines and Energy Ships

by

Patrick Connolly
B.Sc., University of Prince Edward Island, 2018

Supervisory Committee

Dr. C. Crawford Main, Supervisor
(Department of Mechanical Engineering)

Dr. B. Buckham, Committee Member
(Department of Mechanical Engineering)

ABSTRACT

Given the bleak current and projected global climate trends, society is transitioning the energy systems that we rely upon away from fossil fuel based systems to reduce global CO_2 emissions. There are now well-established technologies for providing renewable electricity at utility scales, such as wind turbines and solar panels, being deployed at an ever increasing pace. However, solutions for decarbonizing other sectors where fossil fuels are harder to replace are still needed. Current strategies for reducing fossil fuel use in these sectors rely on replacing them with synthetic fuels instead are produced using renewable electricity, and can therefore be part of a net-zero emissions cycle. The focus of this thesis is to examine a novel class of wind energy systems suitable for powering these fuel synthesis processes. Alternative applications of the proposed systems include powering direct air CO_2 capture systems to support negative emissions technology efforts.

This work develops and presents numerical models for concepts hereafter referred to as mobile offshore wind energy systems (MOWESs). A MOWES is a wind energy system that operates offshore and is not intended to remain stationary during operation. MOWESs would operate far from shore, harnessing a part of the wind resource that would not otherwise be usable. No full- or large-scale MOWES has yet been developed, and there is little work on developing these concepts, even within academia. Steady-state power performance models of two MOWES concepts, namely unmoored floating offshore wind turbines and energy ships, are developed to support further research in this field. Model results suggest that each concept has unique pros and cons and no conclusion can be drawn as to which technology is more efficient overall. A key conclusion of this work is that unmoored floating wind turbines can generate more power by sailing at a constant speed rather than holding station. We also conclude that unmoored floating wind turbines designed for downwind operation can produce as much power as conventional stationary wind turbines given sufficiently high wind speeds. Further work must examine whether the advantages of these technologies are exploitable given realistic wind conditions and when considering the complicated dynamics of the system.

Contents

List of Tables

List of Figures

ACKNOWLEDGEMENTS

I would like to thank:

My parents and my brother, for always supporting me. Even when it was just picking me up from basketball practice, you've helped me grow. And for believing in me, especially when I find it hard to believe in myself.

My supervisor, Curran Crawford, for bringing me on as a student, mentoring me, and not least of all letting me ramble on about topics I'm passionate about.

and my friends, Everyone in our lab group for making me happy to come into work everyday. And my friends from PEI for always being around to laugh with, even though we're spread far apart.

Amaurotic nightingale
I hope that darkness keeps you well
When I can't fall asleep at night
I blindly taught myself to fight
Oh shadow man shadow box, please keep your hands up
And if you get knocked down don't forget to stand up
–Noname

Chapter 1

Introduction

It is apparent that the world is undergoing global climate change due to anthropogenic green house gas emissions, which have steadily increased since the industrial revolution. Economic growth and emissions have been coupled due to the global reliance on fossil fuel combustion to meet society's energy needs. This has resulted in ever increasing emissions, which as of 2021 have resulted in a global average temperature increase of over 1.0°C relative to pre-industrial temperatures [10]. Although the need to decarbonize our energy systems is now recognized globally, action is not being taken fast enough. Climate model projections presented in the latest report from the intergovernmental panel on climate change (IPCC) show that no realistic scenario will limit warming to below 1.5°C, while most scenarios presented exceed 2°C of warming [11]. Most progress has been made in decarbonizing the electricity sector, so far, thanks to the rapid scale-up of renewable energy systems like wind turbines and solar panels. Though these technologies exploit renewable sources of energy, they are variable and unpredictable since they rely on inherently random processes to produce power. Strategies for mitigating this variability, and making sure electrical supply consistently meets demand, are essential, and become increasingly important at higher levels of renewable penetration in a power grid.

Although much progress has been made in decarbonizing electricity systems, many sectors rely on the fact that fossil fuels are a stored form of energy which can be dispatched at will. Moreover, fossil fuels are incredibly energy dense, making them ideal for situations where energy is required far from an energy source, or where it may be impractical to exploit renewable sources of energy. Sectors such as marine shipping, heavy industry (steel, cement, etc.), and heavy duty and air transportation are often referred to as "hard to decarbonize" because they rely heavily on fossil

fuels and have no direct electrification pathway as an alternative. Although battery energy storage is proving a viable alternative for personal transportation and small scale public transport (i.e battery electric vehicles and buses), long-duration, mobile storage is required for other applications. A key part of decarbonizing these sectors is displacing the fossil fuels that are used with alternative zero-emissions fuels, also known as green fuels. For example, a report from IRENA on decarbonizing the shipping sector estimates the sector demand for e-ammonia (one such green fuel) at up to 183 Mt by 2050, in a scenario consistent with 1.5°C of warming [12]. This need for green fuels has spurred development of renewable energy to green fuel projects, such as wind-to-hydrogen projects [13, 14, 15].

Since there is a need for more production of green fuels, as we undergo a transition away from carbon-rich fuels, there is space for innovation in renewable power to X (PtX) systems. This thesis examines a class of novel wind energy systems which are developed specifically to be part of a PtX process. These technologies are referred to as mobile offshore wind energy systems (MOWESs). As the name implies, they generate renewable power from offshore winds, however, contrary to conventional offshore fixed- or floating- wind turbines, MOWESs are not stationary while operating. Since PtX systems can operate on a micro-grid, they are perfectly suited for mobile operations, where grid-connection would be impractical. The primary objective of this thesis is to assess the feasibility of this type of system, since there is a lack of existing research into this concept. Focus is specifically aimed at the conversion of wind energy to electrical power by MOWESs, downstream energy conversion processes and storage are left out of scope.

Another potential application of MOWESs is as autonomous CO_2 capture plants. In this pathway, systems for direct air capture (DAC) of CO_2 are installed on board the MOWES instead of (or in addition to) PtX systems. DAC is a developing negative emissions technology (NET) that functions by chemically reacting ambient air with a sorbent or solvent to trap CO_2, which is then separated in subsequent reaction steps [16, 17]. The captured CO_2 must then be safely stored or sequestered so to not be re-emitted into the atmosphere. Climate and emissions pathways conducive to 1.5°C warming or less now often include deployment of NETs at substantial scales, so there is an impetus for developing new negative emissions solutions [18, 19]. One of the main challenges for DAC is that the concentration of CO_2 in air is very dilute, meaning that DAC systems have large energy input requirements. DAC is also a very expensive process with high cost uncertainty, due to the high energy and material requirements

as well as technological immaturity [17, 19]. MOWESs may be a suitable means for powering these systems, since they represent an additional source of renewable power that may not otherwise be exploited to reduce emissions such as through grid electrification. Electrical power generated by a MOWES may be used to meet the energy requirements of an onboard DAC system, captured CO_2 can then be stored and periodically offloaded at a site where it is utilized or sequestered. This pathway for MOWESs also relies on efficiently producing electrical power, further motivating the study of the power performance of MOWESs.

1.1 MOWES background

A MOWES is any system that produces renewable energy from offshore wind, and that is not constrained to operate in or about a single place. MOWESs must have (at least) the following subsystems:

Generation system: Dedicated subsystem for conversion of mechanical energy to useful electrical energy (i.e a turbine and generator).

Propulsion system: Subsystem for propelling and course-keeping (or sea-keeping) of the MOWES.

Floating support structure: A base on which all the other subsystems are mounted.

Power to X or CO_2 capture system: Equipment necessary to convert the electrical energy generated to the desired energy storage vector or to power onboard DAC equipment.

Storage system(s): Storage for the produced energy, as well as storage for backup and buffering.

Auxiliary subsystems: Other systems such as data acquisition, monitoring, lights, signals etc.

No MOWES has been developed beyond computational models, or small-scale experimental models [4, 7, 20]. Because existing concepts are currently under-developed, there is room for innovation in proposing wholly new systems, or adaptations to concepts already existing in the literature.

Two specific MOWES concepts are the focus of this work, they are:

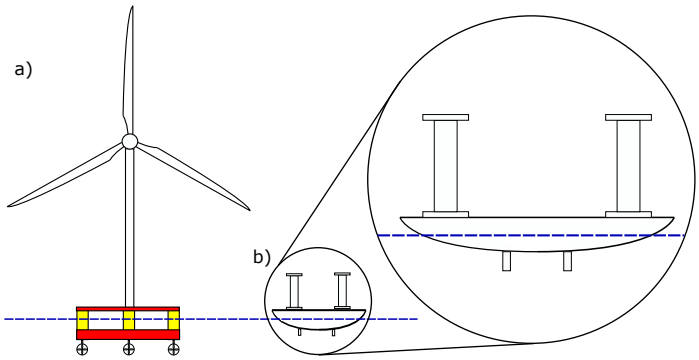

Figure 1.1: The two types of MOWES being considered: a) an UFOWT, b) an energy ship. Systems are drawn to-scale for designs proposed in Chapter 3.

a) Unmoored Floating Offshore Wind Turbines (UFOWTs): The concept of an UFOWT is to generate power from the wind using a floating wind turbine, using propellers to stabilize the system in place of mooring lines. Propellers can be actively controlled to oppose environmental loads and ensure the turbine can operate safely.

b) Energy Ships (ESs): An ES moves quickly through the ocean by harnessing the wind to propel the vessel by way of Flettner rotors (or other suitable systems). It produces electrical power using hydroturbines mounted under the hull which experience inflow because of the velocity difference between the vessel and the water.

A simple depiction of each system is shown in Figure 1.1. Each of these technologies produces renewable power from the wind to be passed to a PtX or CO_2 capture system, however, they do so in different ways. The components of each technology have each been the subject of extensive research, however, not explicitly in the context of the proposed MOWES. For example, there is a vast amount of research into the design and analysis of floating wind turbines including theoretical, computational, and experimental models, but all in the context of a moored system (for example [21, 22, 23]). Existing designs of UFOWTs and ESs are of quite different scales. For example the IEA 15 MW reference wind turbine [1] used as the basis of a UFOWT design herein is 150 meters tall, whereas the Flettner rotors used in the FARWIND ES design are only 35 meters tall [4].

Focus is aimed at these two MOWES configurations since they are the most developed in academic literature. For example, there has been extensive research into

the design of the FARWIND ES concept [4, 24, 20]. This ES design uses Flettner rotors, although other wind propulsion options such as rigid sails, turbo-sails, and kites may also be viable [25]. The option of using hydrofoils to reduce hull resistance for ESs and thereby allow them to travel faster has also been considered, though not studied extensively [26, 27]. UFOWTs have also been studied in several works, though no single design has received significant attention. Some studies focus on an UFOWT that is station-kept by thrusters (such as [7, 28]), while others analyse a mobile UFOWT [29, 30, 31]. Given existing results for flow-driven vehicles, it is expected that UFOWTs may produce more power by being mobile [32], so this work focuses on mobile UFOWTs rather than station-kept ones specifically. Since no explicit UFOWT design is well established, a design is proposed herein based on a reference floating wind turbine [1, 2].

The general flow of energy through a MOWES is described in Figure 1.2 for an UFOWT. Electrical power is produced by the generation system. This power can be directly consumed by the PtX system to convert to a storable form which is then stored onboard the vessel. However, part of the energy generated may first be consumed by the propulsion system, to maintain course, and by the auxiliary subsystems (not pictured) to remain operational. Fuel produced or CO_2 captured by the MOWES must be periodically offloaded, since it will have a fixed storage capacity. This is either done by navigating the MOWES back to shore and offloading in port, or by having another vessel meet the MOWES offshore, offload the stored fuel, and return it to shore [33]. Figure 1.2 shows the system boundary considered for this work. The generation, propulsion, and support systems are considered, while all others are neglected. We choose to ignore the PtX, auxiliary, and storage systems, since they do not have a direct impact on the net power production of the overall MOWES, although they do contribute to the total mass of the system and also take up valuable deck space. This choice of system boundary means that the inputs to the models will be environmental conditions (i.e wind and wave) and the output will be net electrical power produced.

1.1.1 Why MOWES?

There are a few major advantages that MOWESs hold over other similar renewable PtX concepts. One such advantage is that MOWESs can, in principle, operate anywhere in the open ocean. This means that they are able to operate very far from

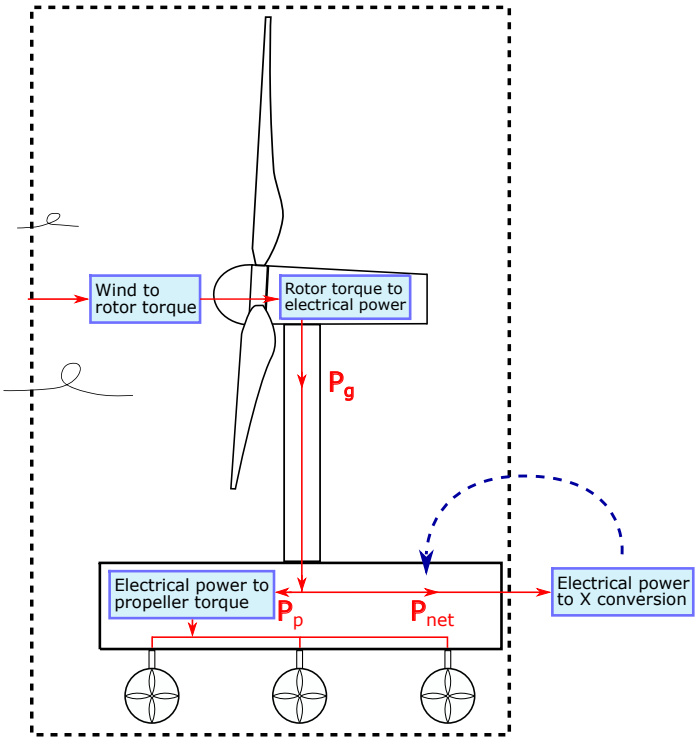

Figure 1.2: Energy conversion process for a UFOWT. PtX processes are outside of the system boundary, but the systems themselves will be onboard the vessel.

shore, where average wind speeds are the highest. Operating in higher average wind speeds will lead to higher average capacity factor (CF) for wind turbines in general. Being free to operate anywhere also means that MOWESs may follow routes to optimally position themselves given current weather and forecasts. The capacity factor is defined as the electrical energy produced (which is the integral of the power produced over a period of time), as a fraction of the electrical energy which would be produced if the system operated at maximum capacity for the given duration:

$$CF = \frac{\sum_{i=0}^{T} P(V(t_i))\Delta t}{P_{rated}T} \tag{1.1}$$

Indeed, one of the main upsides to conventional offshore wind turbines is the relative increase in average wind speed as compared to onshore. Existing floating wind projects have achieved capacity factors over 50%, well over average CFs for onshore wind [34]. No matter the performance of MOWESs compared to existing wind turbines, they represent an additional source of renewable energy which would otherwise remain unused. MOWESs do not compete for land, and may not require building

additional infrastructure associated with onshore wind farms such as roads, power lines, transformers etc.

MOWESs also benefit from the fact that they operate on the high seas. From a legal/regulatory perspective this may be an advantage since installing anchored or fixed OWTs in the seabed may have a more complicated regulatory process. As a new technology, MOWESs can also benefit from existing industries and supply chains. For example, UFOWTs could greatly benefit from the fact that many wind turbines are being manufactured and installed, so a supply chain already exists for manufacturing key parts of the system. Depending on the future growth of the floating wind industry this advantage may also be present for the floating platforms required for UFOWTs. Since MOWES designs are not site-specific they may also be mass-produced more easily than conventional OWTs and FOWTs. MOWESs do not use moorings and are not bottom-fixed so site water depth and seabed conditions are not relevant to their design. In addition, they may return to shore autonomously for maintenance whenever necessary, rather than dispatching crews to conduct maintenance. This is especially important for offshore systems, since servicing them would otherwise require travelling out to the systems by boat. Since MOWESs must return to shore to offload stored fuel/CO_2, necessary maintenance may be scheduled around these regular returns. The impact of MOWESs on wildlife and the environment is also an important consideration. From this standpoint, there is precedent for using large propellers in the open ocean, so this does not pose novel environmental challenges. Although direct environmental impacts of a MOWES are unknown, the mobility of the systems may allow them to avoid specific areas that are important for local wildlife at different times such as protected areas or migratory paths.

1.1.2 Why not MOWES?

By nature of being a novel concept, there are still many uncertainties about MOWESs that make their feasibility unknown. It will be key to understand the dynamics of any MOWES, since they would be subjected to harsh and stochastic wind and wave environments. As of yet, very little research exists on the dynamics of any given MOWES concept. Xu et al. simulated a UFOWT, where the thrusters are controlled to keep the system on station, subject to dynamic wave loading and steady winds [7]. In their study, the dynamic positioning system (DPS) was effective at stationkeeping the system, however, it consumed around 50% of the power generated by the wind

turbine under normal operation. UFOWT dynamics were also investigated by Willeke [29], who modelled a spar-type floating wind turbine with no propulsion system. Results of the study show that the turbine yaws out of the wind while in operation. This is due in large part to the gyroscopic force from the spinning wind turbine rotor, which causes a precession of the rotor; this is evidence that the yaw stiffness that is provided by the mooring system for a conventional floating wind turbine must also be achieved for UFOWTs by way of the propulsion system. In all studies thus far, MOWESs are considered to operate autonomously, despite the fact that there is little precedent for fully autonomous ships operating in the open ocean. There is growing interest in unmanned surface vehicles (USVs) for offshore operations, which may be useful for MOWESs both on the logistics side, and on providing precedent for larger unmanned vessels [35, 36]. However, regulations around autonomous shipping vessels are not yet fully developed by the International Maritime Organization (IMO) which would inhibit the deployment of full-scale MOWESs in the near-term [37].

Another flaw in the concept of MOWESs is that the process of producing green fuels requires several conversion steps, no matter the fuel, and each conversion step will have associated losses. Many of the conversion losses will be substantial, for example the combined efficiency of an electrolyser and fuel cell for H_2 round trip is only 43 % [38]. While battery energy storage has higher round-trip efficiency, popular battery technologies such as lithium-ion batteries have much lower energy density and specific energy than synthetic fuels [39, 33]. Since space and weight may be extremely limited for MOWESs, battery energy storage is not seen as a viable option unless the system is limited to very short trips (such as in [40]). Therefore more direct alternative solutions than green fuels may be more efficient, depending on their own efficiency. An example of where this rationale is applicable is in the case of substituting green fuels for fossil fuels in ship propulsion. Direct wind propulsion for ships is a viable alternative and has existed for millenia. It can equally be implemented to supply part of the propulsion (often referred to as wind-assisted propulsion) and can be used in conjunction with using less carbon intense fuels. Wind-assisted ship propulsion using Flettner rotors has been shown to reduce fuel consumption by up to 30% [6]. In addition, wind-propulsion may require significantly less infrastructure than green fuel usage, since the conversion process is more direct. An illustration of this example is shown in Figure 1.3.

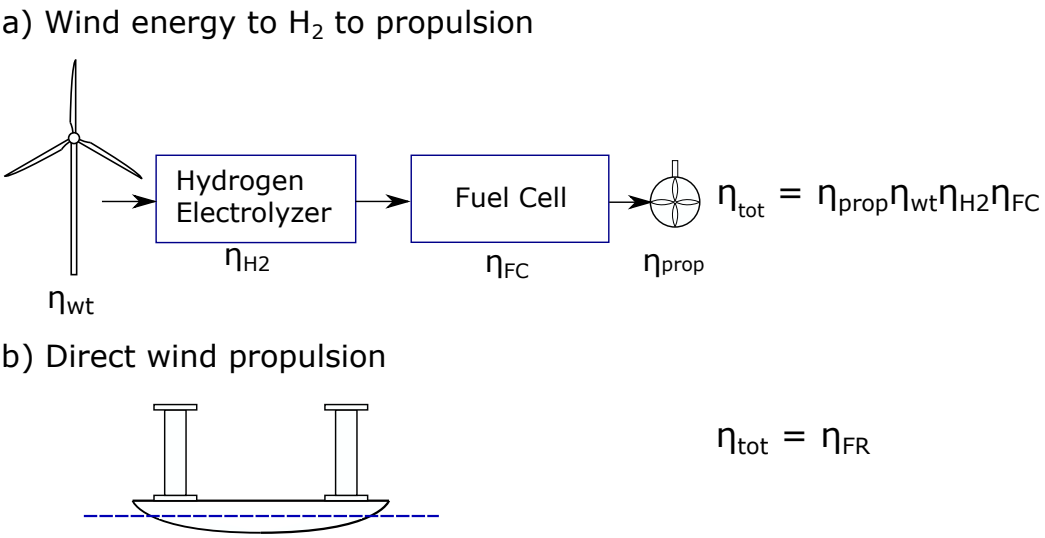

Figure 1.3: A comparison of complete process efficiency of green fuels from wind energy versus direct wind propulsion. The process in a) takes many conversion steps, whereas in b) wind is directly harnessed to propel the vessel

1.2 Research Questions

The overarching goal of this work is to help contribute to better understanding the two MOWES concepts mentioned. Since much work has already been done in modeling and analysis of ESs (see for example [4, 20]), the first focus of this work is developing a simplified first-principles model of an UFOWT to investigate key design and operation considerations. Most existing UFOWT research considers a station-keeping system, whereas theoretical results for flow-driven vehicles suggest that a mobile system may produce power more efficiently [32, 41]. The work of chapter 2 is to investigate two main research questions:

1. Is it beneficial for an UFOWT to move during operation rather than be station-kept? If so, should it move upwind or downwind?

2. How does the relative sizing of the wind turbine, propellers, and support structure affect the performance of an UFOWT?

Since no suitable model existed for investigating these questions, a one-dimensional steady-state UFOWT model was developed. Results of this model motivated the development of a more detailed two-dimensional model.

Ultimately, to be feasible the most important metric for a renewable energy technology is the levelized cost of energy (LCOE). Here, we will not estimate the LCOE

of these technologies, but make steps towards it. This may also be referred to in terms of the energy vector being produced, for example levelized cost of hydrogen (LCOH). LCOE is defined as the cost per unit energy produced by the system, usually in $\$/kWh$. It is used to estimate whether an energy project will be financially viable, since it can be directly compared to how much the energy can be sold for in electricity (or equally hydrogen or other) markets. Calculating the LCOE of a system requires knowing the costs of the system, and the expected energy production over a period of time, often the life of the system. For MOWESs, neither of these things are known to any precision. Indeed, to estimate the energy production of an MOWES requires first knowing the power performance of the system in it's possible operating conditions. This leads to the main research questions of Chapter 3:

3. How much power can each type of MOWES produce under any given set of environmental conditions?

4. What are the ideal operating conditions for each type of MOWES (both environmental and operational)?

5. Does one type of MOWES drastically outperform the other? If so, under what circumstances?

Power performance models of each MOWES type were developed to investigate these questions in a consistent framework. MOWESs were directly compared to one another and to conventional stationary wind turbines. Using the models and model results, design and operation aspects of the MOWESs have been investigated and are reported on in Chapter 3. The models are also suitable for further design studies, such as subsystem design-optimization.

1.3 Document structure

This dissertation follows a paper-based format. That is, the present work has been prepared and submitted as two journal papers and is therefore presented as two independent subjects in the chapters that follow. The complete structure of this thesis is as follows:

Chapter 2 Presents the development and analysis of a one-dimensional steady-state UFOWT model. Model results are used to examine the sensitivity of the power

performance to several system design aspects over a range of operational vessel speeds. This work concludes that UFOWTs can produce more power by moving relative to the wind, rather than attempting to hold station. This result motivated further development of the UFOWT model, to examine their operation in more detail.

Chapter 3 Develops a two-dimensional steady-state UFOWT model based on the model of chapter 2. The model makes improvements in modelling the wind turbine and thrusters, and an optimization method is employed to determine optimal operating points for the system. A similar energy ship model is revisited from existing literature [4], and is used to compare the two MOWES concepts in a consistent way. Results suggest that both technologies have relative merits, and both produce a reasonable amount of power compared to an established reference wind turbine design.

Chapter 4 Draws the main conclusions of the work and discusses how they are relevant to the development of MOWES in the future. What future work may be most useful in this space is also discussed at length.

Chapter 2

Analytical Modelling of Power Production from Un-moored Floating Offshore Wind Turbines

This paper is published in **Ocean Engineering** as of July 6, 2022:

Connolly, P., Crawford, C., 2022. Analytical modelling of power production from Un-moored Floating Offshore Wind Turbines. Ocean Engineering 259, 111794. https://doi.org/10.1016/j.oceaneng.2022.111794

CRediT contribution statement

Patrick Connolly: Conceptualization, Methodology, Software, Validation, Formal Analysis, Investigation, Visualization. **Curran Crawford:** Methodology, Resources, Writing - Review & Editing, Supervision, Funding Acquisition.

Abstract

To avoid the limitations of floating offshore wind turbines (FOWTs) in deep water, and with the increasing push for renewable power to X (PtX) systems, un-moored wind turbine concepts are now being considered. Un-moored floating offshore wind turbines (UFOWTs) are still in the conceptual design stage, but they represent a unique way of harnessing the abundant far-offshore wind resource in deep waters. We examine an UFOWT with bottom-mounted thrusters for station-keeping from an

analytic perspective. A one-dimensional steady-state analytical model is constructed to estimate the net power that can be extracted using such a system. Results of the model are consistent with existing literature in that a significant amount of power is lost to the thrusters for course-/station- keeping. Sensitivity of the net power to substructure design and relative size of the rotors is examined. Model predictions suggest that UFOWTs can produce more power by moving either upwind or downwind as opposed to remaining stationary. Optimal vessel speed and direction is also found to be sensitive to system design parameters. Although major concessions are made for the sake of model simplicity, the results serve to motivate and guide further modelling efforts for mobile wind energy systems (MWES).

2.1 Introduction

Wind energy systems (WESs) have advanced drastically in the last decades, as global efforts to decouple energy consumption and carbon emissions continue [42]. The offshore wind industry in particular is rapidly growing in recent years [43]. FOWTs have now been deployed at full-scale such as in the HyWind Scotland floating wind farm [44], however challenges still exist for further development. One such challenge is the relationship between mooring system cost and site water depth. Although FOWTs are more cost-efficient than fixed-bottom OWTs in deep waters, beyond depths of around 200 m the cost of the floating platform and mooring system becomes prohibitively large. Some cost-savings strategies have been proposed to alleviate this problem, including shared moorings and shared anchors [45, 46, 47]. Despite these other promising concepts, an alternative solution is examined here, namely FOWT systems that do not rely on moorings.

An Un-moored Floating Offshore Wind Turbine (UFOWT) is similar to a conventional FOWT, except it relies on a set of thrusters mounted on the sub-structure to position it under environmental loading (Figure 2.1). UFOWTs are also different in that they must store the generated renewable energy on-board, as opposed to relaying it to shore via electrical cables. This can be in the form of battery electric storage, or the energy could be used for a PtX process such as producing green hydrogen [48]. There is also potential to mount direct air carbon capture systems on-board the UFOWT and use the generated power to power the carbon capture process. Although an expensive pathway, this represents an avenue for UFOWTs to also contribute to negative emissions technology (NET) development. No matter the energy storage or

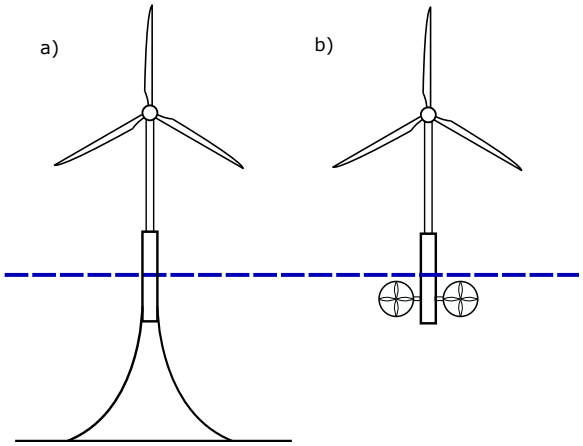

Figure 2.1: Conceptual diagram of a) FOWT b) UFOWT

utilization vector, the absence of mooring lines and power cables allows UFOWTs to be mobile and makes their cost independent of water depth. Mobility also allows them to navigate to locations with higher wind speeds, potentially greatly increasing their capacity factor relative to conventional FOWTs. Servicing UFOWTs may also be more convenient since they are able to return to port autonomously when necessary. Other mobile, far-offshore wind energy systems have been shown to be capable of producing green methanol at a competitive cost [4]. Given this result, there is potential for UFOWTs to also be viable in PtX applications, provided that they have a high enough efficiency.

Although the problem of mooring system costs and their scaling with water depth does not exist for UFOWTs, other challenges and downsides exist. The most major downside is that a fraction of the energy generated by the wind turbine must be used to power the thrusters for station-keeping. The energy, cost, and reliability of the thrusters are a potentially substantial trade-off for eliminating the mooring system. Although ultimately this trade-off may be best analysed through a comparison of costs over the lifetime of each system (FOWT and UFOWT), we must first fundamentally understand how much net power an UFOWT is capable of generating. The aim of this work is to provide a basis to this understanding, whereby the performance of different designs may be estimated and compared to conventional FOWTs.

In section 2.2, existing research into UFOWTs and relevant topics are summarized, and the goals of this work are outlined. Following this, the modelling method is described in section 2.3 and the results are presented in section 2.4, along with discussion of their implications. Section 2.5 concludes the paper with a summary of

major results.

2.2 Background

2.2.1 Existing Research

Although UFOWTs are still in the conceptual design phase, some studies have already focused specifically on them. Time-domain simulation work has been conducted for an UFOWT system by Xu et al. [7]. Their work analysed the dynamics as well as power produced by the system when subjected to dynamic waves and steady winds. A key result of their simulations is that 50-80% of the power generated by the wind turbine must be consumed by the thrusters for station-keeping. However, in their work the goal of the control system was to operate the thrusters in a way to keep the turbine and platform stationary. Herein we explore the possibility of allowing the system to move either directly upwind or downwind, motivated by existing flow-driven vehicle research [32, 41]. Another existing work on UFOWTs is that of Martinez Beseler [31]. In their work, they looked at the problems of system design and routing with some focus on different energy storage options. Other dynamic simulations for UFOWTs have been conducted, but without thrusters or any dedicated sub-system for station-keeping [29]. A spar-type platform was considered and it was found that large motions in pitch and yaw occur, confirming that thrusters (or another similar system) are necessary for an UFOWT. Attempts were made to redesign the spar platform to help in preventing excessive motions; although their attempts were unsuccessful, this elucidates the fact that conventional FOWT platforms are not necessarily optimally designed for UFOWTs. The design of each component of an UFOWT has also been looked at for a unique concept called Wind Trawler [30]. Wind Trawler differs slightly in that it uses hydro turbines in place of omni-directional thrusters to balance the thrust force, limiting it to down-wind operation. They ensure ideal operation by designing the hydro turbines such that they will achieve rated power when the wind turbines are also operating at rated conditions. Results show that Wind Trawler concepts can exceed the power produced by a stationary wind turbine in above-rated conditions as well as exceeding the capacity factor of conventional offshore wind turbines when operating far enough from shore.

Many other works are relevant to the UFOWT concept, although they do not specifically focus on it. Bøckmann and Steen investigated the design and use of wind

turbines mounted on shipping vessels to generate propulsive power[49]. They use a blade-element theory approach to design a uniquely optimized wind turbine rotor, raising the important point that stock wind turbines and thrusters are likely not ideal for mobile offshore operation. The rotor thrust and power generation characteristics should be specifically tailored for being mobile. A strong motivating factor for pursuing UFOWTs is their ability to be deployed far-offshore. It is well understood that in general available wind energy increases with distance from shore. This has been shown by Abd Jamil et al. [50, 40], where simulated stationary wind turbines achieved capacity factors of up to 80% in the north of the Atlantic Ocean. These capacity factors were calculated for the sake of comparison to another mobile wind energy system known as energy ships, which reached similar capacity factors. Energy ships are novel wind energy systems that use wind propulsion technologies such as Flettner rotors, rigid sails, or kites to propel a ship through open water [24, 51, 52]. Power is generated by hydro turbine(s) mounted on the bottom of the hull and is subsequently stored or used in a PtX process. In their work, they focused primarily on the problem of navigation for energy ships, a challenge which is also present for UFOWTs. Because UFOWTs are mobile, it will be essential for them to continuously navigate to areas of high wind speed, until it is time to unload the stored energy. An optimization approach to solving the routing problem was done by Abd Jamil et al. [50] for the energy ship case. The routing problem has also been examined by Tsujimoto et al. [53] for a sailing wind farm with many wind turbines and thrusters on a single platform. They achieve much lower capacity factors than the aforementioned energy ship results, however, the sailing wind farms were restricted to an area much nearer to shore than the area used for energy ship routing. Another challenge of energy ships is that to produce power they must move very fast, sometimes at the same speed as the wind [51]. This means the hull must be designed to have very low resistance. Some studies have also considered the use of hydrofoils to allow the energy ship to travel faster [27].

More generally, an UFOWT can be thought of as a specific type of flow-driven vehicle. Past work by Gaunaa et al. [32] focused on creating a general framework for analysing any vehicle that propels itself based on a difference in velocity between two "media". Their work is a strong motivator for this paper; we will draw frequently from their work and adopt many of their conventions. They used their framework to show several important results. Most relevant for this work is that a wind turbine may increase its net power output by using some power to propel itself upwind, given

that the energy conversion processes are efficient enough.

There is a growing interest in dedicated renewable PtX projects as the world looks at decarbonizing sectors beyond connected electrification [48, 54]. Some offshore wind to hydrogen projects are now being planned up to GW scale, such as the Asian Renewable Energy Hub project which is aiming for 16 GW of installed wind capacity alongside 10 GW of solar capacity [55]. Far-offshore wind energy systems are uniquely suited for PtX, since storing the energy onboard is necessary and the wind resource is much more abundant in the open ocean than near-shore[33]. UFOWTs and energy ship concepts are aligned in their objective, since they both look to produce green fuels from far-offshore wind energy. In a techno-economic analysis of energy ships, Babarit et al. state that "...the main cost driver [for hydrogen-producing energy ships] is the electricity cost aboard the wind energy converter." [33]. What this means for UFOWTs is that there may be equal avenues to bring produced green hydrogen to market competitively, so long as the barrier of producing power cheaply enough can be overcome.

2.2.2 Motivation and Objectives

The primary goal of this work is to provide fundamental insight into the viability of UFOWT systems. This requires a better understanding of the fundamental design questions for such a system. As a starting point, one-dimensional steady-state analytical models for UFOWTs are derived from momentum theory equations for a rotor. These expressions allow estimation of steady-state operating points in terms of how the thrusters must operate to station-/course-keep an UFOWT. In turn, this allows estimation of the power produced by the wind turbine and also the power consumed by the thrusters. Several design variables are present in the models and are examined in a sensitivity analysis later (Section 2.4.2). Results of the sensitivity analysis, and the models themselves, serve to aid future design and analysis of UFOWTs.

2.3 Methodology

Consider an UFOWT system in open water in 1-dimension (Figure 2.2). All forces and velocities are aligned with the surge direction and are defined positive to the right. We refer to the wind/air as medium 1 with velocity V_1, and refer to the water as medium 2 moving with velocity V_2 relative to an earth-fixed inertial reference

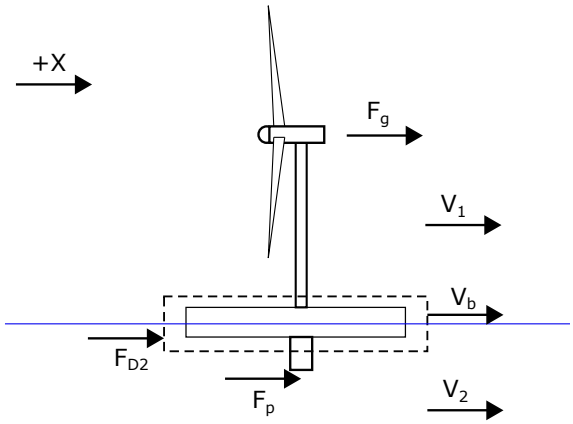

Figure 2.2: Vector diagram describing velocities and forces on a UFOWT

frame. Direction conventions are shown in (Figure 2.2). Relevant properties of the media (i.e density ρ) are labelled similarly, as well as the capture areas of the rotors in each medium (i.e A_1). The velocity of the UFOWT itself is labelled V_b, and referred to as vessel or body speed. For convenience, the velocity of each medium relative to the body is also defined as V_1' and V_2', respectively:

$$V_1' = V_1 - V_b \tag{2.1}$$

$$V_2' = V_2 - V_b \tag{2.2}$$

The vessel speed as a fraction of the wind speed (V_b/V_1) will be frequently used as a non-dimensional variable. Here, a positive wind speed means that the wind is flowing from the -x direction to the +x direction (i.e mass flow is to the right). By convention then, a UFOWT is moving downwind when $V_b/V_1 > 0$ and is moving upwind when $V_b/V_1 < 0$. This is counter to conventions for sailing vessels such as those used in [24, 56, 57].

In labelling the forces acting on the UFOWT, we adopt the convention of Gaunaa et al.[32] wherein the force from the generation system (i.e the wind turbine) is referred to as (F_g) and the force from the propulsion system (i.e thrusters) is referred to as (F_p). A quadratic drag force (F_{d2}) with a non-dimensional coefficient (C_{d2}) is also included for the platform/sub-structure as it moves through the water (equation 2.5). A quadratic air drag force would also be present, however, it is assumed to be negligible compared to the water drag term in most cases and so is excluded. Actuator

disk theory results are used to represent the force on the rotor disk for both the wind turbine and the thrusters (equations 2.3 and 2.4, respectively) [58]. A constant thrust coefficient (C_{t1}) is assumed for the wind turbine thrust All forces are calculated in a body-fixed reference frame. This is the only reference frame where the actuator disc theory results can be applied directly, since they rely on the Bernoulli equation which is not invariant to Galilean transformations[59]. This means equations 2.3 and 2.4 cannot be simply applied in another reference frame (i.e earth fixed frame) by replacing the velocities with the appropriate ones for that frame. The velocity downstream from the thruster in the UFOWT-fixed reference frame ($V'_{p,out}$) is used as a control variable to ensure that steady-state operation is achieved. The choice to use this downstream velocity as a proxy control variable is made both for convenience of future calculations and to keep the formulation reliant only on general momentum theory. Forces are formulated to match the sign convention in Figure 2.2.

$$F_g = \frac{1}{2}\rho_1 A_1(V'_1)|V'_1|C_{t1} \tag{2.3}$$

$$F_p = \frac{1}{2}\rho_2 A_2(V'_2 - V'_{p,out})(V'_2 + V'_{p,out}) = -\frac{1}{2}\rho_2 A_2(V'_{p,out} + V_b)(V'_{p,out} - V_b) \tag{2.4}$$

$$F_{d2} = \frac{1}{2}\rho_2 C_{d2} A_{d2}(V'_2)|V'_2| = -\frac{1}{2}\rho_2 C_{d2} A_{d2}(V_b)|V_b| \tag{2.5}$$

To limit the equation to one variable, the simplifying assumption that $V_2 = 0$ has been made in equations 2.4 and 2.5 (and later 2.7). This is equivalent to assuming no current in the water. It was shown in [7] that current force can drastically reduce the net power output of an UFOWT when current and wind are co-directed. Methods and results for power produced from this model with $V_2 \neq 0$ are presented separately in sections 2.3.1 and 2.4.3 respectively. In all other results, current is neglected.

Next, the associated power for each sub-system is introduced in equations 2.6 and 2.7: the power generated by the wind turbine (P_g) and the power consumed to run the thrusters (P_p). Though not directly included when summing the powers, the propulsive power which is necessary to overcome the drag on the structure is inherently accounted for through the other terms. For example, when moving upwind the thrusters must produce enough thrust force to counter-balance the drag on the structure. This requires a relative increase in power consumed. In the downwind case

the drag allows for a relative decrease in power consumption, owing to the fact that the drag is acting to counter-balance the wind turbine thrust. Only electrical power is of interest, since ultimately the objective is to calculate the net power output that can be used for storage or fuel synthesis. Also introduced are associated efficiencies for the generation system (η_g) and for the propulsion system (η_p), respectively.

$$P_g = F_g V_1' \eta_g = \frac{1}{2}\rho_1 A_1 (V_1')^3 C_{p1} \tag{2.6}$$

$$P_p = \frac{F_p}{\eta_p}\frac{\left(V_2' + V_{p,out}'\right)}{2} = -\frac{1}{4\eta_p}\rho_2 A_2 (V_{p,out}' + V_b)(V_{p,out}' - V_b)^2 \tag{2.7}$$

The aim is to model an UFOWT system and its power production in steady-state conditions. This means ensuring that the net force on the system is zero (equation 2.8).

$$\sum F = F_g + F_p + F_{d1} + F_{d2} = 0 \tag{2.8}$$

Using the steady-state equation as a constraint, the required output velocity of the thrusters ($V_{p,out}'$) is directly solved for:

$$\frac{V_{p,out}'}{V_1} = +\sqrt{\left(\frac{V_b}{V_1}\right)^2 + \frac{\rho_1}{\rho_2}\left(1 - \frac{V_b}{V_1}\right)\left|1 - \frac{V_b}{V_1}\right|\left[\frac{A_1}{A_2}C_{t1} + \frac{A_{d1}}{A_2}C_{d1}\right] - \frac{A_{d2}}{A_2}C_{d2}\left(\frac{V_b}{V_1}\right)\left|\frac{V_b}{V_1}\right|} \tag{2.9}$$

Equation 2.9 for $V_{p,out}'/V_1$ can in principle lead to a complex valued result when the water drag area and/or coefficient are sufficiently large. To avoid this, a rule is adopted for flipping the propeller 180° in yaw, or identically operating the propeller in reverse. Doing this flips the direction, and therefore also the sign, of the propulsive force such that another expression for $V_{p,out}'/V_1$ can be derived for reverse operation:

$$\frac{V_{p,out}'}{V_1} = -\sqrt{\left(\frac{V_b}{V_1}\right)^2 - \frac{\rho_1}{\rho_2}\left(1 - \frac{V_b}{V_1}\right)\left|1 - \frac{V_b}{V_1}\right|\left[\frac{A_1}{A_2}C_{t1} + \frac{A_{d1}}{A_2}C_{d1}\right] + \frac{A_{d2}}{A_2}C_{d2}\left(\frac{V_b}{V_1}\right)\left|\frac{V_b}{V_1}\right|} \tag{2.10}$$

Two things are taken into account to see if the propeller should operate normally (facing upwind) or reversed (facing downwind). Firstly, the direction the UFOWT is travelling is considered. If it is travelling upwind (i.e $V_b/V_1 < 0$), then the propeller must face upwind, since both the drag on the platform and the thrust on the wind

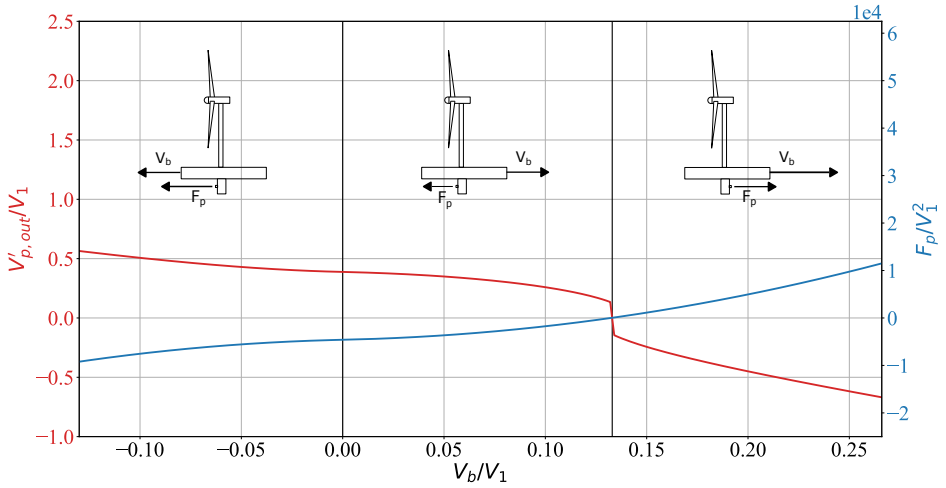

Figure 2.3: Direction of propulsive force, and propeller output velocity

turbine must be opposed by the propeller. In downwind operation, the propeller operates facing upwind so long as: $V_b/V_1 < V'_{p,out}/V_1$. In other words, as V_b/V_1 increases, the propeller chooses to flip operation at the point where it is not acting on the flow $\left(V_b/V_1 = V'_{p,out}/V_1\right)$. This is of course also the point where the propulsive force is exactly zero; the thrust force on the wind turbine is exactly equalled out by the drag on the substructure. Figure 2.3 shows an example of the operation of the UFOWT. It is also worth highlighting that the second (middle) region in Figure 2.3 is the operating range for concepts like WindTrawler [30]. In this region, hydro-turbines could be used in place of a propeller to balance out the other forces, which could of course lead to more power generation. This could also be achieved by using thrusters which are able to double as hydroturbines.

Choosing to operate the propeller in this way may lead to some unique considerations. A real control system for such an UFOWT would need significant safety range around the reversal point, since the propeller either needs to yaw 180°, reverse the direction the blades are spinning, or pitch the propeller blades. There may also be considerations around operating the propeller in negative inflow, sometimes referred to as thrust reversal or astern propulsion (middle region of Figure 2.3). Existing research suggests that propellers can operate safely at some small negative advance ratios, but at larger (i.e more negative) advance ratios the behaviour of the propeller becomes unpredictable [60]. Herein the generous assumption is made that momentum theory remains valid in this case, however, care should be taken when interpreting

results around negative inflows.

Equations 2.9 and 2.10 are non-dimensionalized by the wind speed (V_1). Using this non-dimensional form allows values to be more easily interpreted independent of a specific system design. It is also in line with how the upcoming non-dimensional equations for power are presented.

Next, the net power output from the UFOWT system is derived. Here, the net power P_{net} is considered as the power generated by the wind turbine (P_g) minus the power which is consumed by the thrusters for station-keeping (P_p), assuming there is some transmission efficiency (η_t):

$$P_{net} = P_g - \frac{P_p}{\eta_t}$$

For comparison, the power available to a conventional stationary wind turbine (P_1) is defined as:

$$P_1 = \frac{1}{2}\rho_1 A_1 V_1^3 C_{p1}$$

Then a metric to compare between UFOWT and conventional wind turbines must be defined. Here, the power output of an UFOWT as a fraction of the power available to a stationary wind turbine is defined as $C_{p,net}$, and can be expressed as follows in equation 2.11.

$$C_{p,net} = \frac{P_g - \frac{P_p}{\eta_t}}{P_1} = \frac{P_g - \frac{P_p}{\eta_t}}{\frac{1}{2}\rho_1 A_1 V_1^3 C_{p1}}$$

$$C_{p,net} = \left(1 - \frac{V_b}{V_1}\right)^3 \mp \frac{\rho_2 A_2}{\rho_1 A_1}\frac{1}{2\eta}\left(\frac{V'_{p,out}}{V_1} - \frac{V_b}{V_1}\right)^2\left(\frac{V'_{p,out}}{V_1} + \frac{V_b}{V_1}\right) \tag{2.11}$$

where the sign of the second term is determined by the direction that the thruster is facing. Referring to Figure 2.3, the sign is negative in the left and center regions, but becomes positive in the right region. Noting also that η is defined in equation 2.11 for convenience as:

$$\eta = \frac{1}{\eta_g \eta_p \eta_t} = \frac{C_{t1}}{C_{p1}\eta_p \eta_t}$$

Another metric used to compare across models is the power ratio (R_p). This is defined as the ratio of the power consumed by the thrusters to the power generated by the wind turbine i.e:

$$R_p = \frac{P_p}{P_g} \tag{2.12}$$

This was used in [7] and will also be used here since it is not directly scale/size-

dependent.

2.3.1 Model for Non-Zero Currents

Equations for $V'_{p,out}/V_1$ for the case where $V_2 \neq 0$ will be different from those of equations 2.9 and 2.10. This is owing to the fact that V_2 cannot be excluded from equations 2.4 and 2.5. Equations including currents are derived by the same process as was done for the $V_2 = 0$ and are shown below in equations 2.13 and 2.14 for normal and reversed orientations respectively.

$$\frac{V'_{p,out}}{V_1} = +\sqrt{\left(\frac{V'_2}{V_1}\right)^2 + \frac{\rho_1}{\rho_2}\left(1 - \frac{V_b}{V_1}\right)\left|1 - \frac{V_b}{V_1}\right|\left[\frac{A_1}{A_2}C_{t1} + \frac{A_{d1}}{A_2}C_{d1}\right] + \frac{A_{d2}}{A_2}C_{d2}\left(\frac{V'_2}{V_1}\right)\left|\frac{V'_2}{V_1}\right|} \tag{2.13}$$

$$\frac{V'_{p,out}}{V_1} = -\sqrt{\left(\frac{V'_2}{V_1}\right)^2 - \frac{\rho_1}{\rho_2}\left(1 - \frac{V_b}{V_1}\right)\left|1 - \frac{V_b}{V_1}\right|\left[\frac{A_1}{A_2}C_{t1} + \frac{A_{d1}}{A_2}C_{d1}\right] - \frac{A_{d2}}{A_2}C_{d2}\left(\frac{V'_2}{V_1}\right)\left|\frac{V'_2}{V_1}\right|} \tag{2.14}$$

Similarly, the result for $C_{p,net}$ when $V_2 \neq 0$ is different from the no current case and is shown in equation 2.15 for the same direction convention of equation 2.11.

$$C_{p,net} = \left(1 - \frac{V_b}{V_1}\right)^3 \mp \frac{\rho_2 A_2}{\rho_1 A_1}\frac{1}{2\eta}\left(\frac{V'_2}{V_1} + \frac{V'_{p,out}}{V_1}\right)^2\left(\frac{V'_2}{V_1} - \frac{V'_{p,out}}{V_1}\right) \tag{2.15}$$

2.4 Results and Discussion

2.4.1 Verification

For the purpose of verification, and for further analysis, the UFOWT design of Xu et al. will be used [7]. A set of design parameters are listed to define the system in Table 2.1. Data for wind turbine radius, thruster radius, and number of thrusters are taken directly from [7]. The efficiency of the thrusters is assumed constant at 40% for this work, roughly the average efficiency of the thrusters used. To estimate the drag on the substructure the quadratic drag coefficient for the NREL semi-submersible platform is used [61], noting that $B_{d2} = C_{d2}A_{d2}\rho_2$.

Figure 2.4 shows verification of power ratio results for the model presented here

against the results from Xu et al. [7]. Figures 2.4a and 2.4b show the variation of power ratio with the size of each rotor disk. Results mostly agree, although Figure 2.4a has a roughly constant offset, whereas in Figure 2.4b the slope is slightly too large. These discrepancies are likely owing to model differences, such as varying propeller efficiency and accounting for wave force. More generally, the relationship between the ratio of the rotor sizes (A_2/A_1) to power ratio is shown in Figure 2.4c. This shows generally good agreement between the results of this model and those of Xu et al.[7], noting that only the $V_b = 0$ case was considered in that work. It can be seen that for area ratios around 1% and below, the power ratio becomes extremely sensitive to area ratio. Also shown in Figure 2.4c is the power ratio for the maximum achievable power when the UFOWT is not restricted to remaining stationary, as was assumed by Xu et al.. The jump in power ratio occurs when the preferred direction of operation of the UFOWT changes between upwind and downwind, this is further explained in Figure 2.7a. The flaw of power ratio as a metric in the context of a mobile turbine is that minimizing power ratio does not always correspond to maximizing the net power output of the system. This is further discussed below with regards to Figure 2.7b.

	Unit	Value
Wind turbine		
r_g	m	60
C_{p1}	-	0.52
C_{t1}	-	0.664
Thrusters		
r_p	m	1.8
n_p	-	4
η_p	-	0.4
η_t	-	1.0
Sub-structure		
A_{d1}	m^2	0
B_{d2}	Ns^2/m^2	$3.95E5$
C_{d1}	-	0
C_{d2}	-	1

Table 2.1: Parameters to define the UFOWT system used for verification

2.4.2 Sensitivity Analysis

An UFOWT system is an amalgamation of several existing sub-systems, each of which has been historically optimized within a different context. As a preliminary step for designing an UFOWT system, we examine the sensitivity of the results to several design parameters present in the model:

- Relative area of thruster rotor(s) to the wind turbine rotor (A_2/A_1)
- Hull drag area relative to the swept area of the wind turbine rotor ($A_{d2}C_{d2}/A_1$)

Better understanding of these parameters will help in the preliminary design steps

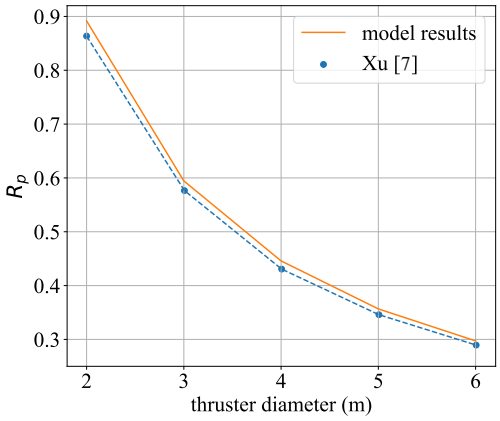

(a) Varying A_2

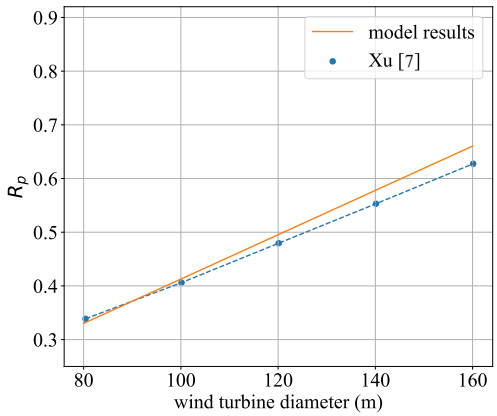

(b) Varying A_1

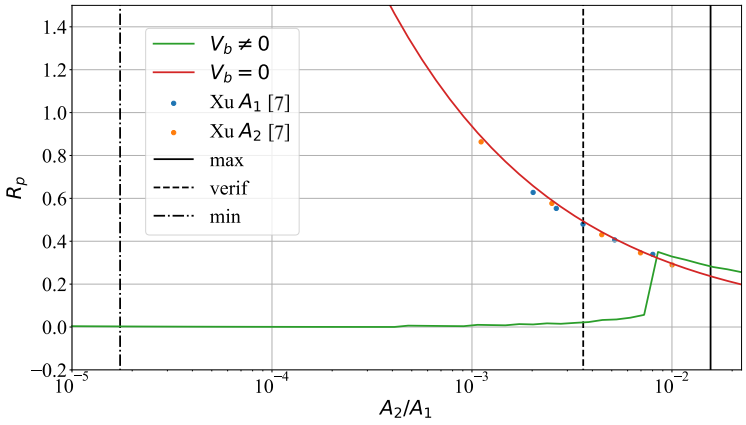

(c) Varying $\frac{A_2}{A_1}$, larger scale

Figure 2.4: Verification of R_p results compared to those of Xu [7], noting Xu only considered the case of $V_b = 0$

of UFOWTs. For example, the rotor area ratio (i.e A_2/A_1) and power extraction is vital to understand since ultimately a choice of wind turbine and thruster sizes are core design choices of an UFOWT.

The relative amount of drag on an UFOWT is also of great importance. Here the quantity $A_{d2}C_{d2}/A_1$ will be analysed, since it is representative of how much drag force there will be on the platform at a given speed. It is referred to hereafter as drag area or drag area ratio for convenience. Drastically different amounts of drag are possible for varying UFOWT designs. For example, a design which uses a semi-submersible platform will have a much larger drag than one which uses a stream-lined ship hull as the base. Consequently, the optimal operating speed of each will be significantly different. Drag area will be examined over a large range (several orders of magnitude) to cover the large possible design space. This is also the case for rotor area ratios, since various sizes of wind turbines and thrusters exist from different contexts. These can range from small, commercially available thrusters used in dynamic positioning systems, to large propellers for cargo ships, or even massive tidal energy turbines.

Operation and efficiency of an UFOWT is much more complicated than is represented in this model. Realistically, each rotor (wind turbine and thruster) will have operational curves, and for the UFOWT system to operate optimally these curves should be designed in tandem. The optimization of the rotors and their operation is beyond the scope of this work, however, it is an essential problem for the design of UFOWTs in the future. Here, the assumption is made that the wind turbine is operating at a point in region II (i.e below rated power) corresponding to the thrust and power coefficients listed in Table 2.1.

First, the range of possible rotor and drag area ratios for the sensitivity analysis will be defined. Data used for calculating the bounds of the sensitivity analysis are listed in Tables 2.2, 2.3, and 2.4. The bounds are listed in Table 2.5 and are not the exact upper and lower limits calculated from values in the other tables, but are instead rounded up or down to the nearest order of magnitude to encompass a wider design range. Since the estimates of extreme values for subsystem sizes are all taken from different contexts, it is prudent to allow some range on either side of these estimates. Commercial offshore wind turbines range from between 2 and 15 MW, with respective rotor diameters of 80 to 240 m. Also referenced is the turbine design from Xu et al., very similar in size to the NREL 5 MW reference turbine [7, 62]. Smaller wind turbines are of course possible, but we do not consider them here since they are not typically used offshore. Reference points for the substructure come from

FOWT and energy ship designs. A streamlined Wigley hull form (like the one used in [24]) is used to represent a low drag scenario. The NREL semi-submersible platform (studied in OC4 [61]), and the NREL spar platform (studied in [63]) are considered as examples of high drag substructures. These platforms are chosen because they are commonly referenced; they do not necessarily represent an ideal choice of platform for this application. It is also noted here that there are no constraints on relative size of components other than using their extreme values as bounds. Realistic design constraints, such as neutral buoyancy of the system, are omitted at this point.

Figure 2.5 shows various operational curves ($C_{p,net}$ vs. (V_b/V_1)) for different rotor area ratios. This shows for an UFOWT operating optimally how much power it can produce relative to a stationary wind turbine, over a range of possible vessel to wind speed ratios. Plotted in Figure 2.5 are the results for the calculated upper and lower bound designs , the design of Xu et al., as labelled in Table 2.5. Other rotor area ratios in between and just outside the bounds are also shown for the sake of completeness. It shows that an increase in thruster size, or a proportional decrease in turbine size, gives an increase in net power output, exactly the result which was used for verification above. Recalling that this power output is a fraction of the power a stationary turbine of the same size would generate, the maximum achievable power in the designs considered is 78% (excluding the design shown in Figure 2.5 that is outside of the considered bounds). Increasing rotor area ratio also has the effect of widening the range of possible operating speeds. Widening this range is useful for ensuring that the UFOWT achieves a high capacity factor, since it will likely need to operate at many different vessel speeds and directions while at sea. The degree to which this is important is impossible to know without further analysis involving

	$r(m)$	$A_1(m^2)$	source
max	120	45200	[1]
verif	60	11300	[7]
min	40	5030	[64]

Table 2.2: Wind turbine size bounds

	$r(m)$	n	$A_2(m^2)$	source
max	5	1	78.5	[65]
verif	1.8	4	40.87	[7]
min	0.5	1	0.785	[66]

Table 2.3: Thruster size bounds

	$A_{d2}C_{d2}(m^2)$	source
max	677	[63]
verif	385	[61]
min	4.94	[24]

Table 2.4: Substructure drag bounds

Name	Min	Verif	Max
$\frac{A_2}{A_1}$	1.00E-5	3.6E-3	2.00E-2
$\frac{A_{d2}C_{d2}}{A_1}$	1.00E-4	3.41E-2	2.00E-1

Table 2.5: Sensitivity analysis bounds.

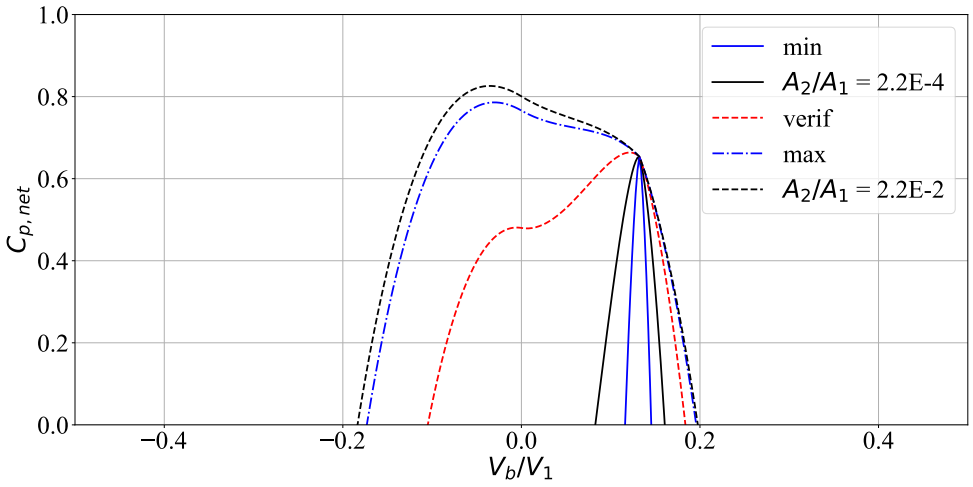

Figure 2.5: Performance of UFOWTs with varying rotor area ratios

routing and environmental conditions. Also shown is that with increasing rotor area ratio, the ideal operating speed for the UFOWT decreases; this is further discussed later with respect to Figure 2.7.

The amount of drag on the substructure is examined in Figure 2.6. It shows several operation curves for different ratios of drag area to wind turbine capture area. Higher drag tends to tighten the operational range, meaning the UFOWT may perform better in perfect conditions, lower drag expands the range an UFOWT could operate over at many different vessel speeds. This again stresses the importance of further work into the routing of UFOWTs.

Some insights into better UFOWT design can be drawn from the relationships seen above. Namely, it has been shown that a decrease in the drag area ratio widens the operational profile and strongly favours upwind operation. This is consistent with intuition, lowering drag reduces the force required by the thrusters to achieve steady-state in all upwind situations. This results in a net reduction in power consumed by the thrusters. In a similar vein, an increase in thruster area ratio has the same effect of widening and shifting the optimal speed more negative. This suggests that an UFOWT designed to operate moving upwind should minimize the drag area ratio and maximize the thruster area ratio, while one designed to operate moving downwind should maximize drag area ratio and the rotor area ratio can be minimized.

Figure 2.7a shows the relationship between rotor area ratio and net power output more directly. It clearly shows the advantage of allowing the UFOWT to be mobile.

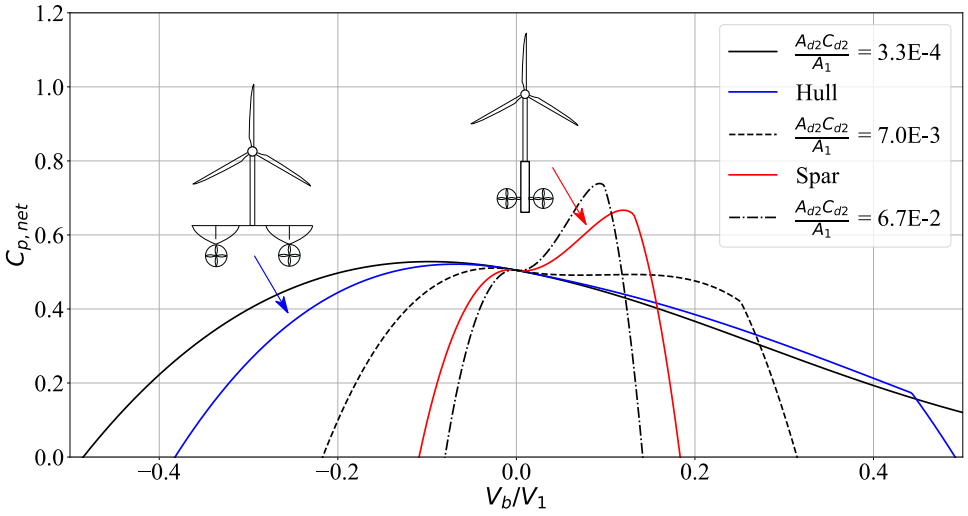

Figure 2.6: Performance of UFOWTs with varying drag area ratios. Representative spar and hull designs shown

For all area ratios, the UFOWT is able to produce a higher net power when allowed to be mobile and operating at its ideal speed, compared to remaining stationary. This is most pronounced at very small area ratios where downwind operation dominates. It is shown that the design of Xu et al. could benefit in terms of power output from operating in downwind motion. The model estimates that the power could be increased for this design by up to 13% by allowing it to be mobile. It is shown again in Figure 2.7b that a lower power ratio does not always correspond to a higher net power output for a mobile UFOWT. The net power always increases with increasing area ratio, however, above around $A_2/A_1 = 1\%$ the power ratio increases drastically. This comes about because the UFOWT's optimal operating direction (i.e upwind or downwind) changes at this point. We can see that above $A_2/A_1 = 1\%$ the preferred direction is upwind. Upwind operation will always require more power consumed by the thrusters, since they must overcome the drag and wind turbine thrust forces. It will be important in UFOWT design to decide whether the principle operating mode will be upwind or downwind, and to design the system accordingly.

Performance of UFOWT designs with varying drag area are examined in Figure 2.8, keeping in mind that these results are for the specific propeller size in Table 2.1. Some representative examples of drag area ratios from Table 2.4 are shown in Figure 2.8 as vertical lines, each of which is taken relative to a wind turbine rotor diameter

of 120 m as was used in [7]. It is again shown in Figure 2.8a that power production of UFOWTs is always greater when the system is able to move. For all drag area ratios there is a non-zero operating speed for which the vessel has a net increase in power compared to remaining stationary. It is also shown that the optimal operating speed for the vessel never exceeds 20% of the wind speed, or equally the optimal V_b/V_1 never exceeds 0.2. This is significant when considering the routing of a UFOWT; existing research into energy ships suggests that they will routinely operate at speeds of 50-

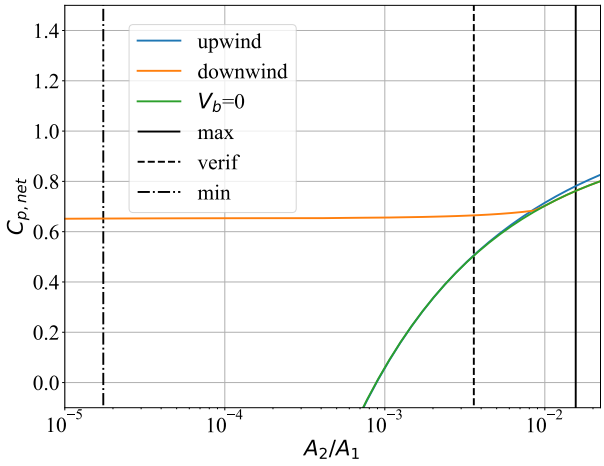

(a) stationary, upwind, and downwind operation

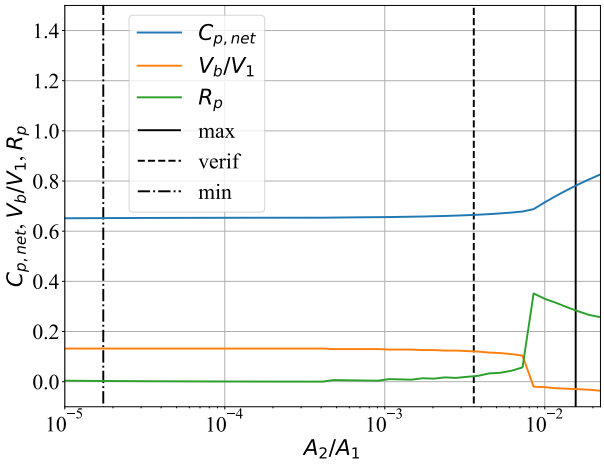

(b) Max $C_{p,net}$, and the corresponding $\frac{V_b}{V_1}$ and R_p

Figure 2.7: Comparison of optimal mobile and stationary UFOWT operation for varying $\frac{A_2}{A_1}$

100% of the wind speed [24]. An implication of this is that for the same time spent at sea, a UFOWT will travel much less distance than an energy ship assuming they are both operating near ideally. Future studies into how these two concepts differ in routing should explore these differences further.

Figure 2.8b shows how drag area ratio has an impact on the preferred direction of operation, upwind or downwind. For relatively low drag situations, such as the hull example, it is preferable to operate moving upwind. The advantage of the hull is that it provides significantly less resistance compared to a typical platform, meaning it requires less effort for the UFOWT to move upwind. Platform type substructures provide significantly more resistance and so designs using these perform best operating moving downwind. In the downwind case, the added drag is an asset, as it helps to counter-balance the thrust force of the wind turbine without directly consuming power.

2.4.3 Non-Zero Currents

Here, results for the model are presented for cases with non-zero current (i.e $V_2 \neq 0$). All results presented are for the verification design described in table 2.1. Figure 2.9 shows how co-directed wind and current result in decreasing net power, but also shows how contra-directed wind and current flows may result in higher net power. This figure looks specifically at the case where $V_b/V_1 = 0$, however, this is generally true for a mobile UFOWT also (as shown in Figure 2.10). It may be possible to strategically navigate UFOWTs through areas with contra-directed wind and currents to increase their power output. However, it is expected that the more common situation will be roughly co-directed wind and current, since ocean surface currents in areas far offshore are largely driven by wind stress [67]. For this reason, exploitation of contra-directed wind and currents for power increase may be difficult. Furthermore, average current speeds far offshore are estimated to be on the range of 1-3% of the wind speed by existing standards and data [68, 67]. A more detailed look at sites where ocean surface currents and wind are often contra-directed would be required to exploit this.

Results presented in Figure 2.9 can be compared with those of Xu et al. for their simulated load case at rated wind speed (labelled as "Xu LC"). Their load case uses a wind speed of 11.2 m/s and a current speed of 1 m/s, corresponding to $V_2/V_1 = 0.89$. For this load case they calculate an average power ratio of 0.8, whereas the present model predicts a power ratio of roughly 0.92. Since the models

differ greatly in their representation of the thrusters, a discrepancy in results is not unexpected. Investigation of these implications is left for future work.

Figure 2.10 shows how constant current speeds change the operating profile of the UFOWT. It can be seen that not only does the net power decrease for co-directed wind and currents, but the preferred operating speed also shifts. In situations with current, UFOWTs being mobile is again a great advantage. As current increases, for the given design the optimal operating speed shifts further from $V_b/V_1 = 0$. This may

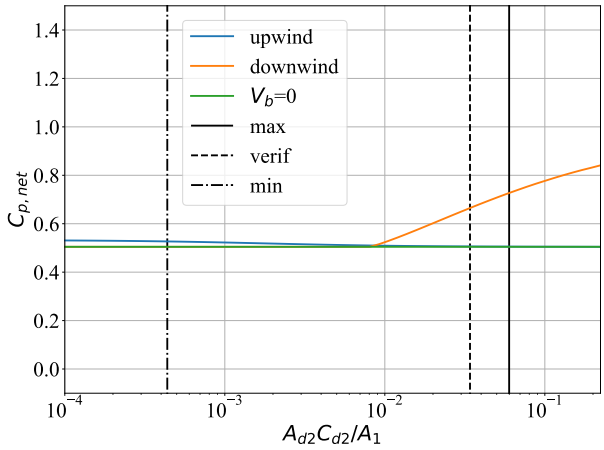

(a) stationary, upwind, and downwind operation

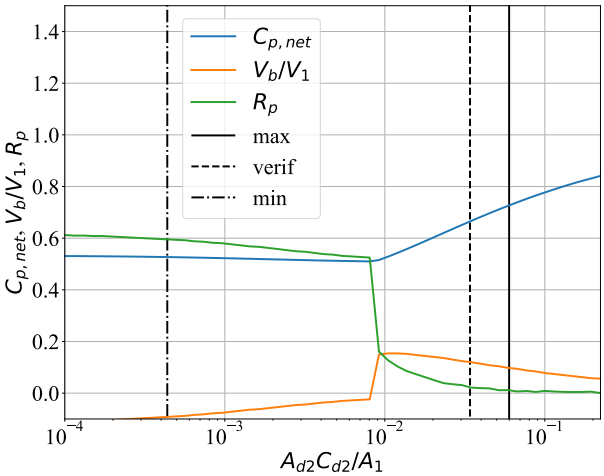

(b) Max $C_{p,net}$, and the corresponding $\frac{V_b}{V_1}$ and R_p

Figure 2.8: Comparison of optimal mobile and stationary UFOWT operation for varying $\frac{A_{d2}C_{d2}}{A_1}$

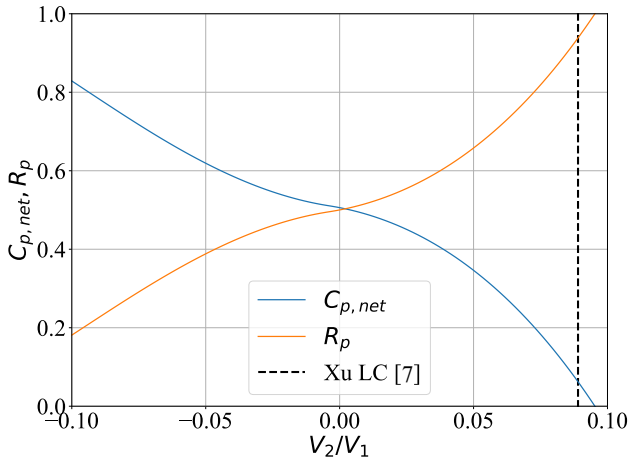

Figure 2.9: $C_{p,net}$ and R_p for $\frac{V_b}{V_1} = 0$

also play a part in how best to design UFOWTs, however, the design implications are unclear at this point.

2.4.4 Model Assumptions

Many assumptions have been made to keep our UFOWT model lightweight; these major assumptions are discussed below. The fact that UFOWTs are designed for operation at sea is largely neglected in this work by the omission of current and wave forces. Only the water drag is represented by the model. These other forces would affect the net force in both steady-state and dynamic conditions, thus changing the power performance of the system. The performance of a UFOWT under fully dynamic environmental conditions is unknown. Low-fidelity modelling was deemed more suitable for this preliminary design study, but a full aero-hydro-servo-elastic simulation study of a UFOWT will be necessary in the future to understand how the system responds under these conditions. By verifying the results of the model against existing results for the dynamics of an UFOWT [7] which does include wave and current forces, some certainty about the quality of the results is gained. As well, by investigating a single design in cases with currents, we gain some insight into the more general case. Although net power output decreases with co-directed wind and current, this effect is partially mitigated when a mobile UFOWT is considered as opposed to a stationary one. The model is also limited to one-dimension, meaning only direct upwind and downwind operation are considered. It is expected that operating

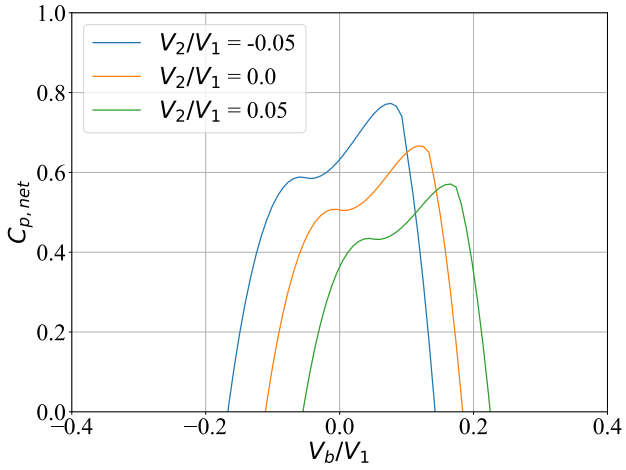

Figure 2.10: $C_{p,net}$ for several choices of V_2/V_1

directly upwind or downwind with perfect yaw represents the best case scenario for producing power for an UFOWT, since the wind turbine will be producing as much power as possible. Despite this, there will be cases where an UFOWT must operate differently (i.e not moving parallel to the wind direction) and these cases warrant investigation. These non-aligned cases will be analyzed and presented in future work.

In examining the sensitivity of power output to UFOWT drag area, we have concerned ourselves with the design of the substructure, but effective drag is not the sole (or even the main) purpose of the substructure. Here, no concern has been given to the moments on the system, steady or dynamic, which in a conventional FOWT are counteracted by the platform and mooring system. As previously mentioned, there is also no consideration to the buoyancy of the system. These are major aspects of designing the substructure and need to be considered in the future. An UFOWT in motion may have very large pitching and rolling moments, even in steady-state, owing to the fact that the wind turbine thrust force and propeller thrust force may both contribute pitching moments in the same direction (as would be the case for the left and center regions of Figure 2.3). This must be considered in the initial design by spacing the propellers such that this is not an issue. Another design consideration is the operation of the wind turbine and propellers. In this work, it is assumed that the wind turbine operates near ideally for any given vessel speed. This completely neglects the fact that a wind turbine has operational curves in terms of thrust force and power output. Also neglected is that the design of the rotors should be specially

tailored to UFOWTs. This is owing to the inherent trade-off between increasing the power generated by the wind turbine and increasing the thrust, as would be the case for a wind turbine operating in region II. When the wind turbine thrust force is increased, the thrusters must also generate more thrust to counter-balance it, and therefore will consume more power. The design and operation of the wind turbine and thruster rotors in view of this trade-off is left for future work. We have only examined the design of an UFOWT system at a point near rated power production; the operation of the wind turbine (and also the propeller) need to be considered in more detail.

No consideration has been given in this model to the energy storage system or PtX system, which is necessary for UFOWTs. Results of our model are the electrical power that would then be either used to charge batteries or to power a PtX process (such as [54, 69, 70]). No matter the storage system chosen, there will be some associated power losses from the efficiency of the process. Power estimates of the model are therefore likely over-estimations of the usable power from an UFOWT system as a whole.

2.5 Conclusions

In an attempt to assess the viability in terms of power performance of UFOWT systems, a simple steady-state power estimation model was developed. Establishing this model sets the foundation for understanding UFOWTs and how they should best be designed. The model is developed completely analytically, making for easy computation of results and analysis of different designs. Model results were verified against existing simulation results from Xu et al. [7] and show only small discrepancies, despite major differences in model fidelity. A main modelling difference which may cause these discrepancies is that this work does not consider any wave or current loading on the system in the sensitivity analysis. Although this is a shortcoming of the model, there is merit to using this simple model as a first step in design, as long as the many assumptions made are kept in mind. The model predicts that within the narrow section of the design space analysed, mobile UFOWTs can produce up to 78% of the power of a stationary wind turbine.

A first glimpse into the massive design space of UFOWTs is made through a sensitivity analysis. Model parameters of non-dimensional thruster area and drag area have been examined. The main findings of the sensitivity analysis are as follows:

- No matter the design of the UFOWT, the best operating speed for the system is always non-zero
- Ideal direction of operation (moving upwind or downwind) is determined by the relative size of the wind turbine and thrusters, and hull streamlining or lack thereof
- Systems designed for upwind operation and downwind operation appear to both be possible based on our model and the range of existing wind turbines, thrusters, and substructures

These findings motivate further work into both the design and operation of UFOWTs, and much work is still necessary to bring UFOWTs beyond the conceptual design stage. Two of the biggest areas which require focus in the future are the problems of optimal system design, and optimal routing. Although propeller, wind turbine, and floating platform design are each rich fields with considerable investigation, the specific combined problem of optimizing the design of an UFOWT has yet to be addressed. The routing of an upwind UFOWT versus a downwind UFOWT may vary drastically, and hence may make one design superior than the other in a way not encapsulated by this model. Despite these challenges for future research and development, this model shows the merit of UFOWTs and that more investigation is warranted. A future study will focus on the power performance of UFOWT systems in 2-dimensions over all possible wind speeds and directions relative to the vessel speed and heading. Other future works should include high-fidelity dynamics simulations of a UFOWT under realistic environmental load cases.

Chapter 3

Comparison of optimal power production and operation of unmoored floating offshore wind turbines and energy ships

This paper is in preparation for submission to **Wind Energy Science** as of July 6, 2022:

Connolly, P., Crawford, C., 2022. Comparison of optimal power production and operation of unmoored floating offshore wind turbines and energy ships. Wind Energy Science, Manuscript in Preparation.

CRediT contribution statement

Patrick Connolly: Conceptualization, Methodology, Software, Validation, Formal Analysis, Investigation, Visualization. **Curran Crawford:** Methodology, Resources, Writing - Review & Editing, Supervision, Funding Acquisition.

Abstract

As the need to transition from global reliance on fossil fuels grows, solutions for producing green alternative fuels are necessary. Mobile offshore wind energy systems (MOWESs) have been proposed as one such solution. These systems aim to harness

the far-offshore wind resource, which is abundant and yet untapped because of installation and grid-connection limitations. Two classes of MOWES have been proposed in the literature: unmoored floating offshore wind turbines (UFOWTs) and energy ships (ESs). Both systems operate as autonomous Power to X (PtX) plants, powered entirely by wind energy. The two technologies differ in form; UFOWTs are based on a conventional FOWT but include propellers in place of mooring lines for sea-/course-keeping, while ESs operate like a sailing ship and generate power via hydroturbines mounted on the underside of the hull. Though much research and development is necessary for these systems to be feasible, the promise of harnessing strong winds far offshore, as well as the potential to avoid siting regulatory challenges, are enticing.

This paper develops models of each MOWES concept to compare their power production on a consistent basis. The performance of the technologies are examined at steady-state operating points across relative wind speeds and angles. An optimization scheme is used to determine the values of the control variables which define the operating point for each set of environmental conditions. Results for the each model show good agreement with published results for both UFOWTs and ESs. Model results suggest that UFOWTs can generate more power than ESs under ideal environmental conditions, but are very sensitive to off-design operating conditions. In above-rated wind speeds, the UFOWT is able to produce as much power as a conventional, moored FOWT, whereas the ES cannot, since some power is always consumed to spin the Flettner rotors. The models developed here and their results may both be useful in future works that focus on the routing of UFOWTs, or holistically designing a mobile UFOWT. Although differences in the performance of the systems have been identified, more work is necessary to discern which is a more viable producer of green e-fuels.

3.1 Introduction

Renewable fuels are an essential part of decarbonizing many sectors of the global economy. Although battery energy storage systems are proving to be a viable short-term storage solution, renewable e-fuels are more suitable for mid- and long-term energy storage and transport applications. Some sectors, such as shipping, will need to rely heavily on the use of e-fuels to reduce their CO_2 emissions to stay in line with current global emissions targets [12]. Far-offshore wind energy systems have been proposed as systems for producing long-duration, renewable, stored energy harnessing a resource that could not otherwise be tapped for grid-connected electric power

generation [33]. Although they are less mature technologically than other renewable power to hydrogen systems, it has been shown that if implemented at a large enough scale, energy ships in particular can produce e-methanol at costs competitive with predicted markets [4].

In principle, mobile, far-offshore wind systems function similarly to other power to X (PtX) plants. That is, the energy in the wind is converted to electricity which is then used to power one of several processes, depending on what fuel is being produced. Many fuel-production pathways are possible, the most promising of which are the production of green hydrogen (H_2), green e-methanol, and green e-ammonia [12]. The latter liquid hydrogen carriers can be more easily stored than neat H_2 and are the front-runners for long distance marine transport markets. All e-fuel pathways imply electrolysis for the base 'green' H_2 production, aligning with global conventional wind electrolysis efforts and electrolyser production scale-up. Carbon based fuels (such as methanol), rely also on having available carbon dioxide (CO_2) to synthesize the fuel. For produced methanol to be considered green the CO_2 must be extracted from the atmosphere, such as via direct air capture or direct ocean capture. In this case, the fuel is part of a net-zero emission cycle, but with challenging system efficiencies when re-emission of the CO_2 is considered at the point of fuel use [38]. Sourcing the CO_2 from other processes such as point-source carbon capture will lead to lower overall emissions than fossil fuels, but not net-zero emissions. Ammonia has the advantage of not being carbon based, and therefore results in no direct CO_2 emissions, but NO_X combustion emissions and ammonia toxicity must be considered. Ammonia is already an established global commodity for fertilizer production, alongside its H2 carrier potentials. No matter the process, there is a significant electrical energy input required to synthesize e-fuels. Associated system efficiency challenges may be obviated to some extent by harnessing far-offshore winds that would not otherwise be usable for global decarbonization efforts. Here, the focus is on the generation of renewable energy from far-offshore winds to power these processes; energy conversion and storage steps after conversion to electricity are ignored in the present work. Any significant or novel differences in fuel synthesis and storage in non-stationary conditions fall outside the scope of this work which is instead focused on a direct comparison of wind capture modalities.

A MOWES consists of several subsystems. In general, there are systems for energy conversion, energy storage, vessel stabilization, and auxiliary subsystems. In this work, we will focus on two specific MOWES concepts: unmoored floating offshore

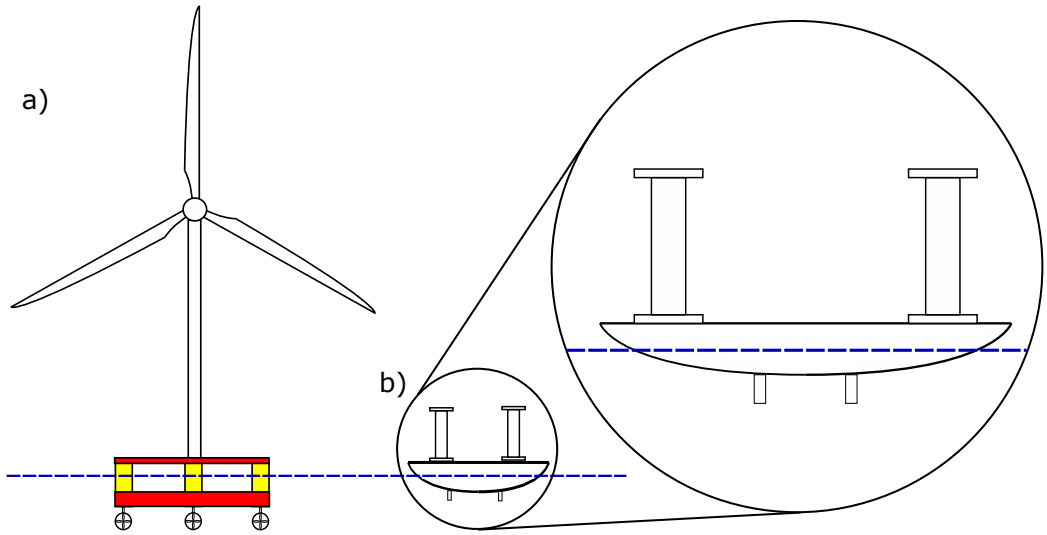

Figure 3.1: The two types of far-offshore wind energy devices being considered: a) an UFOWT, b) an ES. The systems are shown to-scale with one another, for the designs used herein, to show the large difference in height between the two.

wind turbines (UFOWTs) and energy ships (ESs). A simple depiction of each is shown in Figure 3.1. Although there is dedicated research into each concept, they remain at very-low levels of technological readiness [28, 7, 4]. The subsystems that are present in each technology that will be the focus of this work are the power generation system, the propulsion system, and the substructure. These subsystems require a controller to manage power production while maintaining the desired course and keeping the system within dynamical constraints. Many design aspects must also be considered for each subsystem, few of which have been explored in detail. More details of each concept are provided in the sections that follow.

MOWESs are a relatively novel concept, and have some distinct differences to other renewables. One such difference is that existing far-offshore wind concepts are not moored, unlike conventional floating wind turbines. This eliminates the difficulty of installing the moorings in deep water sites, and allows them to, in principle, operate anywhere in the open ocean. Since wind speeds are generally much higher farther from shore (see for example [71]), this may drastically increase the expected capacity factor for MOWESs compared to conventional wind energy systems. The other major advantage of not being anchored to the seabed is that these systems can be mobile. This allows the system to navigate in real-time to areas where wind speeds are locally highest, which may further increase expected capacity factors. Indeed, it has been shown that average capacity factors for ESs can exceed 80% because of these two

effects [50]. They are also able to avoid many siting and regulatory challenges as they are classed as vessels and not permanently installed generating infrastructure. They may also periodically return to port for maintenance as opposed to being serviced at sea. Another distinct difference is that MOWESs are not designed to be grid connected. Instead, as previously mentioned, on-board PtX systems must be installed to store the generated power which must then be unloaded either in port or by vessels dedicated to retrieving the fuel. The major downside to MOWESs is that power must be consumed by the propulsion system for course-/station- keeping [7]. This results in lower net power than for conventional wind turbines for given wind conditions.

3.1.1 Background

UFOWTs

The first MOWES technology considered is the UFOWT (see a) in Figure 3.1). The three main components of a UFOWT are the wind turbine, the sub-structure, and the thrusters. Conceptually, a UFOWT is similar to a conventional FOWT, except that the function of the mooring system is taken up by a set of thrusters mounted on the bottom of the sub-structure. Wind turbine and floating platform design for FOWTs is a mature area of research that can be leveraged for studying UFOWT design (for example [21, 72]), while existing manufacturing capabilities can be leveraged to develop scale-models and prototypes. Existing FOWT designs will not be optimal for mobile operation, however, FOWT design processes may be modified to be applied to the UFOWT case. Although the wind turbine, thrusters, and platform designs should all be re-examined for a first-of-a-kind UFOWT design, this falls beyond the scope of this work. Indeed, to derive the objective functions necessary to optimize these subsystems the power performance of a given UFOWT design must first be readily understood; this is a main goal of the present work.

Stabilization using multiple thrusters is commonly used in the form of dynamic positioning systems (DPSs) for ships. A study by Xu et al. examined a UFOWT design that uses a DPS to maintain a constant position [7]. They simulated the dynamics and power production of the system when subjected to constant wind and stochastic waves. They showed that about 50% of the power generated by the wind turbine is required to stabilize the system when current loads are not considered. When also subjected to current loads, up to 80% of the generated power is consumed for stabilization. It was implicitly assumed in their work that the system should

remain in a fixed position while operating. We will not make this assumption, working under the assumption that the UFOWT is allowed to move at constant velocity, as was assumed in [73]. This is motivated by the work of Gaunaa et al. which shows that there are potential cases where a moving system of this type can generate more power than a stationary one [32]. In fact, the optimal operation of such a system depends on design, and could be either propelling the UFOWT upwind or allowing the UFOWT to drift downwind [73]. Mobile operation introduces new problems that are not present for moored FOWTs, such as weather routing and logistics, both of which will require further study in the future.

Another difference in methodology is that previous works have assumed that the wind turbine operation should adhere to a conventional wind turbine power curve, or simply scale based on constant thrust and power coefficients. Instead we will perform an optimization over possible operating points (ranges of tip-speed ratio λ and blade pitch β). This is motivated by the fact that in the case of an UFOWT, power must be consumed to prevent the turbine from drifting in the wind direction, introducing a direct trade-off between the net power produced by the UFOWT and the thrust force on the turbine. In principle a UFOWT-specific rotor design could be pursued to balance power production and thrust characteristics. However, here an established wind turbine design is used, but its operation is optimized for the case of a mobile UFOWT.

Other works have also looked at UFOWT systems. Martinez Beseler considered a similar system referred to as an Autonomously-Driven Offshore Wind Turbine (ADO-WT) [31]. For the ADO-WT, the wind turbine was mounted on a catamaran hull instead of a conventional floating platform (i.e spar or semi-submersible) allowing it to move through the water with less resistance. This is similar to a design proposed by Annan et al. called Wind Trawler [30]. The premise of Wind Trawler is to generate additional power from the motion of the UFOWT by way of hydro-turbines mounted under the hull; Wind Trawler combines some aspects of an UFOWT and an ES. It is shown that Wind Trawler can produce more power than a conventional, stationary wind turbine, however, the cost of installing hydro-turbines and propellers has not yet been considered. Willeke examined the dynamics of a spar-based UFOWT system and showed the necessity of using thrusters to stabilize the system [29]. Without thrusters, they showed that the turbine yaws uncontrollably. They turn to redesigning the platform as a means to give the platform additional rotational stability. This is evidence that existing platform designs may not be ideal for mobile operation,

however, the problem of platform design is not one we will focus on. In addition, a semi-submersible platform is used here which should provide more resistance to yaw motions than a spar. An effective stiffness in yaw may also be achieved through control of the propellers, as was done in [7]. Alwan et al. have also proposed methods for modelling an UFOWT in steady-state [28]. As was the case for Xu et al., they assume that the system should remain stationary during operation. They also consider the mean drift wave loading on the system, and show that at high wind speeds it may dominate over other forces such as wind turbine thrust force. It is expected that the mean drift force experienced by a barge-type platform, as was used in their work, will be much higher than that on a semi-submersible platform. Since we have chosen to use a semi-submersible platform, mean drift loads will be ignored. The computation of mean drift loads would also not be straight-forward for a mobile UFOWT, since the platform will encounter the waves at different frequencies depending on the direction and velocity of the UFOWT relative to incident waves.

Energy Ships

An ES functions by using the energy in the wind to propel the vessel, and converting the motive power of the vessel through the water to electrical power by way of hydro-turbines. This power is then used in a PtX process and the produced fuel is stored onboard. In principle, an ES could make use of several different technologies to propel the vessel including rigid sails, turbosails, Flettner rotors, or parafoils. These options were examined and compared in a study by Clodic et al. that determined that all of them may be feasible, but each have unique pros and cons [25]. Wind propulsion technologies are maturing thanks to a growing interest in them as a method of decarbonizing the shipping sector, with a number of full-scale Flettner rotor equipped ships in operation [57, 74]. Studies by Babarit et al. have examined an ES design known as FARWIND which employs Flettner rotors [4, 51]. These studies demonstrate the expected power performance and economic case for the FARWIND ES concept. A key finding of these works is that ESs can produce green e-methanol at a competitive cost once fleets of 100s of GW scale operating capacity are reached. Experimental work has further shown that ESs can produce similar amounts of electricity to conventional wind turbines [20]. Power performance models presented herein are adapted from the work of Babarit et al. [4]. In general, ESs must move at significant speeds in order to create the relative flow past the hydro turbines; wave and slamming loads in more

extreme sea states may therefore limit the practical sailing conditions possible and requires further investigation [75].

A key problem for MOWES, which has been studied for the case of ESs, is weather-routing. Routing for ESs (and also UFOWTs) differs from that of conventional ship routing. Courses for ships are typically chosen to minimize travel time as well as the fuel consumption, thus minimizing operating costs and emissions [76]. In the case of ESs, the objective is instead to maximize power production along the voyage, while ensuring that the vessel is able to offload the produced fuel. Abd-Jamil et al. developed a method for optimizing the routes of ESs based on available wind speed data [50]. This study showed that ESs can achieve very high capacity factors when optimal routes are followed. A subsequent study showed that ESs may also be used to supply power to small, coastal communities, but that capacity factors may be significantly lower in near-shore operation [40]. There is clearly a large scope for future work to optimize routing based on fuel production/offload, O& M, and wind/sea-state forecasts.

3.1.2 Objective

Although some research exists on modelling, design, and operation of each individual kind of MOWES, there is so far little effort given to cross-comparing these systems as each proponent only considers their preferred approach. There is also insufficient modelling directed towards UFOWTs in general, so far mostly ignoring the possibility of allowing them to be mobile rather than station-kept. Herein, we endeavour to provide a consistent basis to compare these different classes of MOWESs. This consists of steady-state, power performance models of each system in two degrees of freedom. By constructing these models and comparing their results we provide a foundation for the more specific and detailed research into these kinds of systems that is necessary to bring them to higher levels of technology readiness.

In section 3.2 the general modelling methodology is presented, and the preliminary system designs are outlined. Results for the performance of the two systems are presented in section 3.3, and are compared to one another as well as the steady-state performance of a reference conventional floating wind turbine [1]. The implications of the differences between the two concepts and the limitations of the models are discussed in section 3.4 and the findings of this work are summarized in section 3.5.

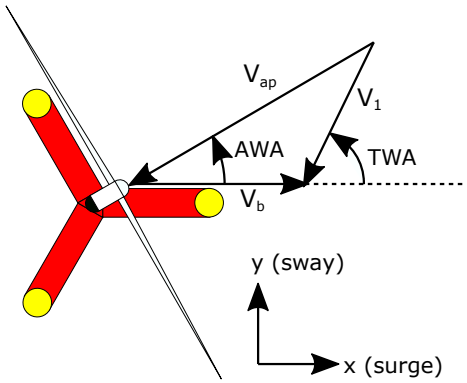

Figure 3.2: Wind vector illustration from above a UFOWT.

3.2 Methodology and modelling

The goal of a far-offshore wind energy system is ultimately to harness power from a velocity difference between two media and convert it to a usable form. Throughout we will refer to the air as medium 1 and the water as medium 2. Number subscripts are used to refer to each of these media. For example V_1 refers to the velocity of the wind, as seen from a stationary reference frame, also commonly referred to as true wind speed (TWS). The speed of the vessel/body is denoted as V_b, and is always directed in the positive surge direction. The angle between the true wind and heading of the vessel is referred to as the true wind angle (TWA). Wind speed as experienced by the vessel is referred to as the apparent wind speed (V_{ap}) and the angle between this and the vessel heading is known as the apparent wind angle (AWA). By convention, the vessel heading is always in the $+x$ direction, and the TWA is measured positive counter-clockwise with zero degrees corresponding to a direct headwind (i.e sailing directly upwind) as shown in Figure 3.2.

In developing the models, each system (UFOWT and ES) is considered to be composed of several sub-systems. Each component contributes a force on the system as a whole, and may also contribute to the net power of the system. The subsystems considered here are a power generation technology (subscript g), a propulsion technology (subscript p), and a sub-structure (subscript d). Although in principle the water will be moving at a velocity (V_2) due to currents, for this work it is assumed that there is no ocean current (i.e $V_2 = 0$). It has been shown that ocean surface currents will have an impact on the power production of UFOWTs, however, here it is neglected for simplicity [7, 73]. Both an UFOWT and an ES will be considered. The models of each system are presented in the sections that follow.

To assess the performance of each technology, the net power output of the system is calculated over a range of environmental conditions. The forces on the system are modelled in two dimensions (surge and sway) and it is assumed that the system is operating at steady-state (Equation 3.1).

$$\begin{gathered} \sum \vec{F} = \vec{0} \\ F_x = 0, F_y = 0 \end{gathered} \tag{3.1}$$

Since the model presented is for steady-state solutions, time-varying components of environmental loads are ignored. Further analysis that includes these loads will be a necessary step to assess the dynamic stability of the systems. However, the high-fidelity simulations that would be required for this are time consuming and would necessitate the development of new models or modification of existing ones. We are first concerned with determining whether one or both of the concepts being studied can produce sufficient power to merit continued research.

Subject to the steady-state constraint, the power performance of each system (UFOWT and ES) is examined over a range of TWSs and TWAs. In general, there are many possible sets of values for the control variables that lead to steady-state solutions, so an optimization method is employed to arrive at the operating point which maximizes the net power output of the system. Each system has several control variables; these form the domain that the optimization searches over. The net power is the objective which is to be maximized, subject to the steady-state force balances (Equation 3.1) and other constraints. The control variables are also bounded to keep them within feasible ranges. These bounds are discussed more specifically for each system individually. The optimization problem can be expressed as:

$$\begin{gathered} \text{maximize } \Gamma_{p,net}(\{x\}) \\ \text{subject to } \{x\} \in \mathbf{C} \\ \mathbf{C} = \left\{ \sum \vec{F}(\{x\}) = \vec{0},\ B_{u,i} \geq x_i \geq B_{l,i},\ O \leq f(\{x\}) \right\} \end{gathered} \tag{3.2}$$

Where $\mathbf{C}$ refers to the set of constraints, and $B_{u,i}$ and $B_{l,i}$ are members of the set of upper and lower bounds for each of the input variables (index i) to the optimization, respectively. Other constraints are also implemented, such as for example constraining the rated power of the wind turbine to not exceed the generator rated power. These are referred to generally as O in the last part of Equation 3.2. To compare across

the two systems, each system's net power is normalized by its respective rated power. This quantity is referred to as $\Gamma_{p,net}$ (Equation 3.3).

$$\Gamma_{p,net} = P_{net}/P_{rated} = \frac{P_g + P_p}{P_{rated}} \tag{3.3}$$

We will also consider the ratio of power consumed to power generated, referred to as power ratio (R_p), as was done in [7]:

$$R_p = \frac{P_p}{P_g} \tag{3.4}$$

The optimization problem is solved for each set of chosen environmental conditions. By sweeping through a range of possible wind speeds and angles, maps of optimal power performance are generated along with the values of the control variables that define the optimal operating points. Optimizations are performed using a particle swarm optimization code implemented in Python called PySwarm. PySwarm is open-source and open-access and allows for implementation of bounds and constraints. Although particle swarm optimization generally does not guarantee the global optimum solution is found, it was used here since the gradient of the objective function is not trivial to compute. As well, the control variable space searched by the algorithm is only two or three dimensional (for ES and UFOWT respectively), meaning that optima are computed quickly using only a personal computer. To ensure global optima were computed, future work may include verifying solutions by way of other optimization processes.

The power performance models of each technology are described separately in the following sections, Section 3.2.1 for the UFOWT and Section 3.2.2 for ESs.

3.2.1 UFOWT

The thrust force on the wind turbine ($\vec{F}_g$) is defined in Equation 3.5 according to actuator disk theory [58]. It is assumed that the wind turbine rotor is always perfectly yawed in the wind direction so there is no yaw error to account for. Thus, the thrust force is always acting in the direction of the apparent wind (i.e along the apparent wind angle, AWA). Future work may explore thrust vectoring by misaligning the rotor yaw to help steer the UFOWT. Wind turbine thrust and power coefficients ($C_{t1}(\beta, \lambda)$ and $C_{p1}(\beta, \lambda)$) are functions of the blade pitch and tip-speed ratio (β and λ). These are two of the control variables used in the control optimization process

for the UFOWT case, and are conventional wind turbine control variables.

$$\vec{F}_g = -\frac{1}{2}\rho_1 A_1 \left|V_{ap}\right|^2 C_{t1}\left(\beta,\lambda\right)\left[\cos\left(AWA\right)\hat{x},\sin\left(AWA\right)\hat{y}\right] \tag{3.5}$$

Viscous drag on the floating platform ($\vec{F}_{d2}$) is accounted for in Equation 3.6. The drag coefficient (C_{d2}) is sourced from existing literature, and is generally dependent on the size and shape of the platform elements. As mentioned earlier, by convention the UFOWT is always moving in the positive surge ($+x$) direction, so the drag force will always act opposite this direction of motion.

$$\vec{F}_{d2} = -\frac{1}{2}\rho_2 A_{d2} V_b^2 C_{d2}\left(V_b\right)\left[\hat{x},0\hat{y}\right] \tag{3.6}$$

Lastly, the thrust force exerted by the propellers ($\vec{F}_p$) is defined according to standard propeller theory in Equation 3.7 [77]. Conventional thrust and torque coefficients ($K_{t2}(J)$ and $K_{q2}(J)$) for fixed-pitch propellers are used, and depend in general on the number of blades and their shape, as well as the advance ratio (J). The yaw angle of the propellers (θ) is controlled to ensure steady-state motion in the surge and sway directions. It is determined analytically by Equation 3.8 for a given set of environmental conditions and a specific vessel speed, i.e. the propellers are yawed to produce a sideways (sway) force to counteract the wind turbine rotor force in the sway direction. Propeller rotational frequency (f) must be solved for numerically according to the implicit relationship in Equation 3.9 which was derived from the force balance. It is not varied directly by the optimizer, but instead determined iteratively during each evaluation of the steady-state constraint and the objective function.

$$\vec{F}_p = -n_{wt}\rho_2 D_2^4 f^2 K_{t2}\left(J\right)\left[\cos\left(\theta\right)\hat{x},\sin\left(\theta\right)\hat{y}\right] \tag{3.7}$$

$$\theta = tan^{-1}\left(\frac{\sin\left(AWA\right)}{\cos\left(AWA\right) - \frac{\rho_2 A_{d2} V_b^2 C_{d2}}{-\rho_1 A_1 V_{ap}^2 C_{t1}(\beta,\lambda)}}\right) \tag{3.8}$$

$$K_{t2}(J)f^2 = \frac{-\frac{1}{2}\rho_1 A_1\left|V_{ap}\right|^2 C_{t1}\left(\beta,\lambda\right)\cos\left(AWA\right) - \frac{1}{2}\rho_2 A_{d2} V_b^2 C_{d2}\left(V_b\right)}{n_{wt}\rho_2 D_2^4\cos\left(\theta\right)} \tag{3.9}$$

To determine the net power generated by the UFOWT system, the power generated from the wind turbine (P_g) and the power consumed by the propellers (P_p) are

computed according to Equations 3.10 and 3.11, respectively. These equations follow from the same theories stated above for the forces, namely actuator disk theory and propeller theory for the wind turbine and propeller, respectively.

$$P_g = \frac{1}{2}\rho_1 A_1 V_{ap}^3 C_{p1}\left(\beta, \lambda\right) \tag{3.10}$$

$$P_p = -2\pi n_{wt}\rho_2 D_2^5 f^3 K_{q2}\left(J\right) \tag{3.11}$$

$\Gamma_{P,net}$ can be computed for the UFOWT according to Equation 3.3 by way of Equations 3.10 and 3.11.

Control

Using the relationships described above, an optimization with the objective of maximizing net power is performed (according to Equation 3.2) for each vessel operating condition (i.e V_1 and TWA). The control variables that the optimizer iterates on for the UFOWT case are: wind turbine blade pitch (β), wind turbine tip-speed ratio (λ), and UFOWT vessel speed (V_b). That is, in the UFOWT case:

$$\{x\} = \{\beta, \lambda, V_b\} \tag{3.12}$$

The full set of variables that describe a given operating point for the UFOWT model are the set of control variables $\{x\}$, as well as the propeller frequency and yaw angle. Bounds on the tip-speed ratio and blade pitch are chosen to remain within the available performance data. Vessel speed was assigned a lower bound of 0 m/s, since negative values of vessel speed would lead to redundant solutions when scanning a full 360° of TWAs. No upper bound was set for the vessel speed, although in practice one may be necessary when the dynamics of the UFOWT are considered in dynamic sea states. In addition to the bounds on the control variables, a constraint on maximum rotor speed for the wind turbine is implemented. Minimum rotor speed is not used as a constraint. The power generated by the wind turbine is also constrained to not exceed the rated power of the generator.

Design

A preliminary UFOWT design is presented here for the purpose of demonstrating power performance. The objective of the design used here is to be easily repro-

Table 3.1: Specifications of the UFOWT subsystems (from [1, 2, 3]).

Wind Turbine	
$r\ (m)$	120
$h_{hub}\ (m)$	150
$V_{1,rated}\ (m/s)$	10.6
$P_{rated,UF}\ (MW)$	15.0
$C_{t1}(\beta, \lambda)\ (-)$	Fig. 3.3
$C_{p1}(\beta, \lambda)\ (-)$	Fig. 3.3
$\omega_{max,WT}\ (rpm)$	7.56
Platform	
$B_{d2}\ (N(m/s)^{-2})$	$9.22E5$
Propellers	
# of blades	4
$h_{hub}\ (m)$	150
P/D	1.1
A_e/A_o	0.9
$D\ (m)$	8.0
# of props	4
$K_{t2}(J)\ (-)$	Fig. 3.4
$K_{q2}(J)\ (-)$	Fig. 3.4

ducible. For this reason the design is based on the International Energy Agency (IEA) 15 MW reference wind turbine and the UMaine VolturnUS semi-submersible platform, the most recent standard reference floating wind turbine [1, 2]. In the spirit of reproducibility, the propeller performance coefficients are derived from the Wageningen B-series propellers [3]. Table 3.1 presents all relevant specifications of the UFOWT system.

Wind turbine performance coefficients are presented in Figure 3.3 for various blade pitch settings. Thrust and torque coefficients for the chosen propeller are shown in Figure 3.4. Although conventionally propeller thrust and torque coefficients are only used over the range where the coefficients are positive, in the case of UFOWTs it may also be possible to operate the propellers under conditions where they are negative. This is further discussed in the following section (Section 3.2.1). The propellers may also operate at small, negative advance ratios ($J < 0$). The performance coefficients are assumed to be constant under these conditions [60]. Negative advance ratios correspond to situations where the propellers may operate as turbines, however, more detailed design and optimization may be required to fully exploit this.

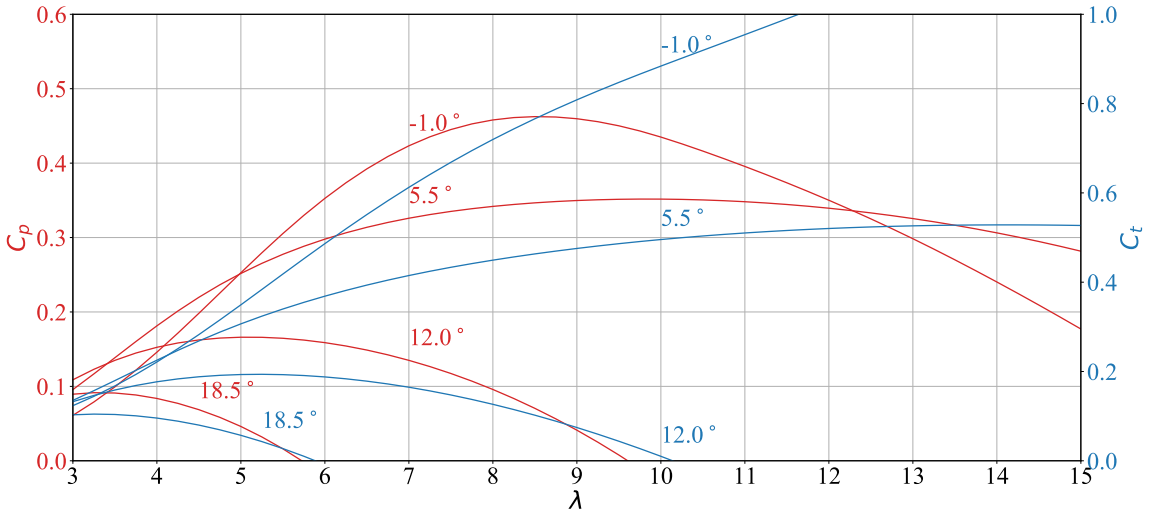

Figure 3.3: Thrust and power coefficient traces for the IEA 15 MW reference wind turbine, full data available in [1] and the associated github page.

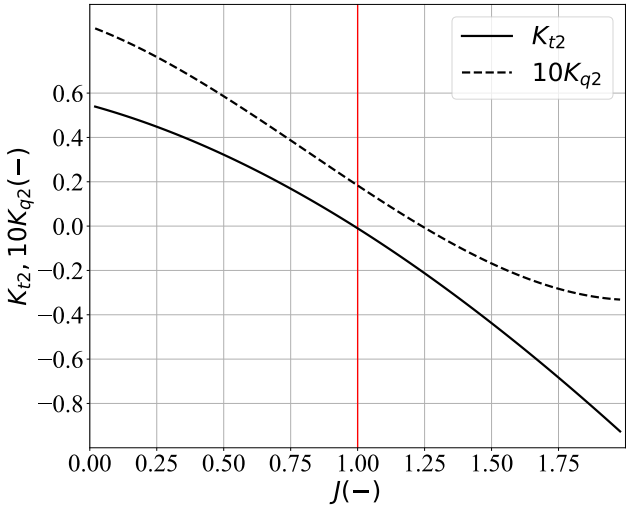

Figure 3.4: Performance maps for the chosen Wageningen B-series propeller [3].

Propeller power take-off (regeneration)

Although the primary purpose of the propellers is to consume power to counter-balance environmental forces on the system, there may be cases where it is possible to extract power through the propellers rather than consuming it. One instance where this may be possible is when the UFOWT is travelling directly downwind. In this case the wind turbine thrust is pushing the vessel downwind, while the drag on the sub-structure resists this motion. It may be possible to use the propellers as if they were water turbines to provide added resistance to achieve steady-state. This is similar to the principle of regenerative braking that is used in electric vehicles [78]. It can also be used with electric or hybrid-electric ships and planes by operating the propellers outside of their normal operating ranges. Though regeneration (as it is referred to when using a propeller) is currently being used in private and small commercial ships, little is published on the design or operation of the propeller [79, 80]. Some research has been conducted on the application of regeneration to electric aircraft, however, the data presented is not directly applicable to the UFOWT application since it is for small propellers used in air [81, 82].

To explore this possibility, the UFOWT model includes an option to consider solutions where the propellers generate power, rather than consuming it. This requires using advance ratios outside the range of what is presented in [3]. Data for propellers operating in this mode are scarce and are mostly for the case of propellers operating in the air. For this reason, the regression polynomials in [3] are used to extrapolate the performance coefficients beyond the intended range. Some results for this case are presented separately in Section 3.3.2. Under this case, the complete range of performance coefficients in Figure 3.4 is used, whereas in the baseline case only values where the thrust coefficient is positive are allowed.

3.2.2 Energy ship

The ES model presented is based directly on that of Babarit et al. [4]. Forces on the ES from the Flettner rotors, water turbines, and hull are considered. Flettner rotors are considered here over other propulsion options to remain in line with existing literature, especially the FARWIND design. Thrust force on the water turbines ($\vec{F}_g$) is calculated according to actuator disk theory and is shown in Equation 3.13. As was the case for the wind turbine in the UFOWT case, the water turbines are considered to be perfectly aligned with the flow. Since the vessel is assumed to only move in the

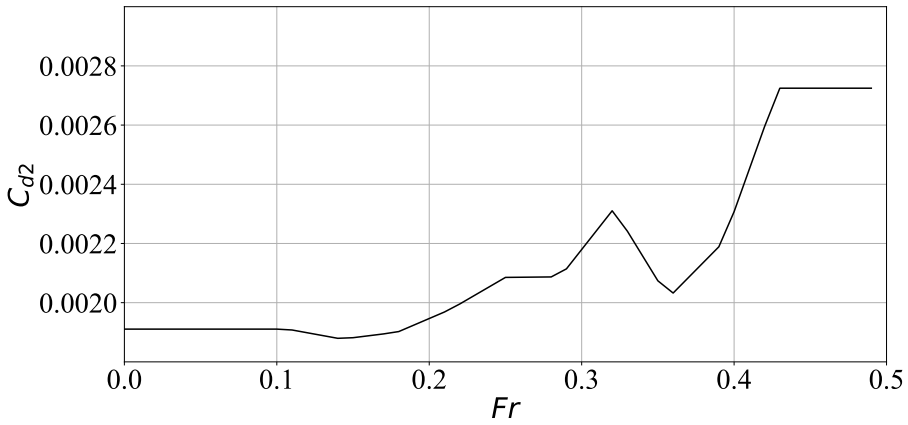

Figure 3.5: Hull resistance coefficient as a function of Froude number (Fr), sum of the frictional and residuary coefficients used in [4].

positive surge direction, the thrust is always along this direction as well.

$$\vec{F}_g = -2\rho_2 A_2 V_b^2 a(1-a)\,[1\hat{x}, 0\hat{y}] \tag{3.13}$$

The hull resistance ($\vec{F}_{d2}$) is also directed opposite the motion of the ship. Resistance coefficients ($C_{d2}\,(Fr)$) are shown in Figure 3.5 and are taken to be the sum of the residuary (wave) resistance and frictional resistance coefficients from [4].

$$\vec{F}_{d2} = -\frac{1}{2}\rho_2 A_{d2} V_b^2 C_{d2}\,(Fr)\,[1\hat{x}, 0\hat{y}] \tag{3.14}$$

Thrust provided by the Flettner rotors ($\vec{F}_p$) is the sum of the aerodynamic lift ($\vec{L}$) and drag ($\vec{D}$) as shown in Equations 3.15, 3.16, and 3.17. These equations assume the Flettner rotor is spinning counter-clockwise, but since the rotors are symmetric they can perform equally as well spinning clockwise, which would reverse the direction of the lift. Flettner rotor lift and drag coefficients ($C_{lp}(\gamma)$ and $C_{dp}(\gamma)$) are presented in Figures 3.6a and 3.6b and the power coefficient for the Flettner rotor motor ($C_m(\gamma)$) is shown in Figure 3.6c. These coefficients are calculated from empirical relationships derived by Tillig and Ringsberg [6]. Since the Flettner rotors are spaced quite closely together, the wakes of upwind Flettner rotors may affect the inflow velocity at rotors downwind. As is recommended in [4], a coefficient that reduces the total thrust is introduced to account for the interaction between the rotors and their wakes ($C_{t,int}$). Although $C_{t,int}$ will generally depend on wind speed, wind angle, and spin ratio, it is assumed to be constant to remain consistent with existing models.

$$\vec{L} = -\frac{1}{2}\rho_1 A_1 V_{ap}^2 C_{lp}(\gamma)\left[\sin(AWA)\hat{x}, -\cos(AWA)\hat{y}\right] \tag{3.15}$$

$$\vec{D} = -\frac{1}{2}\rho_1 A_1 V_{ap}^2 C_{dp}(\gamma)\left[\cos(AWA)\hat{x}, \sin(AWA)\hat{y}\right] \tag{3.16}$$

$$\vec{F_p} = \left(\vec{L} + \vec{D}\right) C_{t,int} \tag{3.17}$$

Power generated by the water turbines is modelled consistently with the thrust force and is shown in Equation 3.18. An efficiency (η_g) is added to remain consistent with [4] to account for losses in the conversion of mechanical (i.e shaft) power to electrical power by the turbine and generator.

$$P_g = 2\rho_2 A_2 V_b^3 a(1-a)^2 \eta_g \tag{3.18}$$

The power consumed to spin the Flettner rotors is computed according to Equation 3.19. It is in line with existing research on Flettner rotors [6, 83, 84]. Equations 3.18 and 3.19 give enough information to calculate $\Gamma_{p,net}$ via Equation 3.3.

$$P_p = -\frac{1}{2}\rho_1 A_1 V_{ap}^3 C_m(\gamma) \tag{3.19}$$

Control

Although the UFOWT is constrained to steady-state solutions in both surge and sway, the ES must only satisfy steady-state in surge. This is because it is assumed that any side-force on the vessel will be counteracted by the force developed from

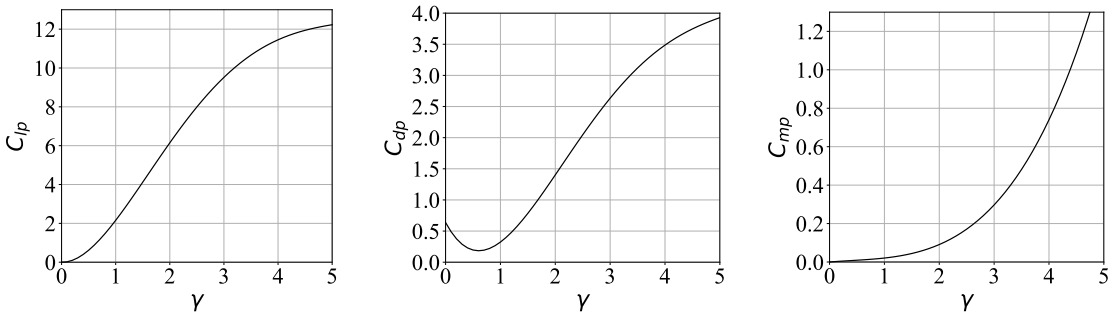

(a) $C_{lp}(\gamma)$ (b) $C_{dp}(\gamma)$ (c) $C_m(\gamma)$

Figure 3.6: Flettner rotor performance coefficients computed from [6].

the ship's keel and the associated leeway angle is assumed small. Only two control variables are passed to the optimizer for the ES, they are the spin ratio of the Flettner rotor and the vessel speed. Thus for the ES case:

$$\{x\} = \{\gamma, V_b\}$$

Rotational frequency of the Flettner rotors is also constrained to a maximum of 180 rpm according to [5]. The axial induction factor (a) is calculated numerically according to Equation 3.20 to ensure steady-state in surge.

$$\begin{aligned} a(1-a) &= \frac{1}{4}\left[\frac{\rho_1 A_1 V_{ap}^2}{\rho_2 A_2 V_b^2} C_x(\gamma) C_{t,int} - \frac{A_{d2}}{A_2} C_{d2}(Fr)\right] \\ C_x &= C_{lp}(\gamma)\sin(AWA) - C_{dp}(\gamma)\cos(AWA) \end{aligned} \tag{3.20}$$

Design

Relevant specifications of the ES are presented in full in Table 3.2. The FARWIND ES design is used here, as it is the most developed and best documented design available [24, 4]. FARWIND uses a catamaran ship hull with four Flettner rotors mounted onboard and two water turbines mounted under the hull.

3.2.3 Design differences

To establish a fair comparison, UFOWT and ES designs were both chosen based on the largest, in terms of rated power, readily available designs in the literature. This decision was based on the established trend for conventional wind turbines that cost decreases for increasing rated power. However, the physical scales of the two system designs, UFOWT and ES, are quite different The rated power of the ES design is only 1.6 MW compared to the UFOWT rated power of 15 MW, however, comparison results are non-dimensionalized to account for this discrepancy. This implicitly assumes that net power results scale linearly with rated power, which is further discussed in section 3.4.2. In terms of physical scale, the heights and weights of the two proposed designs are very different. The discrepancy in height will create a difference in wind speeds experienced by the UFOWT and ES because of the wind shear. This effect is accounted for below in section 3.2.4. By virtue of being larger, the UFOWT design uses a much larger amount of steel than the ES. The combined mass of steel used in the platform, wind turbine tower, and nacelle is on the order of

Table 3.2: Specifications of the ES subsystems (from [4, 5, 6]).

Hydro Turbines	
$r\ (m)$	1.0
# of turbines	2
$\eta_g\ (-)$	0.75
$\omega_{max,FR}\ (rpm)$	180
$P_{rated,ES}\ (MW)$	1.6
Hull	
$A_{d2}\ (m^2)$	1107.5
$C_{d2}(Fr)\ (m^2)$	Fig. 3.5
$L_{hull}\ (m)$	80
Flettner Rotors	
# of Rotors	4
$h_{mid}\ (m)$	22.5
$h_{FR}\ (m)$	35
$D_{FR}\ (m)$	5.0
$C_{t,int}\ (-)$	0.7
$C_{lp}(\gamma)\ (-)$	Fig. 3.6a
$C_{dp}(\gamma)\ (-)$	Fig. 3.6b
$C_m(\gamma)\ (-)$	Fig. 3.6c

6200 tons for the UFOWT, whereas the ES hull and Flettner rotors use about 880 tons of steel [2, 4]. This amounts to the UFOWT using a about seven times more steel than the ES, but producing about nine times as much power. More rigorous accounting of the materials used in each design is necessary to draw any conclusions on if one MOWES is more efficient than the other in this aspect, especially since the weight of the UFOWT thrusters has not been accounted for here. The only dimension in which the two MOWES designs proposed have similar scales is in the length of the sub-structures, the ES hull being about 80% as long as the distance between the pontoons of the semi-submersible platform. This may be relevant when accounting for the space on deck or on board required for the PtX, storage, and other subsystems.

3.2.4 Wind shear

An important differentiating factor between ESs and UFOWTs, which is not inherently captured in the power performance models, is the difference in local incident wind speeds that each would experience due to the difference in height between the two technologies. Current ES designs employ 35 meter tall Flettner rotors, the largest

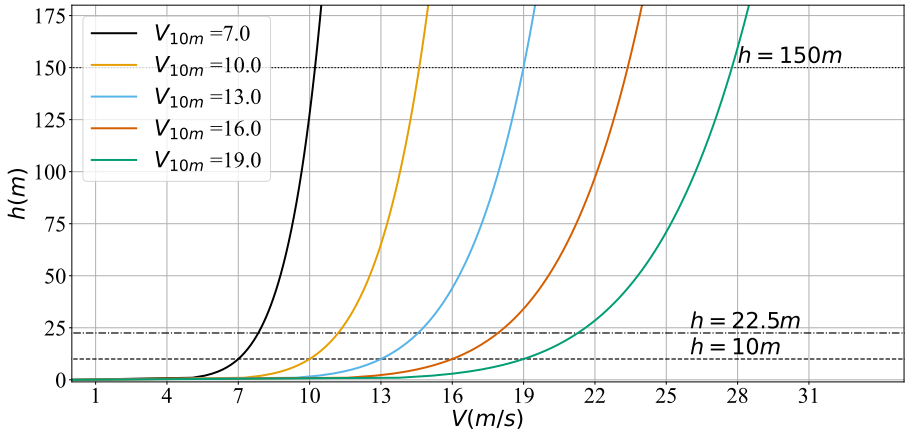

Figure 3.7: Vertical wind shear profiles for the chosen wind speeds.

commercially available from Norsepower [5]. In contrast, there are commercially available offshore wind turbines with hub heights well over 100 meters, and the IEA 15 MW reference turbine used throughout this work has a hub height of 150 meters [1, 2]. This large difference in height means that under the same wind conditions, the two would experience very different average wind speeds depending on the wind shear. Accounting for this effect allows the two to be compared across identical environmental conditions, instead of at equal, but arbitrary, local wind speeds. Model results/comparisons for wind speeds which account for the wind shear difference are presented separately in Section 3.3.4. Relative device sizing may change in the future as larger Flettner rotors may be available, or smaller wind turbine rotors preferred for dynamic reasons.

To account for this difference, power performance curves are generated for equal reference wind speeds (i.e at a reference height of 10 meters). TWSs are scaled using a power law relationship shown in Equation 3.21. A wind shear exponent of $\alpha = 0.14$ is used in accordance with common practice for offshore winds [85, 4]. The effect of applying the shear scaling to the wind speeds is shown in Figure 3.7. Exact wind speeds used during the analysis are listed in Table 3.3.

$$V_1 = V_{ref} \left(\frac{h}{h_{ref}} \right)^{\alpha} \tag{3.21}$$

Table 3.3: Wind speeds (m/s) at reference height, Flettner rotor midpoint, and wind turbine hub height used in the analysis of the effect of vertical wind shear.

$h_{ref} = 10m$	$h_{FR} = 22.5m$	$h_{hub} = 150m$
7.00	7.84	10.23
10.00	11.20	14.61
13.00	14.56	18.99
16.00	17.92	23.38
19.00	21.28	27.76

3.3 Results

Optimized power performance results for each system are presented in the sections that follow. First, the model results were verified against existing literature in Section 3.3.1. Power performance maps for the UFOWT and ES are presented separately in Sections 3.3.2 and 3.3.3 respectively, and are then compared to one another in Section 3.3.4.

3.3.1 Verification

For the ES model, power performance results were verified against those of Babarit et al. [4], however, there is a distinct lack of published results for mobile UFOWTs meaning that it is not possible to directly verify the results. For the case of a station-keeping UFOWT, model results were verified against those of Xu et al. [7]. Power generated and consumed for several wind speeds are shown in Figure 3.8. This verification case is run using a different UFOWT design which uses a 5 MW turbine and smaller thrusters. The model results show good agreement, though slightly less power is consumed by the present model. This may be because wave forces are accounted for in the model of Xu et al. whereas they are not accounted for in the present model. Of note for the results presented in Figure 3.8, no rated wind speed was considered by Xu et al. and therefore the power simply scales with the cube of the wind speed indefinitely. This is not the case for the model results presented hereafter, but this exception was made for verification purposes.

3.3.2 UFOWT

The net power performance for the proposed UFOWT design is shown in Figure 3.9a for a range of wind speeds and for all possible TWAs. Also shown are the

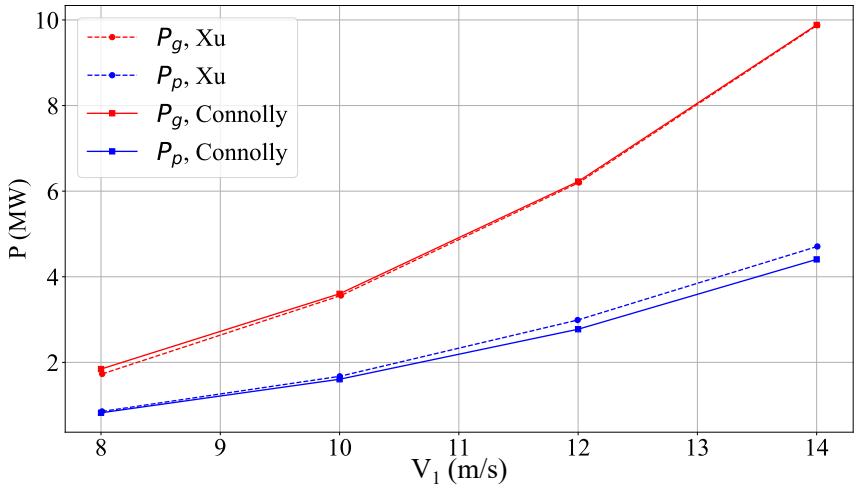

Figure 3.8: Results of the UFOWT model for $V_b = 0$ compared to those of Xu et al. [7].

power generated by the wind turbine (P_g) and the power consumed by the thrusters (P_p) in Figures 3.9b and 3.9c, respectively. Most net power is produced at a TWA of 180°, or heading directly downwind. This is owing to the fact that in this case the viscous drag on the platform helps to counteract the thrust force from the wind turbine, and so the propellers need not produce as much (or in some cases any) thrust to maintain steady-state velocity. This results in potential operating points where UFOWTs are capable of producing as much power as a conventional wind turbine, albeit only for above-rated wind conditions. Drag on the platform is clearly a key design aspect, as was suggested in [73]. A problem which may need to be considered should a high-drag platform be designed is that changing the platform size and/or shape to increase the viscous drag may also increase wave-platform interaction. It is also evident from Figures 3.9a, 3.9b, and 3.9c that for many wind angles the UFOWT operates identically. For more windward (i.e more upwind) headings the optimization converges to results where the best operating speed is around 0 m/s, as is shown in Figure 3.9d for upwind TWAs between 270° and 90°. When there is no potential to benefit, in terms of net power, from platform drag the default is therefore for the platform to remain stationary. This will have implications on the routing of the UFOWT, since sometimes it may be desirable to move upwind to reach an area with higher local wind speeds or to maintain distance from shore. The proposed UFOWT is capable of producing some net power under all environmental conditions considered.

The power ratio is also presented in Figure 3.10. Previous studies have shown that

power ratios of 50% are to be expected for station-kept UFOWTs [7]. However, model results here suggest that this represents the worst case power ratio. The worst case is when the wind turbine is operating in region II, i.e below rated wind speed, and the thrust is increasing with the square of the wind speed. In above-rated conditions, although the power stops increasing, the thrust begins to decrease. This results in the propellers consuming less power, and therefore an overall increase in net power. This effect shows that to accurately predict power performance of a UFOWT, the wind turbine power and thrust coefficients must be considered.

Although not well illustrated by Figure 3.9a, UFOWTs may operate at very high

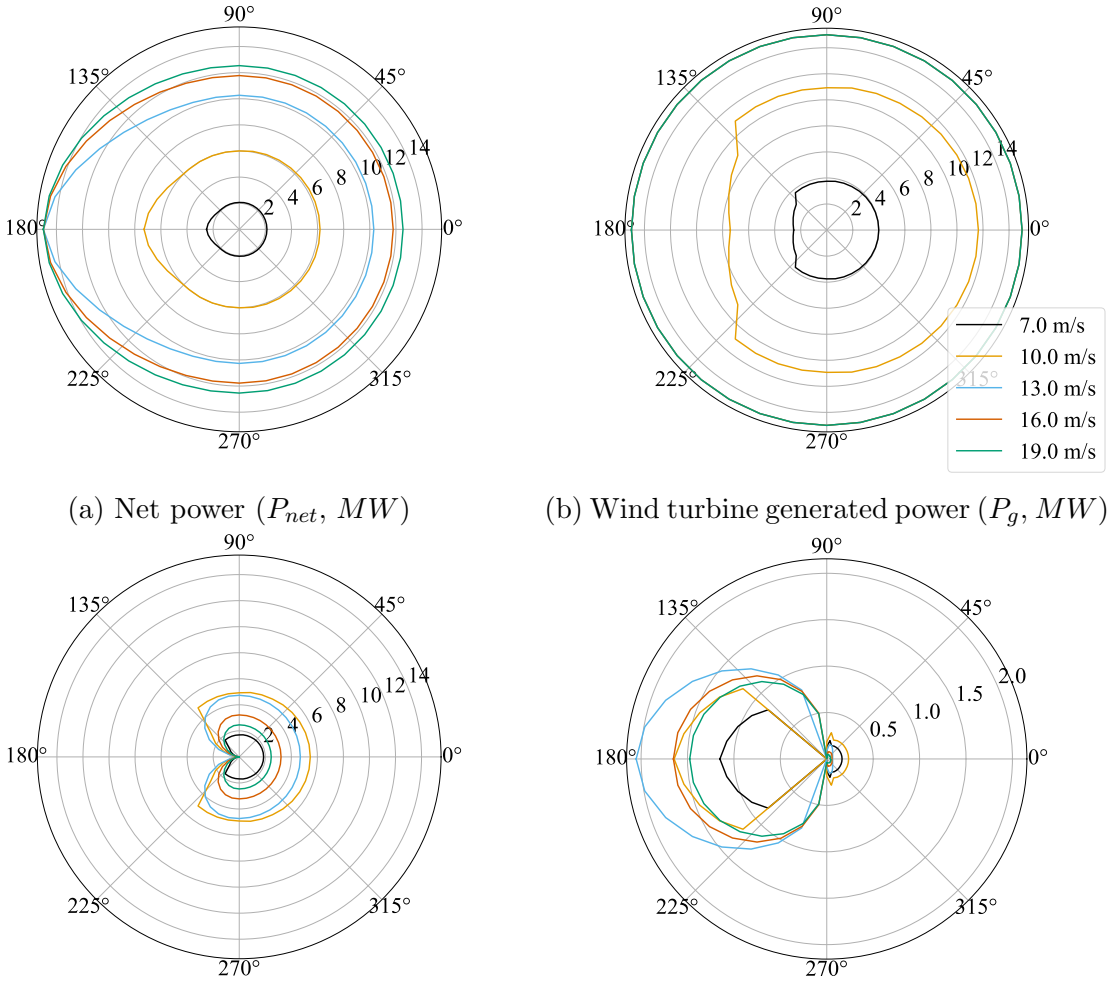

(a) Net power (P_{net}, MW)

(b) Wind turbine generated power (P_g, MW)

(c) Propeller consumed power (P_p, MW)

(d) Optimal vessel speed (V_b, m/s)

Figure 3.9: Power polar results for UFOWT optimization as a function of V_1 (m/s) for all TWAs.

true wind speeds, above the conventional cut-out speed of a conventional stationary wind turbine. This is owing to the fact that by moving downwind the wind turbine rotor will experience a lower apparent wind speed than the true wind speed. The effect of this is shown in Figure 3.11 which shows the power curve of a UFOWT for the ideal wind direction (i.e 180°) compared to the IEA 15 MW reference turbine. Note that the regeneration and baseline UFOWT cases overlap perfectly, meaning regeneration is not exploitable for the proposed design. Only the final wind speed differs, at this point the optimizer failed to converge for the regeneration case. Of course, there will be an upper-bound to the velocity of the UFOWT owing to constraints on the system dynamics, however, at this stage it is not evident what this limit should be. Figure 3.11 also illustrates how at low TWSs the UFOWT cannot produce as much power as the stationary turbine. For example, at $V_1 = 11m/s$ just above the rated wind speed of the IEA 15 MW turbine the UFOWT is only able to produce 9.1 MW or 61% of the power of the stationary turbine. However, by $V_1 = 13m/s$ the UFOWT is able to generate rated power. Also shown is the power curve of an UFOWT constrained to only operate at $V_b = 0\ m/s$, as was assumed by most prior studies [7, 28]. It is obvious that much more power may be produced by a mobile UFOWT than a stationary one. However, allowing the UFOWT to move introduces dynamics and logistical challenges which are not present for a stationary turbine.

The control variable values for a scan of true wind speeds and $TWA = 180°$ are shown in Figures 3.12a, 3.12b, and 3.12c. These are the values which result in optimal

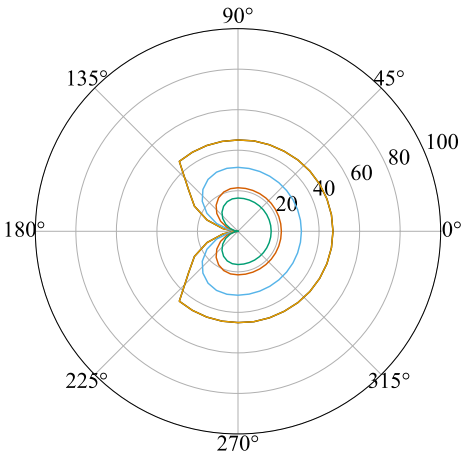

Figure 3.10: UFOWT power ratio ($R_p, \%$) at optimal operating points as a function of V_1 (m/s) for all TWAs. Note 7 m/s result is hidden by 10 m/s result since they match exactly.

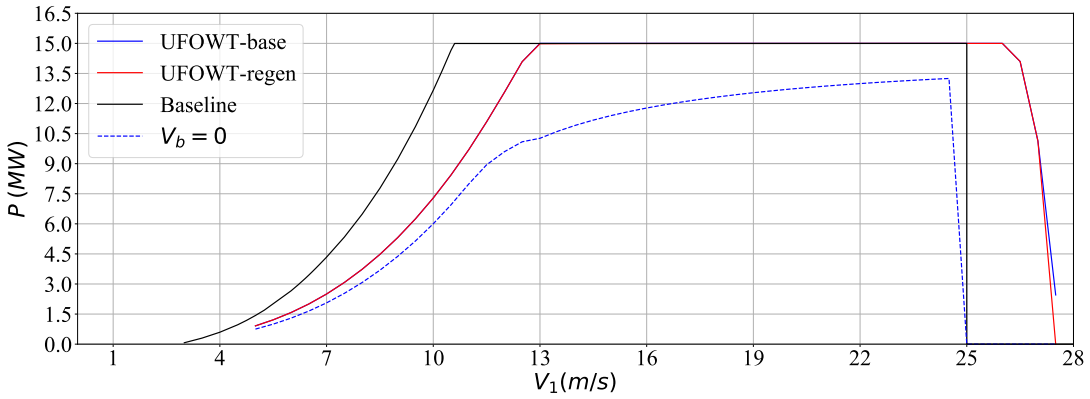

Figure 3.11: UFOWT power curve at $TWA = 0°$ for the UFOWT baseline case, UFOWT regeneration case, UFOWT with $V_b = 0$ case, and baseline IEA 15 MW power curve. Note that the UFOWT baseline case ("base") is hidden by the regeneration case ("regen") since they match each other exactly until about 27 m/s.

net power production, for each of the cases examined. Obviously, for both the base IEA 15 MW case and the case where the vessel speed is restricted to be zero, the vessel speed is zero for all wind speeds. Trends for the TSR and pitch are similar across all cases. TSR is constant in region II and decreasing in region III, while pitch is zero in region II (except for the UFOWT case where $V_b = 0$) and then increasing pitch through region III. Since the blades pitch to feather in above-rated speeds, thrust force decreases as V_1 increases and so less drag is required to counteract the thrust to achieve steady-state velocity. This means that the UFOWT's optimal V_b decreases in above rated conditions. Above the conventional cut-out wind speed, the optimal vessel speed will again increase, because the blades reach their maximum allowable pitch (25°) and can no longer reduce rotor thrust. In this region, call it region IV, the propellers must push the wind turbine downwind to reduce the apparent wind speed at the rotor to below the cut-out wind speed. These control and performance results both suggest that developing optimized UFOWT rotors would be beneficial, since the trade-off between wind turbine rotor thrust and power can be included in the design optimization process.

Regeneration

Although it may be possible to generate more power by operating the propellers outside of their normal operating range, as is shown in Figure 3.11 this is not exploitable for the proposed design. Indeed, optimal net power for the UFOWT in both the

baseline case and the case where regeneration was considered are identical. This may be because the propellers perform very inefficiently as turbines. Future studies may consider a variable-pitch propeller that has been designed for this application. Alternatively, dedicated water turbines could be installed in addition to the propellers as was done for the WindTrawler concept [30]. In this case, the system was designed holistically around a specific operating speed to guarantee wind and water turbines operate at rated power at the same point.

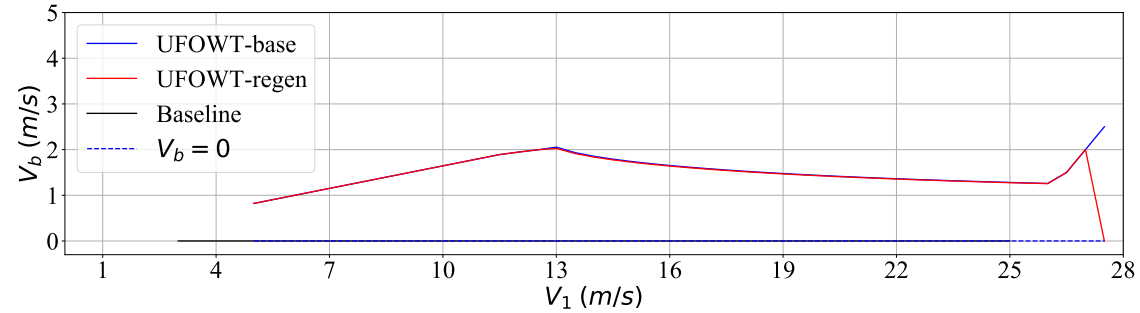

(a) Vessel speed, V_b

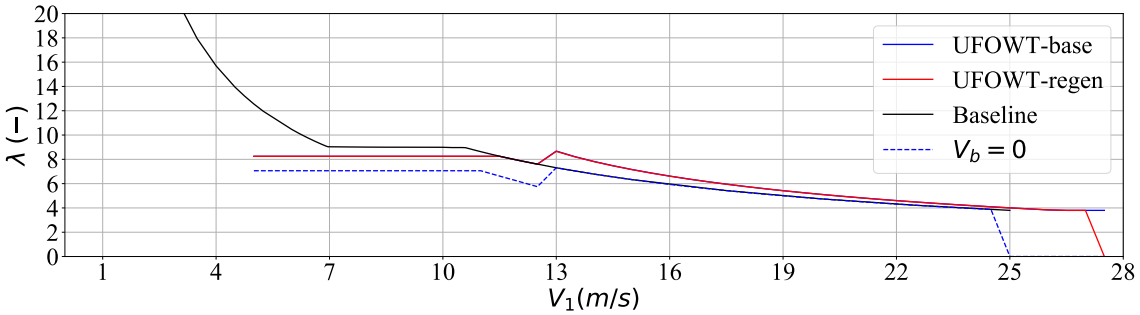

(b) Tip-speed ratio, λ

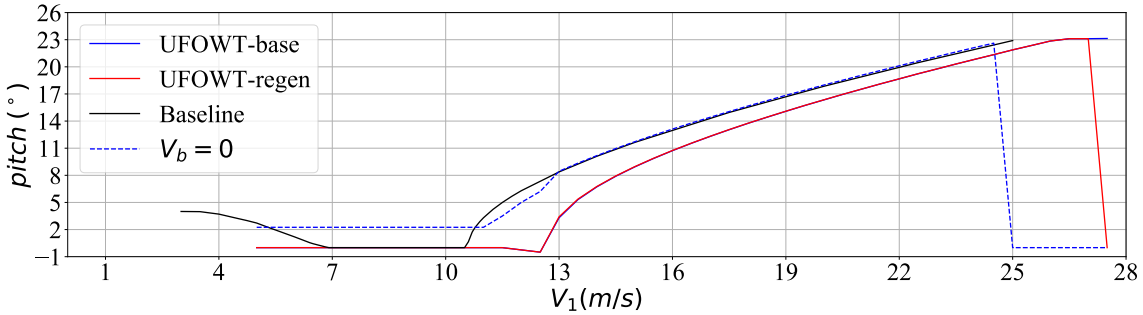

(c) Blade pitch, β

Figure 3.12: Control variables of the UFOWT at optimal operating points for $TWA = 0°$. UFOWT baseline results are hidden by the regeneration case for the most part, since regeneration was not exploitable.

3.3.3 Energy ship

The net power generated by the FARWIND ES concept is shown in Figure 3.13a. Power produced by the water turbines and consumed to spin the Flettner rotors for each set of wind conditions are shown in Figures 3.13b and 3.13c respectively. The ideal vessel speed for the ES is shown in Figure 3.13d. For many sets of conditions the optimal vessel speed is 10 m/s, this is owing to the shape of the drag curve for the ship hull, which reaches a local minimum at this speed (see Figure 3.5); it is not a ceiling effect from a constraint applied to the optimization. For direct headwinds (i.e TWA = 0°) and nearby angles, the optimization converged to results which suggested net negative power production. Realistically, this means that the ship cannot operate under these conditions as expected, so the results for these wind angles are defaulted to zero. Like the results for the UFOWT, the power generation of the ES has reflectional symmetry across the x-axis. This is because the Flettner rotors can operate equally as well spinning clockwise or counter-clockwise. Unlike the UFOWT, ESs power performance does not fall off symmetrically on either side of its optimum point. This is owing to the fact that the lift generated by the Flettner rotors to propel the ship is perpendicular to the AWA, while the drag is parallel. The most efficient TWAs for ES operation are driven mostly by the most efficient wind angles for sailing.

3.3.4 Comparisons

Here the performance of the two technologies predicted by the models are compared to one another. First, Figure 3.14 shows the effective power curve of the two technologies compared to the standard power curve for the IEA 15 MW reference turbine. It is assumed that each technology is operating at its optimal wind angle for each wind speed, and the net power is presented as a fraction of each technology's respective rated power (i.e $\Gamma_{p,net}$). The shaded blue region indicates where the UFOWT outperforms the ES, whereas the shaded red region shows where the ES performs better. As was expected, neither technology is able to perform as well as a stationary wind turbine over all wind speeds. However, at above-rated wind speeds the UFOWT is able to generate rated power whereas the ES is not. No matter the conditions, the ES must always consume some power to spin the Flettner rotors, meaning that it is not possible for it to reach the rated power of the water turbines. Although this suggests that the UFOWT is performing better on a scale of $\Gamma_{p,net}$, it is also indicative that

$\Gamma_{p,net}$ as a metric is not sufficient for comparing the two technologies. This is further discussed in section 3.4.

Also of interest is the performance of the two technologies under non-ideal conditions. Since the wind and wave loads are stochastic, unpredictable, and harsh when far offshore, the systems actual operating points will differ from their optimal ones

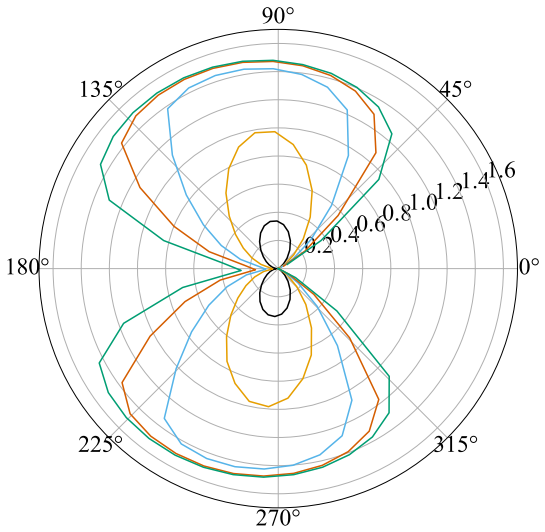

(a) Net power (P_{net}, MW)

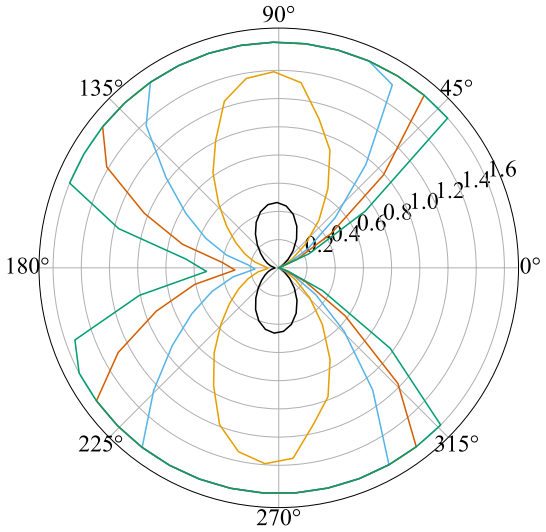

(b) Hydroturbine generated power (P_g, MW)

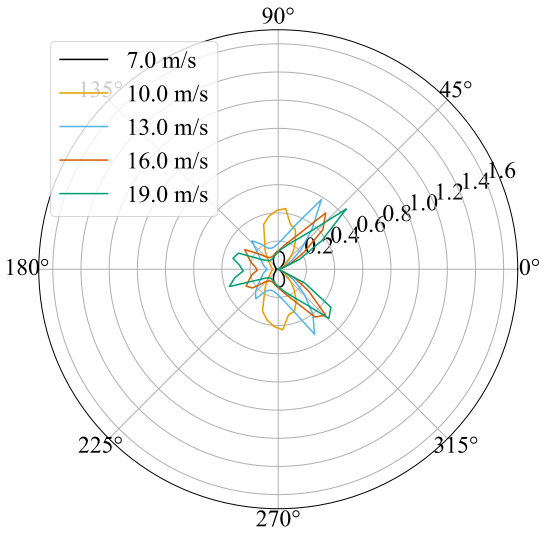

(c) Flettner rotor consumed power (P_p, MW)

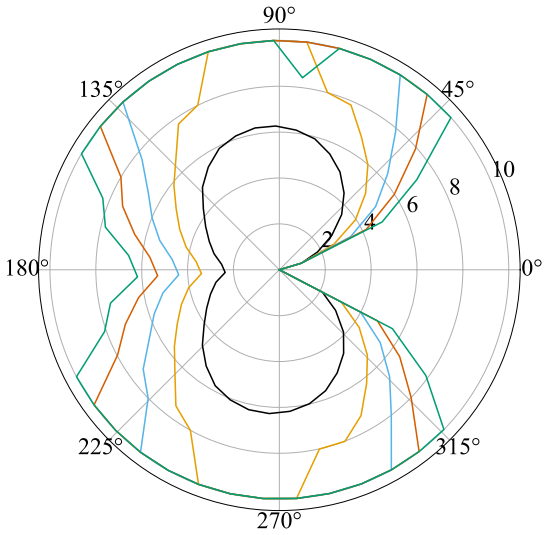

(d) Optimal vessel speed (V_b, m/s)

Figure 3.13: Power polar results for ES optimization as a function of V_1 for all TWAs.

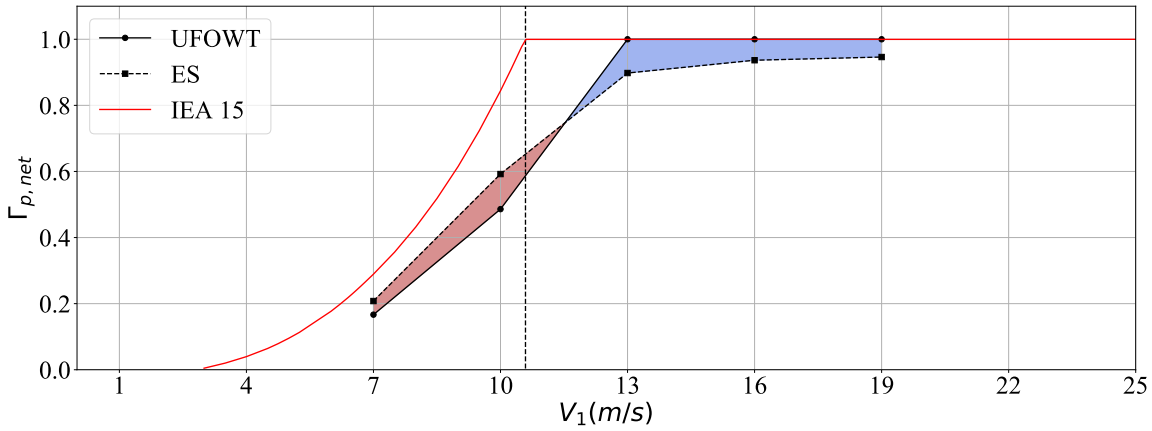

Figure 3.14: Effective power curve of each technology for their ideal TWAs. Wind speed is assumed equal at the reference height of each technology, as if there is no wind shear, so that both technologies have the same inflow speed.

frequently. In addition to errors in heading from stochastic wind and waves, performing well over a wide range of headings/wind angles may also be advantageous for routing a course for the system. Although this is not reflected in the power curve, it may result in increases in average capacity factor. The reduction in power performance of the technologies when at sub-optimal operating points is examined here for deviations in true wind angle and vessel speed separately. In these analyses, the net power is presented as a fraction of the maximum obtainable net power (instead of as a fraction of rated power) for each technology for each wind speed to isolate the effect of changing each variable.

The sensitivity of the net power of the two technologies to varying TWAs on either side of the optimal TWA is shown in Figure 3.15. From Figure 3.15 it is shown that for smaller deviations in wind angle ($\pm 20°$) the ES maintains better relative power performance in higher wind speeds. Beyond deviations of 20° which technology performs better depends mostly on whether the wind angle is increasing or decreasing. This is because the ES's power performance is not symmetric about its optimal TWA, whereas the UFOWT's is symmetric. Since the energy ship relies on Flettner rotors which are lifting surfaces to propel them, they perform relatively better for more downwind TWAs than more upwind ones.

The sensitivity of net power production to changes in vessel speed is examined in Figure 3.16. Both MOWESs sensitivity to relative changes in vessel speed is quite similar, with ESs only barely outperforming UFOWTs at high wind speeds. UFOWTs' change in net power is noticeably asymmetric over all wind speeds. This is because

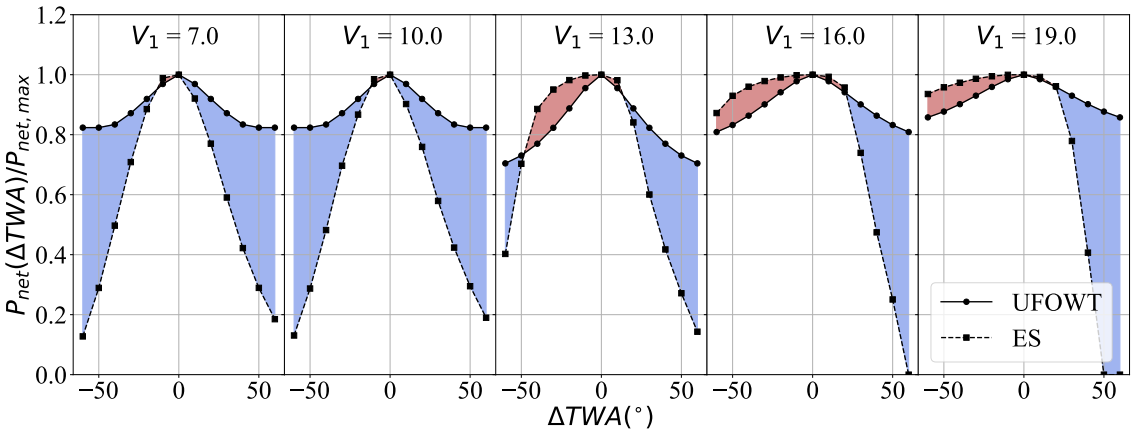

Figure 3.15: Net power loss for operation at sub-optimal wind angles. Panels show individual wind speeds (V_1, m/s) and ΔTWA is measured relative to the optimal wind angle for each technology for each wind speed. Power loss ($P_{net}(\Delta TWA)/P_{net,max}$) is defined relative to the maximum net power for a given wind speed for a given technology, to isolate the effect of changing wind angle.

the optimal TWA for UFOWTs is 0°, meaning increasing vessel speed corresponds to sailing downwind faster. Both a decrease in AWS at the wind turbine (thus decreasing P_g) and an increase in propeller thrust to overcome drag (thus increasing P_p consumed) come as a result of this increase in speed. At a TWS of 13 m/s, there is a local optimum for UFOWT performance after increasing vessel speed by about 20 %. This comes about because the wind turbine rotor was initially designed around a rated wind speed of 10.6 m/s, so at this point it achieves maximum C_p. A caveat to Figure 3.16 is that vessel speeds are plotted relative to the optimal vessel speed of each MOWES at each wind speed. This means that, for example, a 20% increase in vessel speed for the ES will often correspond to a total increase of about 2 m/s whereas the same relative increase for a UFOWT will be between 0.2-0.4 m/s. Absolute differences in vessel speed can be seen from Figures 3.9d and 3.13d; from these it is evident that energy ships travel much faster which is likely an advantage in terms of operation and routing. Overall, similar to the result for sensitivity to TWA, Figure 3.16 suggests that ESs will perform somewhat better from a capacity factor perspective than UFOWTs, since they are more flexible to plan routes.

Wind shear effect

All figures presented thus far show power production at the reference height for each technology respectively. However, the two technologies are very different heights. As

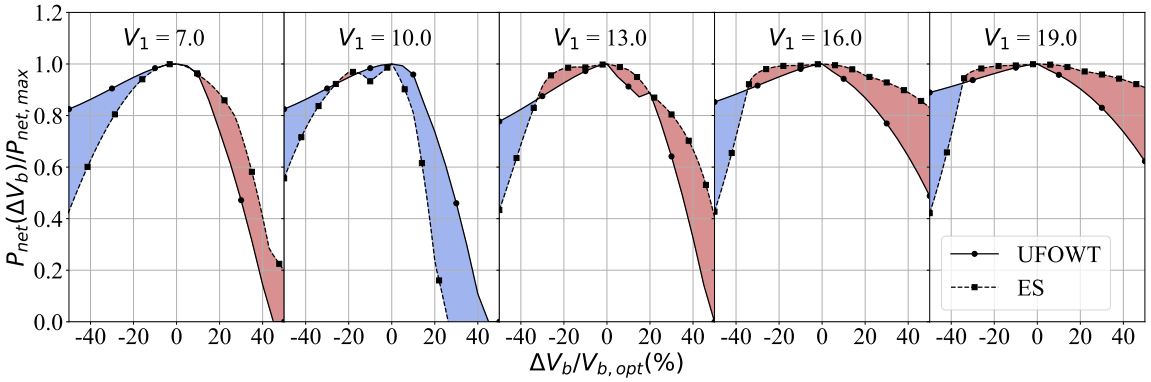

Figure 3.16: Net power loss for sub-optimal vessel speeds. Panels show individual wind speeds (V_1, m/s). Vessel speed is plotted as a percentage of the optimal vessel speed ($\Delta V_b/V_{b,opt}$, m/s) over a range of $\pm 50\%$ of the optimal vessel speed for the given V_1 and the optimal TWA.

discussed in section 3.2.4, this means that the UFOWT will experience much higher average wind speeds than the ES owing to the wind shear effect. Correcting for this, the normalized net power performance of each technology is shown in Figure 3.17 as a function of the TWS at a constant reference height of 10 m. When accounting for this difference, the UFOWT outperforms the ES for all wind speeds for an ideal TWA except for the last one, $V_{10m} = 19\ m/s$. As seen in Table 3.3 at wind turbine hub height this corresponds to $V_1 = 27.76\ m/s$, well above the cut-out speed for the conventional wind turbine. Although UFOWTs tend to reduce the local wind speed by moving downwind, in this case the UFOWT is not able to move downwind fast enough to reduce the wind speed to below the cut-off speed. This is an aspect of UFOWT design which can be explored further in future studies. Because of wind shear, the performance comparison in Figure 3.14 may be misleading, however, it was included since it is conventional to present power curves as a function of the wind speed at hub height, not at a reference height. The impact of wind shear is heavily design-dependent, since it relates directly to the height of the technologies. However, the designs proposed use the largest available Flettner rotors and the largest published reference wind turbine to make the comparison as fair as possible. This point must be carefully considered in the overall comparison of MOWESs, as scale will impact both dynamic feasibility as well as component and sub-system design and availability.

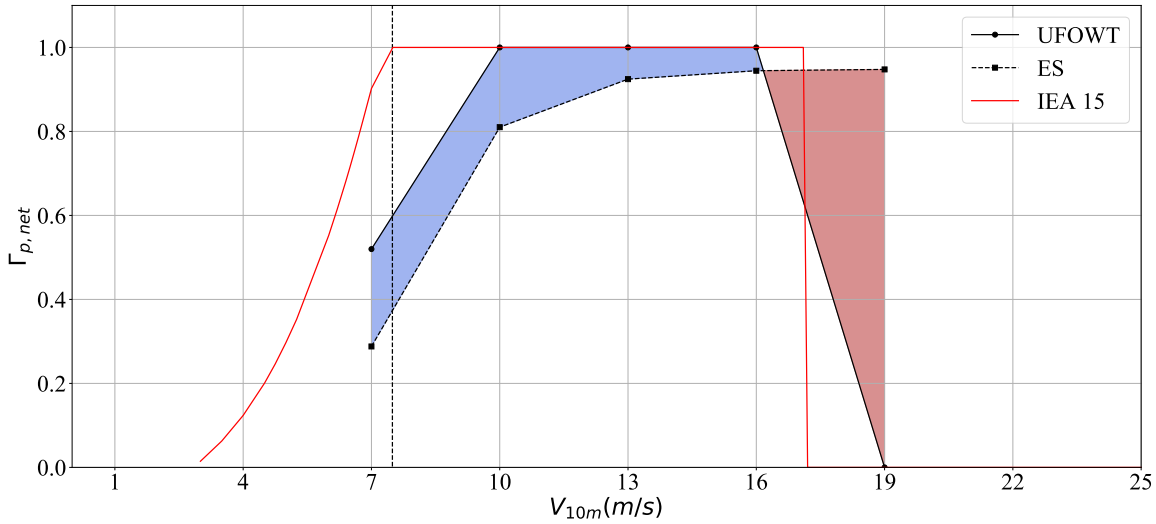

Figure 3.17: Effective power curve for each MOWES after accounting for wind shear effects.

3.4 Discussion

In the subsections that follow the limitations of the models and analysis are discussed. By virtue of being a preliminary idealized analysis of the performance of these technologies, many facets of the design and operation of a MOWES were overlooked.

3.4.1 Model concessions

Operating points that maximize the net power for each technology were computed in a two degree of freedom steady-state model of the system. Two bulk assumptions are made for these models: the assumption of steady-state, and the modelling of only two degrees of freedom. Each of these assumptions leads to omissions of details that should be considered by other models in the future. Firstly, analysing only the steady-states of the system allows the omission of dynamic wind and wave loading. Studying the response of these systems to these loads, as has been done for moored FOWTs, is imperative to understanding whether they are feasible and what design and controls modifications are required. Standard operational design load cases and extreme events will need to be analysed, since the system loads and response may differ greatly from a moored FOWT in both cases. These studies may also help refine estimates of power performance by considering power production under dynamic inflow conditions. Secondly, by only modelling the surge and sway degrees of freedom, much is left out

of the analysis. Modelling only surge and sway is adequate for representing the dominant steady loads on the system, however, future studies should consider more degrees of freedom. It will be especially important to analyse the pitching of each system when operating in severe wave conditions. The yaw behaviour of the UFOWT is also important to analyse. There may be a net yaw moment on the wind turbine rotor from variations in local AWA vertically, since the AWS will vary vertically due to wind shear. To effectively operate at sea, the propellers will need to prevent the UFOWT from yawing out of the wind.

In addition to the assumptions above, some steady loads have also been omitted from the analysis. These are namely mean drift wave loading, and loads from ocean currents. As mentioned in Section 3.1, mean drift loads were considered in a previous modelling study of UFOWTs [28]. However, for the semi-submersible platform used here it was expected that mean drift loads should be relatively small compared to other loads such as wind turbine thrust and platform drag. Whereas for a barge type platform, mean drift loads may be much larger and therefore should be considered. The effect of ocean current is omitted for simplicity, although it has been shown that currents can have a significant impact on the power generated by an UFOWT [7, 73]. Currents will effect UFOWTs and ESs differently, and therefore will impact the comparisons presented here, but as of yet the effect of currents on the performance of ESs has not been considered in any study. Ocean currents should also be considered in larger scale routing analysis as well, as they will impact on overall system trajectories.

There are many aspects which should be kept in mind when evaluating the comparisons between ESs and UFOWTs presented here (Figures 3.14, 3.15, 3.17). One such aspect is that the design of both systems should undergo further iteration. Neither design has yet been optimized, in terms of subsystem design or overall sizing, for cost or power production. To establish a more fair comparison between the two technologies would require design optimization studies for each, however, this is far beyond the scope of the present work.

3.4.2 Metrics of performance

The power performance of these systems has been compared under many environmental conditions, however, this alone is not adequate for determining if one or both of these technologies is feasible. More information is also required for clearly determining if one technology is a better candidate for further development than the other.

Ideally, the two technologies would be compared on a basis of levelized cost of energy (LCOE) first, as well as other metrics such as the life-cycle emissions of the technologies and their impact on other sustainable development goals. Although there is existing and ongoing research into additional study of ESs, including cost predictions, so far UFOWTs have many more research gaps. To reasonably estimate the LCOE of an UFOWT will require dedicated design optimization work as well as implementation of a weather-routing algorithm for capacity factor optimization of UFOWTs, as has been done for ESs. The present work has performed some preliminary steps which are necessary for these proposed further works.

Comparing the two technologies on the basis of power performance has some inherent flaws. By directly comparing the power performance of the two, it is as if all other dimensions are assumed equal (or perhaps irrelevant) for the two technologies. In reality, there are many other dimensions which are equally as important. The first of which, as was mentioned above, is the cost of the system. Since ultimately the viability of MOWESs depends on whether or not they will be able to produce a valuable product (i.e green e-fuel) at a profit, ultimately the cost per unit power should be considered. Here, the net power is instead normalized by the rated power of the system ($\Gamma_{p,net}$), which provides a less valuable means of comparison. An issue with $\Gamma_{p,net}$ is that ESs can fundamentally never reach their nameplate rated power, specifically, the nameplate capacity of the water turbines installed. Thus $\Gamma_{p,net}$ may be misleading, since at first glance it may seem that under ideal conditions both technologies should reach $\Gamma_{p,net} = 1$. This shows that for ESs the water turbine generators must be designed to be oversized, since some power will always be consumed to run the Flettner rotors. Indeed, ESs might also benefit from the use of rigid sails or kites as alternative propulsion technologies to avoid this issue. Normalizing by the rated power of each system also implies that the power curves/polars for each system would scale linearly with increasing rated power. This assumption is valid in the case where multiples of the same design are deployed, i.e a fleet of ten 1.5 MW ESs could be directly compared to a 15 MW UFOWT. However, for individual systems with different rated powers (i.e a 5MW wind turbine vs. a 15MW wind turbine) this assumption may not hold exactly, since many design aspects may change with changing size.

There are many factors other than power production that are also important for the feasibility of MOWESs. One such factor is the system stability while in operation, as discussed earlier. The operational vessel speeds will strongly play into the dynamics of each system, and so it is important to also compare them. Under most operating

conditions where the ES is producing considerable power, it is travelling at a speed of 10 m/s or about 20 kn (see Figure 3.13d). This is comparable to average speeds of container ships which range from $18 - 24$ kn [76, 86], but is much slower than the largest high-speed catamarans which travel at around 38 kn [75]. For high-speed vessels in severe wave environments, wave-slamming loads and subsequent whipping effects may be crucial to the operation and lifetime of the vessel, and so should also be considered for ESs in the future [75, 87]. While the UFOWT travels much slower, only around $1-3$ m/s (see Figure 3.9d), it is a much taller and heavier structure. No matter the effect of speed on the dynamics of the systems, moving faster may be an asset operationally, since it means the system can return to offload fuel more quickly and also travel to far-offshore areas with high wind speeds more quickly. This effect, and the robustness of each technology to operate in non-ideal TWAs and headings, come into play when determining routes for the system which maximize fuel/energy production, such as in [50].

3.4.3 Other Differences

Although this work has focused on quantitatively comparing the two MOWES technologies discussed, other important qualitative differences also exist between the two. One such difference is that each will rely on different supply chains to be manufactured at a large-scale. UFOWTs will benefit greatly from the existing wind turbine manufacturers, and port infrastructure that is being developed for FOWTs, and continues to develop as power grids become more electrified. On the other hand, ESs may benefit from growth of the wind propulsion sector, as the shipping sector decarbonizes. While some examples of deployed full-scale wind propulsion technologies exist, the global manufacturing capacity for wind turbine components is much greater.

3.5 Conclusions

As the offshore wind industry grows, far-offshore wind systems should be considered as an option for green e-fuel production. Steady-state, two degree of freedom models of two candidate MOWESs, the ES and the UFOWT, are presented. The ES model is reproduced from the work of Babarit et al. [4] to compare the power performance of ESs to that of UFOWTs. The UFOWT model achieves steady-state in surge and sway by determining the thrust required by the propellers to sustain wind turbine thrust

loads as well as platform drag. Both technologies have dedicated subsystems for power generation and subsystems which consume power for propulsion. An optimization is employed to determine operating points for these systems that maximize net power generation over a range of possible wind speeds and TWAs.

Model results presented show some relative strengths of the ES and the UFOWT when compared to one another. While an UFOWT is able to produce a higher fraction of its rated power under ideal wind conditions compared to an ES, an ES is more robust to operating in various headings/TWAs as well as various vessel speeds. Both peak operating efficiency and robustness to operating in sub-optimal conditions will impact the capacity factor of the systems. A relative advantage of UFOWTs over ESs is that they benefit more from the effect of wind shear because of their prodigious height. Regeneration via the propellers was not an exploitable means of power generation for the UFOWT design used here, however, it may be exploitable given a more rigorous design process. Further work is required to compute estimates of the capacity factor of an UFOWT to be compared to published ES capacity factors. Neither technology should be ruled out as a potentially cost-effective, novel, means of producing green e-fuels that are necessary for the ongoing global energy transition.

Chapter 4

Conclusions

Herein I have endeavoured to examine the feasibility of MOWESs through the development and analysis of numerical models. More specifically, this work focuses on determining the power production of these systems to assess how they perform relative to conventional wind turbines. Two unique numerical models of UFOWTs were developed and an ES model was produced based on a well established model. A one-dimensional steady-state model of a UFOWT was developed first to analyse large-scale design choices, such as subsystem sizing, and operational choices, such as upwind versus downwind operation. Subsequently, a two-dimensional steady-state model was developed to look at UFOWT power production in more detail. A two-dimensional ES model was also developed based on the work of Babarit et al. for the sake of comparison [4]. An optimization scheme was employed to guarantee that the latter models arrive at operating points that correspond to optimal power production under any given set of wind conditions. All models were developed to allow for investigation into key design and operation questions for MOWESs, outlined in section 1.2. Model results have given promising direction for further MOWES research in terms of dynamics modelling, design optimization, optimal control, and routing.

The main metric of interest for this work has been net power production. Power production is a core metric in itself, and is also useful for subsequent analyses. Indeed, to evaluate the cost of energy, to evaluate system design choices, and to determine the consequences of system dynamics the power production of the system must first be well understood. The main contribution of this work is in producing a readily-reproducible power performance model of a UFOWT that predicts it's optimal power production for a given design under any wind conditions.

4.1 Key Findings

Model results lead to several important conclusions on the design and operation of MOWESs, discussed in turn here:

1. *No matter how the UFOWT is designed, it may always achieve higher net power production by moving than by remaining stationary.*

   Despite the consensus in existing literature of modelling UFOWTs only to be station-kept, results of both models suggest that mobile UFOWTs generate more power. Figure 2.6 shows that for low-drag systems it is best for the system to operate moving upwind, whereas for high-drag systems moving downwind is better. This is corroborated by the results of the 2D model developed in chapter 3. The design used in this case was a high-drag one, using a semi-submersible platform, and the optimization determined that moving downwind can lead to rated power production whereas moving upwind produces much less. This result should serve to direct further research into mobile concepts instead of strictly station-kept unmoored systems. In particular, research directed at hull/platform optimization and wind turbine rotor design to optimize UFOWT operating points will be necessary.

2. *Both UFOWT designs that are intended to move upwind or downwind may be feasible. Higher maximum power production is predicted for downwind UFOWT designs than upwind designs.*

   Results of the one-dimensional UFOWT model show that designs based on existing concepts for upwind and downwind UFOWTs may both be feasible. While downwind designs seem to produce more power under ideal conditions, upwind designs may have other logistical and operational benefits. Upwind concepts require a low-drag subsystem such as a ship hull and will tend to move faster than downwind systems. Because of this, they may be able to reach areas of high wind quicker, resulting in an increase in CF. Also similarly to ESs, they may be more robust to operating at non-ideal vessel speeds. Downwind concepts can produce more power under ideal conditions, but as shown in Figure 3.16, they are extremely sensitive to changes in vessel speed. Although it was not directly exploited in model results presented, power take-off by the thrusters in downwind operation may also be possible to further increase net power above

conventional wind turbine rated power. Both design types merit further investigation, especially at the level of routing optimization to see if the potential upsides of upwind UFOWTs can be exploited.

3. *UFOWTs can produce as much power as a stationary turbine in above-rated wind speeds.*

Although not predicted by the one-dimensional UFOWT model, the two-dimensional model shows that UFOWTs can produce up to the same rated power as a conventional wind turbine when operating in above rated wind speeds. This result is not present in the one-dimensional model, and indeed is not present in other existing literature, since it does not account for the thrust and power coefficients of the wind turbine and how they change in the different regions of operation. Figure 3.11 shows that the power curve for the UFOWT reaches rated power at wind speeds about 2 m/s higher than the conventional FOWT. However, given that wind speeds are higher offshore, this shift may be effectively offset by operating in the open ocean. More detailed design studies should consider this when sizing the wind turbine rotor and generator for UFOWTs. Power production will also be affected by the system dynamics, and so this result should be confirmed using future dynamic UFOWT simulations.

4. *Under ideal conditions, an UFOWT produces more power than an ES, however, ESs are more robust to non-ideal conditions.*

Figure 3.14 directly compares power production of the two technologies, showing that UFOWTs are able to produce more power at high wind speeds. When wind shear is accounted for (Figure 3.17), UFOWTs produce more power at all wind speeds within their operating range. Together these results suggest that no matter the relative physical scale of the technologies, UFOWTs' power production under ideal conditions is greater than that of ESs. This result comes in part from the fact that ESs will always consume some power to spin the Flettner rotors, meaning they will never reach their nameplate rated power. The advantage of ESs is that their power production remains relatively higher than UFOWTs' for sub-optimal vessel speeds. This illustrates the importance of further research into routing of UFOWTs, so that an estimate of their CF can be calculated and see if the operational/routing benefits of ESs outweigh the better peak performance of UFOWTs.

5. *Both types of MOWESs discussed merit further research.*

Many differences between UFOWTs and ESs are described in chapter 3, but ultimately the discrepancies between their predicted performance are not substantial enough to dissuade continued research into either concept. The significant differences presented herein may guide intuition into expected results of future work. For example, since UFOWTs tend to move much slower than energy ships, it is expected that their CF over a short period will vary much more than for ESs, since they cannot as easily reach areas with locally high wind speeds. UFOWTs also tend to incur greater losses for operating in non-ideal conditions, which may also increase the variance in CFs. On the other hand, the higher speeds of ESs create greater risk of wave-slamming events which may limit their operational sea states. Much more research, as outlined in section 4.2, is necessary to conclusively say if one technology is more economical, more efficient, or otherwise more feasible than the other.

MOWESs have proven to be a potentially viable means of producing renewable energy far-offshore and for off-grid processes at this level of analysis. Models developed here have built upon existing models, and advanced modelling methodology for UFOWTs. Results for ES and UFOWT power performance are promising, though in most cases they are not able to produce as much power as conventional FOWTs. That said, MOWESs need not produce as much power as existing renewables since they are exploiting an otherwise unused part of the wind resource. From a global climate and decarbonization perspective, MOWESs may appear to be a distraction away from more well-established renewable energy systems. However, MOWESs occupy a niche in that they can provide green fuels, a commodity which there is a growing need for, without competing for grid power or space on- or off-shore. Many technical barriers remain before MOWESs may be technologically ready, however, these can be tackled through research and development in academia or industry, leveraging existing institutions in wind energy. Existing manufacturing capacity of important parts for MOWESs (such as wind turbine blades or Flettner rotors) developed for the wind energy and wind propulsion sectors may help MOWESs scale-up faster than concepts relying on wholly novel energy generation strategies. Although MOWESs may seem far-fetched at first, that is often true of innovative technologies, especially those that reshape our world.

4.2 Future Work

Although the main focus of this work was to understand the fundamental power performance of MOWESs and how they relate to design and operation, many other related and important research questions remain unanswered. Other aspects of MOWESs such as dynamics may directly impact power performance. Still others such as routing will not directly impact power performance, but will impact the energy production and therefore the CF. The goal of this section is to outline the most important research questions which were not the main focus of this work, but that require attention in the future. This chapter focuses on three main topics for future MOWES development:

1. System Dynamics: All MOWESs will interact with stochastic winds and waves. The response of the system under these conditions may directly impact power performance and will also need to be verified against system dynamics constraints. Changes in system loads may also affect the fatigue life of system components, potentially resulting in more frequent maintenance.

2. Course Routing: To achieve optimal CFs, MOWESs must choose courses which maximize power production along the way. Although research exists on weather routing of energy ships, this has not yet been generalized to other concepts [50].

3. Holistic System Design Optimization: MOWESs have several component systems, each of which can vary in many aspects. Thus far, MOWES designs are based on reference designs used in other contexts; this means that a power/energy optimal or cost optimal system design has not yet been identified. Component level optimization may also be necessary, such as optimizing the wind turbine rotor for UFOWTs to tailor thrust and power coefficients to optimal operating points. Design of other subsystems that were not studied here is also necessary, such as sizing and control of the PtX or CO_2 capture system with associated storage systems to use the produced power efficiently.

It is important to note that although these topics are presented independently, they are, realistically, interconnected. For example, an algorithm may be developed to optimize the course of a given MOWES, but the solutions produced for that given system depend inherently on the design of the system. The course may also depend upon results of system dynamics studies, since the harshest environmental conditions may need to be avoided for system safety. Here each research topic is addressed in

isolation and it is expected that results of each should be used to guide subsequent studies. This section may also serve to guide future research projects focused on MOWESs.

Other important research topics will also arise, that are not directly addressed below. These may include lifecycle emissions assessments, environmental assessments, supply-chain and scalability assessments, operational and maintenance assessments, and other yet unknown challenges. Furthermore, the models developed herein can be used directly for further analysis, such as a combined sensitivity analysis of MOWESs to operation in any TWA and at any vessel speed. This would combine the results from Figures 3.15 and 3.16, and would explore a space that combines the ranges of these to understand MOWES performance over all possible operating conditions.

4.2.1 System Dynamics

UFOWTs

As of yet, the dynamics of UFOWTs have not been studied to a satisfactory extent. Multi-DOF, coupled simulations of aerodynamics, hydrodynamics, flexible body dynamics, and control dynamics are commonplace for FOWT research, however, so far UFOWT simulations have been limited to only some of these aspects. The work of Xu et al. focused on time-domain simulation of an UFOWT, but used a simplified aerodynamics model and was limited to a stationary UFOWT [7]. Willeke simulated a fully-coupled UFOWT system, however, the results were limited by the omission of a propulsion system to stabilize the UFOWT, resulting in failed simulations due to large rotations of the system [29].

Novel modelling methodology may be required to construct an accurate dynamics model of a UFOWT. Multi-physics models such as OpenFAST represent different physical phenomena through separate modules, however, in the case of OpenFAST there is no module to represent the propellers of an UFOWT [88, 89]. OpenFAST in particular has been extended to include more modules (i.e MoorDyn for dynamic mooring system simulation [90, 91]), and also adapted for different applications such as airborne wind energy and the program KiteFAST [92]. For UFOWTs, the propellers must be actively controlled based on changing environmental conditions, and so a coupled modelling approach including propeller control system integration is likely necessary. Existing FOWT models may also need to be adapted for the fact that UFOWTs should operate about a constant (and non-zero) velocity in most cases

to maximize power production. This will have an impact on the wind-system and wave-system interactions. Wind and wave conditions are represented using frequency dependent spectra. Since UFOWTs will move during operation they will tend to encounter the wind and waves at different frequencies (referred to as encounter frequency) than their ambient frequencies. The implications of this are that depending on the heading of the UFOWT relative to the wind and wave directions, the UFOWT will experience forcing in different proportions at different frequencies than for a conventional FOWT. System natural frequencies may be excited or potentially avoided because of this shift, so some parts of UFOWT designs such as tower design and controller designs may need to be reconsidered based on dynamics simulation results. A coupled model will be necessary to capture all relevant effects, such as the well-known problem of negative-damping that can occur when a floating wind turbine's blade pitch controller acts at a similar frequency to the rigid-body pitch natural frequency of the system [93]. For UFOWTs, a controller for the propeller system will also need to be designed and similar effects with the effective damping due to the controller should be considered.

Representative and extreme load cases (LCs) will also be very different for UFOWTs than for FOWTs. Given the fact that the system operates far-offshore, it is reasonable to assume that the average sea state that it operates in will be more severe than those of conventional FOWTs in shallower waters. This will have an effect on the ultimate loads experienced by the UFOWT, for example since a 1-year wave event far offshore will be much worse than a 1-year wave event near shore. More severe average sea states will also impact fatigue loads. A representative operational sea-state will be more severe for UFOWTs than FOWTs, so average wave-loading will increase and therefore so will the response of the UFOWT. This means that in normal operation UFOWTs may be heaving and pitching more than a conventional FOWT under analogous LCs, which could be detrimental to the fatigue life of the system. Standard sets of design LCs exist for FOWTs (see [94, 95]), but these will need to be revised for UFOWTs considering the system is unmoored and mobile while operating.

Energy ships

No work has yet been published on the dynamics of an ES. Similarly to an UFOWT, ES system dynamics will impact the power production since power generated depends on the vessel speed. For a course project during my degree program I developed a

model of an ES in ProteusDS to examine the effect of system dynamics on stability and power production [96]. Model results suggest that the effect of wave-loading on the ship can positively affect power production in cases where waves propagate in the same direction as the ship, whereas large power losses occur when the ship sails against the waves. In terms of stability, the ship showed large pitch and roll rates when subjected to harsh wave environments. A more detailed model is required to verify the results of this model, however, these results show that investigating the dynamics warrants further research. Results of such an ES model may better inform system design, such as through analysing ultimate loads on the Flettner rotors under various environmental conditions and headings. Similarly to UFOWTs, active control systems will need to be designed for the propulsion and generation subsystems; coupled dynamics models of ESs should include these to fully capture coupled effects.

4.2.2 Course Routing

Determining a route for a MOWES is an essential problem in determining it's energy production. Typically, for stationary wind turbines the annual energy production (AEP) is determined by simply numerically integrating the power produced by the wind turbine given the wind speed at each point in time, over a period of time. This is analogous to the numerator of equation 1.1. However, since wind speeds vary spatially and MOWESs are mobile, the summation must consider the wind speed locally in both time and space:

$$AEP_{MOWES} = \sum_{i=0}^{T} P(V_i(t_i, x_i, y_i))\Delta t$$

where x_i and y_i indicate the position of the vessel at time t_i. The fact that the system is mobile in this case introduces an optimization problem which is not present for stationary wind turbines. Since the MOWES has control over the course it takes, it may maximize energy production by intelligently choosing its path relative to stochastic weather systems. Optimal courses for each individual route may vary greatly depending on weather system variation. Moreover, the design of the system will greatly influence routing decision-making based on factors such as operational vessel speeds, optimal headings, limiting extreme weather conditions, and quantity of storage onboard the vessel. Re-evaluating MOWES designs based on routing results may also be necessary, although this combined design and operation problem may be very

complex.

Weather routing for energy ships has been studied by Abd Jamil et al. [50, 40]. Their work modifies an existing routing optimization program, traditionally used for planning optimal routes for shipping vessels, to instead optimize energy production. For routes in the north Atlantic ocean, they compute CFs of up to 95%, with an average capacity factor of above 80%. Existing floating offshore wind farms have reported CFs of 50% or more, suggesting that energy ships can be effective at taking advantage of the higher wind speeds that are present far offshore [34]. Despite this, it is important to recall that the CF is a relative measure of energy captured to what is possible based on the nameplate rated power of the system (see equation 1.1). This means that a system with very large generator capacity, such as a 15 MW wind turbine, with a much lower CF may out-perform a smaller capacity system with much higher CF. At this level, it becomes apparent why LCOE is an important metric to compare across multiple systems in a fair and unambiguous way, since it accounts for the energy production dimensionally. Although it is promising that energy ships can produce such high CFs, no similar published result exists for UFOWTs. Based on the results of chapter 3, UFOWTs may have a much higher variability in their CFs since their power output reduces more in sub-optimal environmental conditions than ESs'.

As part of the coursework for my degree program, I developed a similar routing model and applied it to the case of energy ships, but examined the area off the coast of the Pacific Northwest [9]. Figure 4.1 shows the mean wind speed at each point in the space available to the energy ship in the model. Instead of using an optimization approach, a weighted rules-based controller was developed that makes use of several parameters: local wind speed, local average wind power density, efficiency of the energy ship under current conditions, and change in heading. Several model tunings were tested, and most performed quite similarly to one another, achieving average CFs of 57% over many random trials. CFs were also calculated for hypothetical stationary wind turbines at each grid-point. The maximum CF achieved by a wind turbine over the chosen area was 0.65; less than the maximum for ESs computed in [50], but greater than the average for any model tuning. These results show that CFs may vary largely depending on the location where energy ships are deployed, as evidenced by [40].

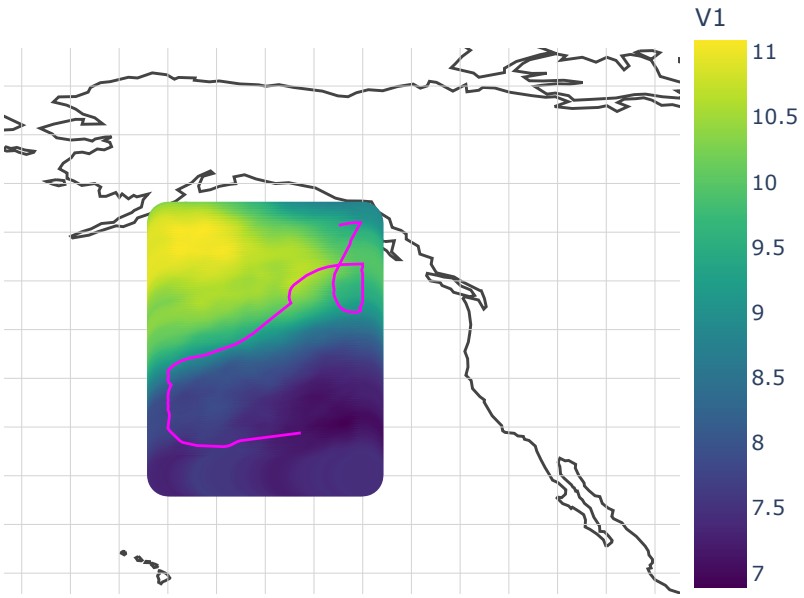

Figure 4.1: 6-month (Jul.-Dec. 2017) mean wind speed (m/s) off the coast of the Pacific Northwest from the ERA5 re-analysis dataset [8]. A sample ES route is plotted for a one week voyage. Based on course work from [9].

4.2.3 System Design Optimization

The problem of system design is mentioned throughout this work, since the design of the system affects all model results. No design optimization studies have been conducted yet for UFOWTs or ESs. It is reasonable to assume from this that improvements may be made in the design of each type of MOWES in terms of efficiency and cost. System design optimization could be performed at many levels from rotor/platform sizing down to wind turbine blade optimization. Results presented in chapters 2 and 3 show the importance of analysing MOWES designs at various levels. Figures 2.5 and 2.6 show the impact of large-scale subsystem design on power performance and on ideal system operation. In addition, Figures 3.11 and 3.12 show the consequences of operational decisions, which should ultimately be designed for.

MOWESs have many subsystems and therefore many design choices are necessary. Optimizing the design of all components holistically may require significant computational effort since many design variables would be required. There are also multiple possible objective functions to be considered, such as cost metrics, dynamic stability metrics, fatigue life metrics, and life-cycle emissions metrics. It therefore seems prudent to study subsystem design individually first, identifying where major

gains may be possible in this way. Based on the results of this work, for UFOWTs I recommend first looking into thruster design optimization. Results of chapter 3 show that UFOWTs are at their most efficient when the thrusters do not operate at all, however, the thrusters in reality will need to operate often to stabilize and course-keep the system. As well, further investigation of thruster design may show if multi-purpose thruster/turbine designs are feasible using variable pitch thrusters or through other means. Co-design of the platform and wind turbine will also be key for maximizing UFOWT power output, since ideal power production is driven largely by the wind turbine thrust-power tradeoff as well as platform drag to counteract the thrust. This could be done through optimization by using an objective function corresponding to the net UFOWT power output (i.e $\Gamma_{p.net}$ or similar), or combined with a routing algorithm using an objective of system energy production. A vast design space is possible for such an optimization, spanning wind turbine blade characteristics (i.e chord, twist, blade length etc.) as well as platform characteristics (i.e draft, number of columns, column diameter, waterplane area etc.).

In the case of ESs, system design may also still be optimized. Clodic et al. concluded that many propulsion technologies may be suitable for energy ships, but further work has focused on Flettner rotor based designs. Re-evaluation of alternative propulsion technologies may be prudent as the wind propulsion sector grows, since one of the major barriers for other propulsion technologies (such as kite wings and turbo-sails) is a lack of technological maturity. The combined design and routing problem will also be important in this case, since different propulsion technologies will perform best under different wind conditions, thus changing optimal routes.

Bibliography

[1] E. Gaertner, J. Rinker, L. Sethuraman, F. Zahle, B. Anderson, G. Barter, N. Abbas, F. Meng, P. Bortolotti, W. Skrzypinksi, G. Scott, R. Feil, H. Bredmose, K. Dykes, M. Shields, C. Allen, and A. M. Viselli, "IEA Wind TCP Task 37: Definition of the IEA 15-Megawatt Offshore Reference Wind Turbine," Technical Report NREL/TP-5000-75698, NREL, 2020.

[2] C. Allen, A. Viscelli, H. Dagher, A. Goupee, E. Gaertner, N. Abbas, M. Hall, and G. Barter, "Definition of the UMaine VolturnUS-S Reference Platform Developed for the IEA Wind 15-Megawatt Offshore Reference Wind Turbine," Tech. Rep. NREL/TP-5000-76773, 1660012, MainId:9434, July 2020.

[3] M. M. Bernitsas, D. Ray, and P. Kinley, "Kt, Kq, and Effficiency Curves for the Wageningen B-Series Propellers," Tech. Rep. 237, University of Michigan, Departmenet of Naval Architecture and Marine Engineering, University of Michi, May 1981.

[4] A. Babarit, F. Gorintin, P. de Belizal, A. Neau, G. Bordogna, and J.-C. Gilloteaux, "Exploitation of the far-offshore wind energy resource by fleets of energy ships – Part 2: Updated ship design and cost of energy estimate," *Wind Energy Science Discussions*, pp. 1–22, June 2021. Publisher: Copernicus GmbH.

[5] Norespower, "Rotor Sail Technical Specifications," brochure, Norsepower, Helsinki, Finland.

[6] F. Tillig and J. W. Ringsberg, "Design, operation and analysis of wind-assisted cargo ships," *Ocean Engineering*, vol. 211, p. 107603, Sept. 2020.

[7] S. Xu, M. Murai, X. Wang, and K. Takahashi, "A novel conceptual design of a dynamically positioned floating wind turbine," *Ocean Engineering*, vol. 221, p. 108528, Feb. 2021.

[8] H. Hersbach, B. Bell, P. Berrisford, G. Biavati, A. Horányi, J. Muñoz Sabater, J. Nicolas, C. Peubey, R. Radu, I. Rozum, D. Schepers, A. Simmons, C. Soci, D. Dee, and J.-N. Thépaut, "ERA5 hourly data on single levels from 1979 to present," *Copernicus Climate Change Service (C3S) Climate Data Store (CDS).*, 2018.

[9] P. Connolly, "Far Offshore Wind Resource for Mobile Wind Energy Capture: The Case for Energy Ships," tech. rep., University of Victoria, Dec. 2020. (Unpublished coursework, available upon request).

[10] R. A. Rohde and Z. Hausfather, "The Berkeley Earth Land/Ocean Temperature Record," *Earth System Science Data*, vol. 12, pp. 3469–3479, Dec. 2020. Publisher: Copernicus GmbH.

[11] H. Portner, D. Roberts, E. Poloczanka, K. Mintenbeck, M. Tignor, A. Alegria, M. Craig, S. Langsdorf, S. Löschke, V. Möller, A. Okem, and B. Rama, "IPCC, 2022: Summary for Policy Makers," 2022. Contribution of Working Group II to the Sixth Assessment Report of the Intergovernmental Panel on Climate Change.

[12] IRENA, "A Pathway to Decarbonise the Shipping Sector by 2050," technical Report, International Renewable Energy Agency (IRENA), Abu Dhabi, 2021.

[13] T. R. Lucas, A. F. Ferreira, R. Santos Pereira, and M. Alves, "Hydrogen production from the WindFloat Atlantic offshore wind farm: A techno-economic analysis," *Applied Energy*, vol. 310, p. 118481, Mar. 2022.

[14] A. Singlitico, J. Østergaard, and S. Chatzivasileiadis, "Onshore, offshore or in-turbine electrolysis? Techno-economic overview of alternative integration designs for green hydrogen production into Offshore Wind Power Hubs," *Renewable and Sustainable Energy Transition*, vol. 1, p. 100005, Aug. 2021.

[15] Ø. Ulleberg, T. Nakken, and A. Eté, "The wind/hydrogen demonstration system at Utsira in Norway: Evaluation of system performance using operational data and updated hydrogen energy system modeling tools," *International Journal of Hydrogen Energy*, vol. 35, pp. 1841–1852, Mar. 2010.

[16] N. McQueen, K. V. Gomes, C. McCormick, K. Blumanthal, M. Pisciotta, and J. Wilcox, "A review of direct air capture (DAC): scaling up commercial tech-

nologies and innovating for the future," *Progress in Energy*, vol. 3, p. 032001, July 2021.

[17] D. W. Keith, G. Holmes, D. S. Angelo, and K. Heidel, "A Process for Capturing CO2 from the Atmosphere," *Joule*, vol. 2, pp. 1573–1594, Aug. 2018. Publisher: Elsevier.

[18] R. Hanna, A. Abdulla, Y. Xu, and D. G. Victor, "Emergency deployment of direct air capture as a response to the climate crisis," *Nature Communications*, vol. 12, p. 368, Jan. 2021.

[19] G. Realmonte, L. Drouet, A. Gambhir, J. Glynn, A. Hawkes, A. C. Köberle, and M. Tavoni, "An inter-model assessment of the role of direct air capture in deep mitigation pathways," *Nature Communications*, vol. 10, p. 3277, July 2019. Number: 1 Publisher: Nature Publishing Group.

[20] A. Babarit, N. Abdul Ghani, E. Brouillette, S. Delvoye, M. Weber, A. Merrien, M. Michou, and J. C. Gilloteaux, "Experimental validation of the energy ship concept for far-offshore wind energy conversion," *Ocean Engineering*, vol. 239, p. 109830, Nov. 2021.

[21] M. Karimi, M. Hall, B. Buckham, and C. Crawford, "A multi-objective design optimization approach for floating offshore wind turbine support structures," *Journal of Ocean Engineering and Marine Energy*, vol. 3, pp. 69–87, Feb. 2017.

[22] J. M. Hegseth, E. E. Bachynski, and J. R. R. A. Martins, "Integrated design optimization of spar floating wind turbines," *Marine Structures*, vol. 72, p. 102771, July 2020.

[23] A. N. Robertson, F. Wendt, J. M. Jonkman, W. Popko, H. Dagher, S. Gueydon, J. Qvist, F. Vittori, J. Azcona, E. Uzunoglu, C. G. Soares, R. Harries, A. Yde, C. Galinos, K. Hermans, J. B. de Vaal, P. Bozonnet, L. Bouy, I. Bayati, R. Bergua, J. Galvan, I. Mendikoa, C. B. Sanchez, H. Shin, S. Oh, C. Molins, and Y. Debruyne, "OC5 Project Phase II: Validation of Global Loads of the DeepCwind Floating Semisubmersible Wind Turbine," *Energy Procedia*, vol. 137, pp. 38–57, Oct. 2017.

[24] A. Babarit, G. Clodic, S. Delvoye, and J.-C. Gilloteaux, "Exploitation of the far-offshore wind energy resource by fleets of energy ships – Part 1: Energy ship

design and performance," *Wind Energy Science*, vol. 5, pp. 839–853, July 2020. Publisher: Copernicus GmbH.

[25] G. Clodic, A. Babarit, and J.-C. Gilloteaux, "Wind Propulsion Options for Energy Ships," American Society of Mechanical Engineers Digital Collection, Dec. 2018.

[26] M. F. Platzer and N. Sarigul-Klijn, "Wind-Propelled Ship Technology," in *The Green Energy Ship Concept: Renewable Energy from Wind Over Water* (M. F. Platzer and N. Sarigul-Klijn, eds.), SpringerBriefs in Applied Sciences and Technology, pp. 81–87, Cham: Springer International Publishing, 2021.

[27] M. F. Platzer and N. Sarigul-Klijn, "Major Elements and Developmental Status of the Energy Ship Concept," in *The Green Energy Ship Concept: Renewable Energy from Wind Over Water* (M. F. Platzer and N. Sarigul-Klijn, eds.), SpringerBriefs in Applied Sciences and Technology, pp. 37–41, Cham: Springer International Publishing, 2021.

[28] R. Alwan, A. Babarit, and J. C. Gilloteaux, "Investigation of a dynamically positioned floating offshore wind turbine concept," *Journal of Physics: Conference Series*, vol. 2018, p. 012001, Sept. 2021. Publisher: IOP Publishing.

[29] L. Willeke, "Concept study of a sailing offshore wind turbine," 2021. Accepted: 2021-04-27T15:12:52Z Publisher: Stuttgart.

[30] A. M. Annan, M. A. Lackner, and J. F. Manwell, "Wind Trawler: operation of a wind energy system in the far offshore environment," *Journal of Physics: Conference Series*, vol. 1452, p. 012031, Jan. 2020. Publisher: IOP Publishing.

[31] X. Martínez Beseler, "Innovative Autonomously-Driven Offshore Wind Turbines: a prefeasibility analysis," May 2020. Accepted: 2020-05-11T10:42:22Z Publisher: Universitat Politècnica de València.

[32] M. Gaunaa, S. Øye, and R. Mikkelsen, "Theory and design of flow driven vehicles using rotors for energy conversion," in *EWEC Proceedings*, 2009.

[33] A. Babarit, J.-C. Gilloteaux, G. Clodic, M. Duchet, M. F. Platzer, and a. simoneau, "Techno-economic feasibility of fleets of far offshore hydrogen-producing wind energy converters," *International Journal of Hydrogen Energy*, 2018. Publisher: Elsevier.

[34] I. E. Agency, "Offshore Wind Outlook 2019: World Energy Outlook Special Report," world Energy Outlook Special Report, International Energy Agency, 2019.

[35] C. Barrera, I. Padron, F. S. Luis, and O. Llinas, "Trends and challenges in unmanned surface vehicles (USV): From survey to shipping," *TransNav : International Journal on Marine Navigation and Safety of Sea Transportation*, vol. Vol. 15 No. 1, 2021.

[36] K. Tanakitkorn, "A review of unmanned surface vehicle development," *Maritime Technology and Research*, vol. 1, pp. 2–8, Jan. 2019. Number: 1.

[37] I. M. Organization, "Outcome Of The Regulatory Scoping Exercise For The Use Of Maritime Autonomous Surface Ships (MASS)," Tech. Rep. MSC.1/Circ.1638, June 2021.

[38] D. Sutter, M. van der Spek, and M. Mazzotti, "Evaluation of CO2-Based and CO2-Free Synthetic Fuel Systems Using a Net-Zero CO2-Emission Framework," *Industrial & Engineering Chemistry Research*, vol. 58, pp. 19958–19972, Oct. 2019.

[39] T. Placke, R. Kloepsch, S. Dühnen, and M. Winter, "Lithium ion, lithium metal, and alternative rechargeable battery technologies: the odyssey for high energy density," *Journal of Solid State Electrochemistry*, vol. 21, pp. 1939–1964, July 2017.

[40] R. Abd Jamil, J.-C. Gilloteaux, P. Lelong, and A. Babarit, "Investigation of the Capacity Factor of Weather-Routed Energy Ships Deployed in the Near-Shore," American Society of Mechanical Engineers Digital Collection, Apr. 2021.

[41] M. Drela, "Dead Down Wind Faster Than The Wind (DDWFTTW) Analysis," Jan. 2009.

[42] J. Lee and F. Zhao, "Global Wind Report 2021," economic, Global Wind Energy Council, Belgium, Mar. 2021.

[43] W. Musial, P. Spitsen, P. Beiter, P. Duffy, M. Marquis, A. Cooperman, R. Hammond, and M. Shields, "Offshore Wind Market Report: 2021 Edition," Economic DOE/GO-102021-5614, U.S Department of Energy, 2021.

[44] A. Jacobsen and M. Godvik, "Influence of wakes and atmospheric stability on the floater responses of the Hywind Scotland wind turbines," *Wind Energy*, vol. 24, no. 2, pp. 149–161, 2021. _eprint: https://onlinelibrary.wiley.com/doi/pdf/10.1002/we.2563.

[45] C. M. Fontana, S. R. Arwade, D. J. DeGroot, A. T. Myers, M. Landon, and C. Aubeny, "Efficient Multiline Anchor Systems for Floating Offshore Wind Turbines," in *Proceedings of the 35th International Conference on Ocean, Offshore and Arctic Engineering*, (Busan, South Korea), June 2016.

[46] G. Liang, Z. Jiang, and K. Merz, "Mooring Analysis of a Dual-Spar Floating Wind Farm With a Shared Line," *Journal of Offshore Mechanics and Arctic Engineering*, vol. 143, May 2021.

[47] P. Connolly and M. Hall, "Comparison of pilot-scale floating offshore wind farms with shared moorings," *Ocean Engineering*, vol. 171, pp. 172–180, Jan. 2019.

[48] G. Gahleitner, "Hydrogen from renewable electricity: An international review of power-to-gas pilot plants for stationary applications," *International Journal of Hydrogen Energy*, vol. 38, pp. 2039–2061, Feb. 2013.

[49] E. Bøckmann and S. Steen, "Wind Turbine Propulsion of Ships," in *Proceedings of Second International Symposium on Marine Propulsors*, p. 10, 2011.

[50] R. Abd Jamil, A. Chaigneau, J.-C. Gilloteaux, P. Lelong, and A. Babarit, "Comparison of the capacity factor of stationary wind turbines and weather-routed energy ships in the far-offshore," *Journal of Physics: Conference Series*, vol. 1356, p. 012001, Oct. 2019. Publisher: IOP Publishing.

[51] A. Babarit, G. Clodic, S. Delvoye, and J.-C. Gilloteaux, "Exploitation of the far-offshore wind energy resource by fleets of energy ships – Part 1: Energy ship design and performance," *Wind Energy Science*, vol. 5, pp. 839–853, July 2020. Publisher: Copernicus GmbH.

[52] M. F. Platzer, N. Sarigul-Klijn, J. Young, M. A. Ashraf, and J. C. S. Lai, "Renewable Hydrogen Production Using Sailing Ships," *Journal of Energy Resources Technology*, vol. 136, June 2014. Publisher: American Society of Mechanical Engineers Digital Collection.

[53] M. Tsujimoto, T. Uehiro, H. Esaki, T. Kinoshita, K. Takagi, S. Tanaka, H. Yamaguchi, H. Okamura, M. Satou, and Y. Minami, "Optimum routing of a sailing wind farm," *Journal of Marine Science and Technology*, vol. 14, pp. 89–103, Mar. 2009.

[54] M. Kopp, D. Coleman, C. Stiller, K. Scheffer, J. Aichinger, and B. Scheppat, "Energiepark Mainz: Technical and economic analysis of the worldwide largest Power-to-Gas plant with PEM electrolysis," *International Journal of Hydrogen Energy*, vol. 42, pp. 13311–13320, May 2017.

[55] "Asian Renewable Energy Hub." https://asianrehub.com/, Web accessed 07/2022.

[56] G. Bordogna, *Aerodynamics of wind-assisted ships: Interaction effects on the aerodynamic performance of multiple wind-propulsion systems*. PhD thesis, 2020. https://doi.org/10.4233/uuid:96eda9cd-3163-4c6b-9b9f-e9fa329df071.

[57] D. Pearson, "The use of Flettner rotors in efficient ship design," *RINA, Royal Institution of Naval Architects - Influence of EEDI on Ship Design 2014*, pp. 162–169, Jan. 2014.

[58] T. Burton, N. Jenkins, D. Sharpe, and E. Bossanyi, "Aerodynamics of Horizontal Axis Wind Turbines," in *Wind Energy Handbook*, pp. 39–136, John Wiley & Sons, Ltd, 2011. Section: 3 _eprint: https://onlinelibrary.wiley.com/doi/pdf/10.1002/9781119992714.ch3.

[59] C. E. Mungan, "The Bernoulli equation in a moving reference frame," *European Journal of Physics*, vol. 32, pp. 517–520, Feb. 2011. Publisher: IOP Publishing.

[60] Y. Itoh and A. Satoh, "Measurement of Propeller Characteristics at a Negative Advance Ratio Using a Whirling Arm Facility," in *The Proceedings of the 2018 Asia-Pacific International Symposium on Aerospace Technology (APISAT 2018)* (X. Zhang, ed.), Lecture Notes in Electrical Engineering, (Singapore), pp. 1169–1188, Springer, 2019.

[61] A. Robertson, "Definition of the semisubmersible floating system for phase II of OC4 /," technical Report, National Renewable Energy Laboratory, Sept. 2014.

[62] J. Jonkman, S. Butterfield, W. Musial, and G. Scott, "Definition of a 5-MW Reference Wind Turbine for Offshore System Development," Tech. Rep. NREL/TP-500-38060, 947422, Feb. 2009.

[63] J. Jonkman, "Definition of the Floating System for Phase IV of OC3," Tech. Rep. NREL/TP-500-47535, 979456, May 2010.

[64] B. Skaare, F. G. Nielsen, T. D. Hanson, R. Yttervik, O. Havmøller, and A. Rekdal, "Analysis of measurements and simulations from the Hywind Demo floating wind turbine," *Wind Energy*, vol. 18, no. 6, pp. 1105–1122, 2015. _eprint: https://onlinelibrary.wiley.com/doi/pdf/10.1002/we.1750.

[65] L. Nikolopoulos and E. Boulougouris, "A novel method for the holistic, simulation driven ship design optimization under uncertainty in the big data era," *Ocean Engineering*, vol. 218, p. 107634, Dec. 2020.

[66] Thrustmaster, "Portable Dynamic Positioning Systems," 2014. https://www.thrustmaster.net/wp-content/uploads/2013/12/Portable-Dyanmic-Positioning-System-Brochure-2014.pdf, Web accessed 07/2022.

[67] J. Sudre, C. Maes, and V. Garçon, "On the global estimates of geostrophic and Ekman surface currents," *Limnology and Oceanography: Fluids and Environments*, vol. 3, no. 1, pp. 1–20, 2013. _eprint: https://onlinelibrary.wiley.com/doi/pdf/10.1215/21573689-2071927.

[68] "DNV-RP-C205: Environmental Conditions and Environmental Loads," p. 124, 2010.

[69] M. Kim and J. Kim, "An integrated decision support model for design and operation of a wind-based hydrogen supply system," *International Journal of Hydrogen Energy*, vol. 42, pp. 3899–3915, Feb. 2017.

[70] A. Allman and P. Daoutidis, "Optimal scheduling for wind-powered ammonia generation: Effects of key design parameters," *Chemical Engineering Research and Design*, vol. 131, pp. 5–15, Mar. 2018.

[71] W. T. Liu, W. Tang, and X. Xie, "Wind power distribution over the ocean," *Geophysical Research Letters*, vol. 35, no. 13, 2008. _eprint: https://onlinelibrary.wiley.com/doi/pdf/10.1029/2008GL034172.

[72] M. Grujicic, G. Arakere, B. Pandurangan, V. Sellappan, A. Vallejo, and M. Ozen, "Multidisciplinary Design Optimization for Glass-Fiber Epoxy-Matrix Composite 5 MW Horizontal-Axis Wind-Turbine Blades," *Journal of Materials Engineering and Performance*, vol. 19, pp. 1116–1127, Nov. 2010.

[73] P. Connolly and C. Crawford, "Analytical modelling of power production from Un-moored Floating Offshore Wind Turbines," *Ocean Engineering*, vol. 259, p. 111794, Sept. 2022.

[74] I. Rojon and C. Dieperink, "Blowin' in the wind? Drivers and barriers for the uptake of wind propulsion in international shipping," *Energy Policy*, vol. 67, pp. 394–402, Apr. 2014.

[75] G. Jacobi, G. Thomas, M. R. Davis, and G. Davidson, "An insight into the slamming behaviour of large high-speed catamarans through full-scale measurements," *Journal of Marine Science and Technology*, vol. 19, pp. 15–32, Mar. 2014.

[76] H. Wang, W. Mao, and L. Eriksson, "A Three-Dimensional Dijkstra's algorithm for multi-objective ship voyage optimization," *Ocean Engineering*, vol. 186, p. 106131, Aug. 2019.

[77] J. S. Carlton, *Marine Propellers and Propulsion*. Elsevier, 2nd ed., 2007.

[78] M. Yoong, Y. Gan, G. Gan, C. Leong, Z. Phuan, B. Cheah, and K. Chew, "Studies of regenerative braking in electric vehicle," in *2010 IEEE Conference on Sustainable Utilization and Development in Engineering and Technology*, pp. 40–45, Nov. 2010.

[79] S. Enge, E. Fjøsna, and r. Sigurbjarnarson, "Regenerative Hybrid-Electric Propulsion," Tech. Rep. 1, Bellona, North Sailing, Apr. 2013.

[80] G. Gunnarsson, J. B. Skúlason, r. Sigurbjarnarson, and S. Enge, "Regenerative electric/hybrid drive train for ships," Tech. Rep. 2, Nordic Innovation, Oslo, Norway, Jan. 2016.

[81] K. Yokota, H. Fujimoto, and Y. Hori, "Basic Study on Regenerative Air Brake Using Observer-based Thrust Control for Electric Airplane," in *2020 IEEE 16th International Workshop on Advanced Motion Control (AMC)*, pp. 34–39, Sept. 2020. ISSN: 1943-6580.

[82] F. Scholtens, "Electric Aircraft Design Including an In-the-loop Propeller Design Model with Regenerative Mode," Master's thesis, TU Delft, Delft University of Technology, 2021.

[83] M. Traut, P. Gilbert, C. Walsh, A. Bows, A. Filippone, P. Stansby, and R. Wood, "Propulsive power contribution of a kite and a Flettner rotor on selected shipping routes," *Applied Energy*, vol. 113, pp. 362–372, Jan. 2014.

[84] A. Lele and K. V. S. Rao, "Net power generated by flettner rotor for different values of wind speed and ship speed," in *2017 International Conference on Circuit ,Power and Computing Technologies (ICCPCT)*, pp. 1–6, Apr. 2017.

[85] T. Burton, N. Jenkins, D. Sharpe, and E. Bossanyi, "The Wind Resource," in *Wind Energy Handbook*, pp. 9–38, John Wiley & Sons, Ltd, 2011. Section: 2 _eprint: https://onlinelibrary.wiley.com/doi/pdf/10.1002/9781119992714.ch2.

[86] W. Mao, I. Rychlik, J. Wallin, and G. Storhaug, "Statistical models for the speed prediction of a container ship," *Ocean Engineering*, vol. 126, pp. 152–162, Nov. 2016.

[87] G. Thomas, S. Winkler, M. Davis, D. Holloway, S. Matsubara, J. Lavroff, and B. French, "Slam events of high-speed catamarans in irregular waves," *Journal of Marine Science and Technology*, vol. 16, pp. 8–21, Mar. 2011.

[88] "OpenFAST." https://github.com/OpenFAST/openfast, original-date: 2016-08-31T20:07:10Z, Accessed 07/2022.

[89] J. M. Jonkman, "Dynamics Modeling and Loads Analysis of an Offshore Floating Wind Turbine," technical Report, National Renewable Energy Laboratory, Nov. 2007.

[90] M. Hall and A. Goupee, "Validation of a lumped-mass mooring line model with DeepCwind semisubmersible model test data," *Ocean Engineering*, vol. 104, pp. 590–603, Aug. 2015.

[91] M. Hall, "MoorDyn V2: New Capabilities in Mooring System Components and Load Cases," American Society of Mechanical Engineers Digital Collection, Dec. 2020.

[92] J. Jonkman, "Google / Makani Energy Kite Modeling: Cooperative Research and Development Final Report, CRADA Number CRD-17-00569," Technical Report NREL/TP-5000-80635, National Renewable Energy Lab. (NREL), Golden, CO (United States), Aug. 2021.

[93] T. J. Larsen and T. D. Hanson, "A method to avoid negative damped low frequent tower vibrations for a floating, pitch controlled wind turbine," *Journal of Physics: Conference Series*, vol. 75, p. 012073, July 2007. Publisher: IOP Publishing.

[94] DNVGL, "Load and site conditions for wind turbines," Standard DNVGL-ST-0437, Oct. 2016.

[95] DNVGL, "Floating wind turbine structures," Standard DNVGL-ST-0119, July 2018.

[96] P. Connolly, "Developing a model of an Energy Ship in ProteusDS," tech. rep., University of Victoria, Dec. 2020. (Unpublished coursework, available upon request).